DISSERTATION

# EVALUATION OF NITRIC OXIDE RELEASING POLYMERS FOR WOUND HEALING APPLICATIONS

Submitted by

Kathryn A. Wold

Graduate Degree Program in Bioengineering

In partial fulfillment of the requirements

For the Degree of Doctor of Philosophy

Colorado State University

Fort Collins, Colorado

Spring 2015

Doctoral Committee:

Advisor: Melissa Reynolds

Charles Henry
Matt Kipper
Ketul Popat
John Williams

# ABSTRACT


## EVALUATION OF NITRIC OXIDE RELEASING POLYMERS FOR WOUND HEALING APPLICATIONS

Chronic, non-healing wounds afflict millions of Americans and represent a costly burden to the healthcare industry. In addition, the overuse and misuse of antibiotics has triggered the widespread emergence of drug-resistant bacteria, making the treatment of infected wounds more challenging. As a result, improved methods for wound care incorporating antibiotic-alternative bactericidal agents are in high demand. Recent wound care advances have focused on the development of dressings incorporating physical structures and biological components which mimic those encountered in a natural wound environment. Nitric oxide (NO), an endogenously produced molecule upregulated to promote cellular function and bactericidal activity during wound healing, has been harnessed in material systems and studied for wound healing potential. This work describes the characterization, bactericidal activity, cell functionality and processing of two NO-releasing polymer systems, one water-soluble and another water-insoluble. The results of this work demonstrate the capability of these polymeric NO-releasing materials to promote high log reductions of planktonic bacteria. Additionally, polymer dosages that promote cell survival and induce cytotoxicity in eukaryotic cells have been determined and nano-scale polymer fibers that maintain NO release properties have been processed. These results represent qualities beneficial towards the development of enhanced materials for the treatment of chronic infected wounds.

# ACKNOWLEDGMENTS

I would like to thank my advisor Dr. Melissa Reynolds for her support and guidance throughout my time at CSU. I would like to express my utmost gratitude to those who contributed to my work and helped me to become the researcher I am today, especially Dr. Adoracion Pegalajar-Jurado, Dr. Jessica Joslin and Dr. Vinod Damodaran.

Thank you also to Dr. Rupak Rajachar for believing in me and inspiring me to pursue my path of research.

Thank you to my cycling and skiing families, for providing me with an outlet for energy outside of the lab. And finally, I am grateful for my family and friends, both near and far for their support and encouragement.

TABLE OF CONTENTS

# CHAPTER 1: INTRODUCTION

The research presented within this dissertation represents the efforts taken to evaluate and to fabricate novel nitric oxide (NO) releasing polymers for potential use as materials to improve wound healing. Chapter 1 provides background information necessary to understanding the mechanism of wound healing, the role NO plays in the process, as well as current work in the field of wound healing and NO materials development. Chapter 2 introduces the material systems used, along with the synthesis and characterization methods developed for two polymer systems containing covalently attached NO donors. Chapters 3 and 4 describe the processes undertaken to elucidate the antibacterial potential and *in vitro* cellular compatibility of the materials. Chapter 5 details the processing methods for developing nano-scale fibers the NO-releasing polymer.

## 1.1 Evaluation of the wound healing mechanism

The human skin provides an important barrier against the outside world and, when compromised, activates a cascade of events to repair itself and restore homeostasis. From the first moments of injury, blood components from broken vessels at the wound site provide temporary protection to the injured area, initiating the first stage of the wound healing cascade – the *inflammation stage*. The goal of this stage is to halt bleeding, clear the wound site of debris and signal blood and tissue components necessary for proliferation. The cascade starts when platelets aggregate and interact with surrounding matrix and blood cells to form a fibrin clot.[1] From this clot, platelets begin to release growth factors and cytokines, signaling inflammatory molecules to the wound site to start the process of wound repair.[2] Two of the most important

signaling molecules released by the platelets are platelet derived growth factor (PDGF) and transforming growth factor-beta (TGF-β). Neutrophils are the first inflammatory mediator on site, attracted by signaling molecules released from platelets as well as chemical signals released by bacteria invading the wound.[2, 3] The role of neutrophils is to consume bacteria and other foreign material as well as eliminate damaged cells and matrix materials, while releasing pro-inflammatory cytokines to recruit additional inflammatory cells. [4, 5] The mast cells also play an important role in the inflammatory stage. They help to increase vascular permeability through the release of vascular endothelial growth factor (VEGF),[6] important for recruiting cells from the bloodstream to the wound site. Mast cells also release a number of other signaling molecules, including TGF-β, PDGF, fibroblast growth factor (FGF), keratinocyte growth factor (KGF), epidermal growth factor (EGF) and interleukin 1 (IL-1), which all signal monocytes from the blood stream and recruit cells for the next stage of healing. Monocytes migrate from the blood stream to the wound site where they differentiate into wound macrophages that, in the inflammation phase, act to further rid the wound site of bacteria and debris.[7] Macrophages are crucial for their phagocytic role as well as their production of cytokines and growth factors such as TGF-α, TGF-β, VEGF, FGF and PDGF. The redundant signaling events occurring within the inflammatory stage, where platelets, neutrophils and mast cells respond to injury by releasing cytokines and growth factors, act as recruitment mechanisms for fibroblasts and epidermal cells, transitioning the wound into the next phase of healing. The duration of this inflammatory phase will vary depending on the size, severity and health of the wounded individual, but generally, inflammation subsides within 24 h to six days after injury (See Figure 1.1.).[8, 9]

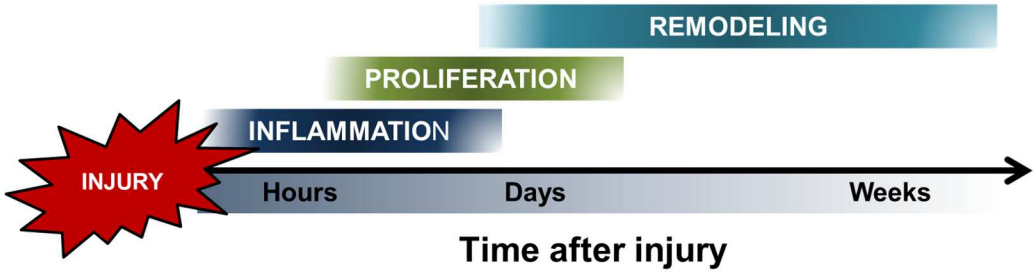


**Figure 1.1.** General time-line of the three stages of acute wound healing

The *proliferation stage* begins as matrix and tissue cells, stimulated by the growth factors and cytokines released during the inflammation stage, migrate into the wound site from the periphery. In this phase granulation tissue consisting of fibroblasts, immature collagen, and newly formed extracellular matrix (ECM) begin to replace the fibrin clot.[10] Fibroblasts replicate from intact margins of the wound site, migrate into the wound by attaching to the fibrin matrix and begin secreting collagen to form the new permanent matrix. Epidermal cells, predominantly keratinocytes, are also active during this phase. Stimulated by KGF expression by fibroblasts, as well as IL-1 and TNF-α released by macrophages and platelets, keratinocytes proliferate along the edges of the wound and remaining hair follicles to create an epithelial bridge, closing the wound below the fibrin clot and accumulating granulation tissue.[11] Due to this active cell and tissue proliferation, the wound site is in need of more blood vessels to support the continued growth. Angiogenesis is primarily stimulated by VEGF released by keratinocytes, and new vessels begin to sprout from intact capillaries around the wounded area and migrate into the wound space. The proliferation stage is brought to an end when the wound begins to contract. A portion of the wound fibroblasts are stimulated to transition morphology into the more contractile myofibroblasts that work to pull the wound together.[9] While initial reconstruction of the dermal tissue begins to occur 3 to 5 days after initial injury, the proliferation phase can last a few days to several weeks.[9]

The last stage of wound healing is the *remodeling stage* where collagen reorganization and maturation take place. The tissue transitions from granulation tissue to scar tissue and the wound is healed. Unnecessary collagen in the matrix is degraded; that which remains undergoes crosslinking, increasing its strength. The remodeling stage can begin just days after injury but lasts anywhere from a few weeks to several months or a year.[9] Although the wound is now closed, the strength of the healed tissue is weaker than the surrounding uninjured tissue, as the scar tissue can only reach 80% of its pre-injured tensile strength.[12]

Chronic or non-healing wounds can arise when the wound healing process does not proceed by these steps. Chronic wounds are a growing and costly medical problem in the U.S. and worldwide with an estimated 1-2% of the population in developed countries suffering from chronic wounds, including approximately 6.5 million in the United States.[13] As a result, the economic burden of chronic wound care in the U.S. alone is estimated at $25 billion dollars.[13, 14]

Chronic wounds most commonly result from complications due to diabetes mellitus, venous stasis, peripheral vascular disease and pressure ulceration.[15] Traumatic wounds such as burns also suffer from impaired healing.[8] Diabetic foot ulcers, pressure ulcers and venous leg ulcers top the list in conditions resulting in long term clinical chronic wound treatment, afflicting an estimated 6 million in the U.S according to a 2012 executive review.[16] Although the healing timeline is relative depending on factors such as type and size, wounds are commonly diagnosed as ‘chronic’ if they remain unhealed within 4 months, or have not shown a 20 – 40% reduction in area after 4 weeks of treatment.[15, 17]

In all chronic wound situations, impaired healing is due to problems in one or more stages of the normal healing mechanism. Two stages where wounds typically become ‘stuck’ are the inflammatory stage, due to hyperactive inflammatory processes or bacterial infection, and the

proliferation stage, due to insufficient tissue growth and integration. In either case, the wound is unable to proceed to the final remodeling phase and is classified as chronic.

## 1.2 Complications in chronic wounds

### 1.2.1 Cellular complications

One hallmark of chronic wounds is chronic inflammation, marked by an excessive infiltration of neutrophils.[12] While these cells are essential to normal wound healing, their larger volume and prolonged presence is detrimental. The enzymes collagenase and elastase released by the upregulated volume of neutrophils leads to the targeted destruction of extracellular matrix components and wound repair mediators including VEGF and PDGF.[18] Additionally, excess reactive oxygen species accumulate in the wound, further damaging the surrounding tissue.[19] Cell growth in chronic wounds is also abnormal. Fibroblasts exhibit low proliferation rates while keratinocytes at wound edges experience hyperproliferation, blockading the migration of fibroblasts and keratinocytes into the wound.[18, 19] Decreased wound fibroblast activity leads to decreased angiogenesis and collagen production, leading to insufficient granulation tissue formation, creating insufficient wound closure and decreased blood flow to support available tissue. This causes inhibited tensile strength of 'healed' wounds, resulting in an increased probability of tissue breakage and a repeat of the wound healing process.[20]

### 1.2.2 Bacterial infection and biofilm formation

In normal wound healing, there is a rapid influx of inflammatory cells to the wound site from the surrounding vasculature. These cells clear the tissue of debris and bacteria so later stages of wound healing can continue in a clean environment. Whereas the presence of bacteria in wounds is common, their concentration burden and growth state are crucial in determining

whether the wound will become chronic. In acute wounds, bacteria exist in a free-floating, or planktonic state, where the infection can be easily accessed by the body's defense systems of antibodies and phagocytic cells.[21] Chronic wounds can manifest when the bacteria burden becomes too great and overwhelms the body's immune system. In general, an excess of $10^5$ bacterial organisms per gram of tissue are sufficient to impede wound healing, but this number is highly dependent on the bacteria strains present and strength of the patient's immune system.[22] For example, diabetics suffer from an inhibited inflammatory phase, impeding the migration of neutrophils and macrophages to the wound and thereby decreasing inflammatory functions like adherence, phagocytosis, and the release of cytokines ultimately leading to inefficient targeting of bacteria.[23] When uninhibited in the body, bacteria have the tendency to attach to wound surfaces, accumulating together and excreting matrix materials to form a biofilm.[24] This process occurs in a series of stages (Figure 1.2).[25] Initially, planktonic bacteria adhere reversibly to a surface. At this stage, the bacteria are still susceptible to antibiotics and free to detach from the surface. However, soon after initial attachment, the attachment becomes irreversible as bacteria multiply and begin secreting exopolysaccharide (EPS), a polymeric matrix. This process begins within minutes of the bacteria first adhering to the surface. In the next stage, bacteria continue to grow, forming microcolonies. They continue to secrete EPS, leading to the formation of a thick film-like substance.[26] As the film continues to grow, bacteria form column-like structures leading to the development of a mature biofilm. In the mature biofilm, bacteria within the film begin to detach, allowing for dispersal and the opportunity for biofilm formation elsewhere within the system. Bacteria biofilms are a challenge for the body to attack as penetrating the EPS is more difficult than targeting individual bacteria cells.[27] The continued presence of bacterial biofim is

recognized by the body, and inflammatory responses are increased, but are ineffective against the biofilm, leading to chronic inflammation in addition to infection.[24, 25, 27]

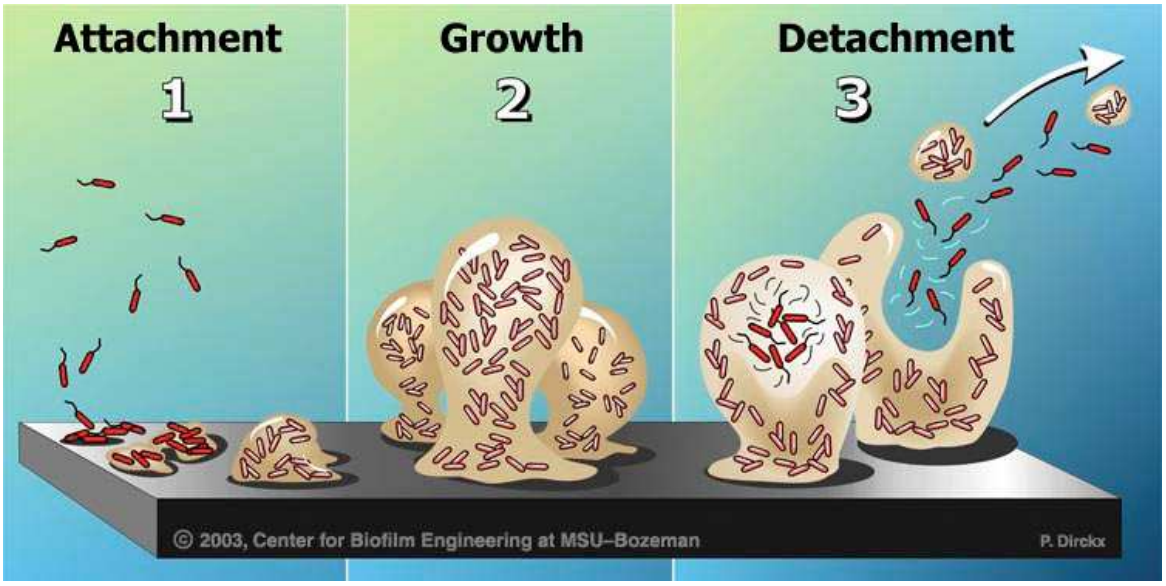


**Figure 1.2.** Steps in biofilm development, reproduced with permission from the Center for Biofilm Engineering at MSU-Bozeman. 1: initial attachment leading to irreversible attachment, 2: biofilm growth and maturation, 3: bacteria detachment and dispersion.

A wide variety of bacteria strains are found to colonize chronic wounds and lead to biofilm development. Common strains include gram positive *Staphylococcus aureus* (*S. aureus*) and *Enterococcus faecalis* (*E. faecalis*) as well as gram negative *Pseudomonas aeruginosa* and *Escherichia coli* (*E. coli*).[28] Additionally, gram negative *Acinetobacter baumannii* (*A. baumannii)* emerged as a common bacterium infecting wounded soldiers in Iraq and Afghanistan and is now prevalent in hospitals throughout the U.S.[29-31] Patients undergoing surgery or being treated for wounds in a hospital are further susceptible to developing hospital-acquired infections (HAIs). Between 2007-2009, post-surgical wound HAIs were estimated to occur in 10% of patients in U.S. hospitals, in turn adding additional days to hospital stays and making these infections a costly problem.[32]

Antibiotics are widely used as a treatment for both acute and chronic bacterial infections, however, they are not equally effective against the two.[25] Antibiotics can easily access free-floating planktonic bacteria, but the thick matrix of biofilms inhibits the penetration of the antibiotic into the film, reducing its effectiveness. Additionally, common antibiotics are designed to target dividing bacteria. They succeed in killing planktonic bacteria but are rendered ineffective against biofilms containing bacteria in a more dormant state.[33] As a result, minimal bactericidal concentrations (MBC) of antibiotics necessary to treat bacteria biofilms are commonly 100 – 1,000 times greater than those used to treat planktonic bacteria.[26, 34]

Despite their ineffectiveness, antibiotics are continually used to treat bacterial infections where biofilms are present. Bacteria survival depends on their ability to adapt to survival in wide variety of environments, and the widespread usage of systemic antibiotics since their commercial development in the 1950s has resulted in strains of bacteria species with genetic mutations rendering them resistant to one or several antibiotics.[35] According to a 2013 report published by the Centers for Disease Control and Prevention (CDC), antibiotic resistant bacteria are responsible for over two million illnesses and 23,000 deaths annually in the United States alone.[36] These resistant strains can run rampant in hospitals where heavy antibiotic use and immunocompromised patients provide an ideal combination for the spread of resistant bacteria. As an example, Methicillin-resistant *Staphylococcus aureus* (MRSA) is one of the most common antibiotic resistant hospital acquired infections found in patients with infected wounds, with over 80,000 severe infections reported resulting in 11,285 deaths in the U.S. in 2011.

### 1.3 Medical wound healing strategies

There is no single effective method for treating all wounds so size, severity and underlying patient health issues are all taken into consideration by medical staff when selecting a wound treatment. The ideal wound dressing would: protect the site from further damage, absorb wound exudate, encourage gas exchange, prevent infection and bacterial invasion, require infrequent changes and avoid inducing allergic or toxic effects on the surrounding wound tissue.[37, 38] Dressing materials used clinically on chronic wounds include polyurethane films, polymer based foams, hydrogels, hydrocolloids and alginates.[22, 39, 40] These particular dressings are designed to provide a moist environment and induce conditions favorable for cell growth to occur. Despite their widespread use, these materials provide no assistance in restoring normal function to the wound tissue or preventing infection from pre-existing bacteria in the wound bed.

One path towards improving these traditional materials is to modify them with structural and functional properties in an attempt to facilitate interaction of the material with the wound site and stimulate natural healing and immune processes. To accomplish this, structural morphology and chemical components are selected to promote other characteristics of an ideal wound dressing mentioned previously.

One potential way to promote wound closure is to encourage cell proliferation across the wound bed by developing wound dressings with fibrous morphology mimicking the ECM, the nanofibrous scaffold on which cells naturally attach and grow. Electrospinning is one processing technique popularly studied for the development of ECM mimicking polymeric.[41-51] Electrospun fibers can be processed from a wide variety of synthetic and natural polymers and impregnated with therapeutic agents.[52] The nanoscale diameter and large surface area provided by electrospun fibers have been shown to increase rates of epithelialization, and the network of small pores

allows for high gas permeability and fluid exudate while inhibiting outside microorganisms from entering the wound.[53]

In addition to enhancing cellular activities, biomimetic wound dressings can be tailored to possess bactericidal properties. Eliminating all bacteria from a wound is not necessary to avoid infection, but current criteria for an efficacious bactericidal treatment are becoming more stringent. Ten years ago, a 3-log reduction, or 99.9% bacteria kill rate, represented a reduction be considered bactericidal and relevant for medical treatments.[54] Today, researchers are aiming for higher bacteria kill rates along the order of 8-log reductions. While drug companies still focus on developing new formulations of traditional antibiotics, the widespread emergence of drug-resistant bacteria necessitates exploring alternative antimicrobials to achieve a higher clinical bactericidal efficacy and replace the drugs to which bacteria are no longer widely susceptible.[55]

### 1.3.1 Antibiotic-alternatives

Silver has long been used as an antibacterial agent,[56, 57] and silver nanoparticles, aided by their large surface to volume ratio, are currently used in clinical and environmental applications for their anti-infective properties.[58-61] Even though it has been shown to be effective in eliminating or reducing certain strains of bacteria from wounded tissue,[62] a downside to the widespread use of silver is the indications of negative health effects, such as cell toxicity and the tendency of the particles to accumulate in the liver.[57] Silver resistance in clinical bacteria strains including *E. coli, P. aeruginosa and A. baumannii* have been recognized for at least the last decade.[63] Silver nanoparticles have been shown effective against silver-resistant bacteria strains, yet bacterial resistance to these nanoparticles have also been reported.[57] Therefore, efforts towards mimicking the body's natural immune system are becoming popular alternative paths to developing next generation antimicrobials agents. Peptides are involved in innate immunity in

animals and are being exploited for use in bactericidal biomaterials.[64] Peptides offer versatility, with hundreds of natural and synthetic antimicrobial varieties available. Peptide-induced bacterial reductions as high as 6-log have been reported, and they have also been shown to be effective on drug resistant bacteria strains including MRSA.[65] Other bioagents, such as nitric oxide (NO), have been considered as promising tools for eradicating bacteria in the wound site.

### 1.4 Nitric Oxide and its biological role in wound healing

The free radical NO is an important molecule produced and released naturally by inflammatory cells, neuronal cells and cells in the vasculature. The NO diffuses rapidly from the site of release and produces localized tissue effects. As such, it does not have long-lasting bloodstream effects. The effects NO has on the body are diverse and include controlling vasculature tone, aiding in the regulation of bone remodeling, and stimulating bactericidal activity.[66-68] The variety of influences NO induces are concentration dependent, varying by the mechanisms by which NO is produced *in vivo*.

L-arginine, a semi-essential amino acid, serves as the precursor for NO production *in vivo*. This production is stimulated by the deamination of L-arginine by the enzyme nitric oxide synthase (NOS) to form NO and L-citrulline.[69-71] Three distinct isoforms of NOS, produced by different genes and responsible for different processes, signal NO production from different cells. Endothelial NOS (eNOS) and neuronal NOS (nNOS) are, as their names suggest, responsible for stimulating NO production from the endothelium and nervous system, respectively, although they can be found in other cells as well. These isoforms induce NO production to stimulate vasodilation (eNOS) and act as a neurotransmitter (nNOS). These isoforms are responsible for signaling a sustained, low-level NO release. The third NOS isoform,

inducible NOS (iNOS), stimulates high-outputs of NO in epithelial, endothelial and inflammatory cells as a response to inflammatory cytokines. iNOS is found to be elevated after skin injury and throughout all stages of tissue regeneration when inflammation, granulation tissue formation and re-epithelialization occur due to the influx of these iNOS susceptible cells. This makes iNOS the most relevant NOS isoform to the wound healing process.

During wound healing process, NO production is most elevated in the inflammatory stage and wanes as the wound moves toward the proliferative phase.[72] During this stage, cytokines such as TNF-α and IL-1 stimulate iNOS in neutrophils and macrophages to produce NO.[39, 69, 70, 73] NO then stimulates vasodilatory properties of the microvascular, increasing blood flow and assisting the influx of inflammatory cells from the blood stream to the wound site. Though neutrophils and macrophages dominate in the inflammatory stage, fibroblasts are the important active cells in the proliferative phase as they are responsible for collagen deposition at the wound site. Fibroblasts isolated in wounds differ from fibroblasts in un-injured skin tissue in that wound site fibroblasts release NO.[74] This NO release capability, unique to wound site fibroblasts, is highly important in the wound healing cascade as NO inhibition in wounded tissue *in vivo* has been correlated with a decrease of wound collagen production, leading to impaired wound healing.[75] Intact keratinocytes in the wound margins also produce NO, stimulating the proliferation and migration of more keratinocytes in the wound.[39]

In the event of a bacterial assault to the body, cytokines, bacterial lipopolysaccharides (LPS) and microbial byproducts act as signals to up regulate iNOS production from macrophages. iNOS then stimulates the production of NO from L-arginine. NO is produced as part of a non-specific immune response to bacterial invasion, yet it acts as an intermediate to bactericidal activity and has insignificant direct bactericidal action. Instead, NO reacts with

oxygen and oxygen radicals to form reactive byproducts that in turn act to target and kill bacteria. One of the most potent interactions involving NO comes from the reaction of NO and superoxide ($O_2^-$). Though NO levels are low in healthy tissue,[76] under inflammatory conditions macrophages and neutrophils produce the free radical, reactive oxygen species through the actions of the enzyme NADPH oxidase. NO and superoxide readily interact to form the reactive oxygen species peroxinitrite ($ONOO^-$). Peroxynitrite exerts strong antimicrobial effects by inducing oxidative stress on DNA nucleotides inside the bacteria cell, cleaving nucleotides in the DNA strands leading to irreparable damage and cell death.[77, 78] Peroxinitrite is also capable of destroying the integrity of the cell membrane by lipid peroxidation. Aside from its interaction with NO, superoxide can also react with hydrogen to form hydrogen peroxide ($H_2O_2$), another oxidative species. $H_2O_2$ is similar to peroxynitrite in that it alone exerts some bactericidal activity, but when combined with NO its bactericidal activity is greatly increased.[79] The combination of NO and $H_2O_2$ causes bactericidal activity by inducing double strand breakage in pathogen DNA. Another mode of bactericidal action of NO is through the interaction of NO with oxygen and other oxygen species to produce $N_2O_3$, $NO_2^{\bullet}$ or $N_2O_4$. These nitrosating agents induce bactericidal activity by also causing breakage of DNA strands by inducing oxidative stress.[80]

Eukaryotic cells are also susceptible to membrane and DNA damage by NO via similar mechanisms that cause bacteria death but at a higher concentration. The reason NO has cytotoxic effects on bacterial cells at lower concentrations than eukaryotic cells *in vivo* is due to the detoxification effects within eukaryotic cells that scavenge nitrogen oxygen species, the reactive byproducts of nitric oxide.[76] One such protective mechanism is metallothionein. This thiol protein is upregulated in eukaryotic cells in the presence of bacteria products and oxidative

stress.[81, 82] Reactive nitric oxide byproducts react with the thiol on the protein, thereby reducing intercellular levels of these harmful species. The antioxidant glutathione can also act to scavenge both NO and reactive NO byproducts, reducing the local concentration within the cell.[76, 83] As the physiological actions of NO are concentration dependent, higher concentrations of NO can eventually overcome the cell's protective mechanisms and induce cytotoxicity, but at a level greater than those necessary for inducing antibacterial activity.[84] It is clear NO plays a vital role across the stages of wound healing, which is why harnessing this molecule could prove beneficial for improving the treatment of clinical wounds.

### 1.4.1 Clinical application of NO

Nitric oxide was first studied for its antibacterial properties over 50 years ago,[85] but it wasn't until the late 1980s when it was determined NO played a role in the innate immune system.[86] In the past few decades, the ability to harness and release NO strategically has been realized and applied toward investigation into the treatment of infection causing bacteria.[87] Unlike traditional antibiotics and antibiotic alternatives like silver, NO has been shown to be unlikely to develop bacterial resistance, even over extended periods of use.[88] Vastly different techniques have been employed to exert therapeutic effects, including gaseous release, small-molecule NO delivery and macromolecular NO delivery. Successful bacteria reduction results have been realized *in vitro* for both free-floating planktonic bacteria as well as the more difficult to treat bacteria biofilms. Despite its recent popularity, therapeutic antimicrobial doses remain varied between material systems as there are several factors behind its killing efficiency including the delivery method, concentration and timeframe over which NO is released.

The most straightforward path to testing NO's effect on bacteria is by administering the molecule in its gas phase. Work with gaseous NO (gNO) has shown that simple application

directly from a gas cylinder to bacteria samples can produce bactericidal activity *in vivo* at levels of 200 ppm.[89, 90] Although gNO is relatively easy to administer in the clinical setting, this method of NO delivery limits patient mobility due to the size of the equipment necessary to administer treatment, namely the gNO cylinder. In addition, as large quantities of NO can be toxic if inhaled, safety risks involving this treatment are great.

### 1.4.2 NO materials systems

To overcome the limitations of gNO delivery, material systems incorporating NO precursors or NO release into medical devices have been developed. The goal is to develop materials capable of releasing tailored or predictable levels of NO under physiological conditions over timeframes from minutes to days. The three broad categories of NO delivery materials developed to date, distinguished by the way NO release or production is incorporated into the material, are: enzymatically producing NO materials, small-molecule NO donor blended systems and macromolecular NO donors.

Table 1.1 provides an overview of NO-releasing material systems tested to date for their bactericidal activity. Jones *et al.* developed a patch where NO is enzymatically created by specialized probiotic bacteria. This method allows gNO to be delivered directly from the patch to the target site through a thin membrane.[67, 81] In terms of the material system variety and publication volume, the Schoenfisch group is a leader in the development and evaluation of NO-releasing material systems with characterized bactericidal activity. The Schoenfisch group has also published a wide array of NO donor systems where NO has been blended into solgels and xerogels, along with macromolecular NO-releasing dendrimers and silica nanoparticles where NO is covalently attached to the carrier.[91-98] These systems achieved a maximum bacterial reduction of 5-log. Recently, NO incorporated zeolites were shown to induce an 8-log reduction

in *E. coli* and *A. baumannii*, representing one of the first NO-releasing systems to achieve a bacterial reduction larger than 5-log.[99]

A limiting factor for NO-releasing systems is the amount and duration of NO release as this capability determines the effectiveness of the material at killing bacteria and promoting wound healing. Therefore, macromolecular donors, where NO is functionalized to or encapsulated within a material system, have been favored over small molecule donors due to their more tailored and targeted NO release capabilities.[100,101]

**Table 1.1.** Published NO-releasing material systems and corresponding results of *in vitro* bactericidal activity

| Material Description | Bacteria | Reported Kill Efficiency | NO Release |
|---|---|---|---|
| **Silica nanoparticles**[102] *Macromolecular donor* | *P. aeruginosa* *E.coli* *S.aureus* *S.epidermidis* (planktonic and biofilms) | >5-log against gram – 2-log against gram + | 60 μmol $mL^{-1}$ |
| **Silica nanorods**[103] *Macromolecular donor* | *S. aureus* *P. aeruginosa* | 3-log | 0.1-0.2 μmol $mL^{-1}$ |
| **Dendrimers**[96-98] *Macromolecular donor* | *P. aeruginosa* *S. aureus* *MRSA* (planktonic and biofilms) | 5-log | 0.01-300 μmol $mL^{-1}$ |
| **Solgel**[91, 104] *Small molecule donor blend* | *P. aeruginosa* | 30-90% reduction | 1-19 pmol $cm^{-2}$ $s^{-1}$ |
| **Zeolites**[99] *Macromolecular donor* | *E. coli* *A. baumannii* MRSA | 8+ log reduction (*E. coli*, *A. baumannii*) 6-log reduction (MRSA) | 1.7-3.5 μmol $mL^{-1}$ |
| **Chitosan oligosaccharide**[105] *Macromolecular donor* | *P. aeruginosa* | 5-log reduction in biofilm | 0.17–0.46 μmol NO/mL |
| **NO producing patch**[67, 106] *Enzymatic production* | MRSA *A.baumannii* *P. aeruginosa* (planktonic) | 4-log after 6 h (MRSA and *A. baumannii*) 5-log after 6 h (*P. aeruginosa*) | 20.3 pmol $cm^{-1}$ $s^{-1}$ |

### 1.4.3 NO interventions and wound healing

The demonstration of bactericidal capabilities *in vitro* is an important step in the development of a wound healing material, but to show potential for clinical use, compatibility with healthy cells and tissue must be demonstrated. *In vitro* cellular studies and *in vivo* animal models are necessary to demonstrate whether NO-releasing materials impact favorable cellular interactions. Factors that must be considered are the material system and structure, NO release levels, as well as the mechanism of NO attachment used in macromolecular donors. As NO at high dosages can be toxic to eukaryotic cells, reported bactericidal dosages could also prove toxic to living tissue.

While fewer NO donor materials have been evaluated *in vivo,* the NO-releasing systems studied for their wound healing potential in small mammal models all exhibited enhanced healing properties. Gaseous NO release from the enzymatic NO-releasing dressing tested on infected wounds in rabbit models exhibited accelerated wound healing and a reduction in wound exudate and microbial load in comparison to control dressings while exhibiting no signs of tissue toxicity.[107] NO-releasing hydrogel based nanoparticles promoted an increased rate of wound healing in *in vivo* mouse models through the enhancement of collagen deposition while also providing antibacterial activity against *S. aureus,* MRSA and *A. baumannii*.[108-110] Bohl Masters *et al.* observed improved strength in the healed wounds in diabetic mice treated with another NO-releasing hydrogel system.[111] Neidrauer *et al*. developed an NO-releasing zinc-exchanged zeolite ointment that, when used to treat wounds in a rat model, was shown to improve healing time while also inducing an absence of inflammation during treatment.[99]

The growing number and variety of macromolecular NO-releasing donor materials, along with the results of the *in vivo* studies showing improved wound healing after the application of

NO-releasing substances, give great precedence for the further exploration and development of these materials for applications towards treating chronic wounds. However, several challenges remain in the fabrication of NO-releasing material systems suitable for a clinical setting including determining ideal NO dosages for increased bactericidal activity while minimizing cell toxicity, improving the handleability of the materials and their bench-top stability.

### 1.5 Hypothesis and aims

**Fundamental hypothesis:** Natural and synthetic polymers incorporating NO through *S*-nitro functionalization provide an advantageous material system for combined antibacterial activity, cell functionality and scaffold processability- leading to enhanced wound healing.

**Hypothesis 1:** *S*-nitrosated polymer derivatives can be synthesized to exhibit reproducible structural and NO release properties.

**Aim 1:** Synthesize *S*-nitrosated dextran and poly(lactic-co-glycolic-co-hydroxymethyl propionic acid) (PLGH) and characterize polymer derivatives and their intermediate synthesis products for thiol incorporation, NO incorporation and real-time NO release. This work is discussed in **Chapter 2**.

**Hypothesis 2:** NO-releasing polymers will exhibit bactericidal activity against gram negative and gram-positive bacteria.

**Aim 2:** Determine the threshold of NO release required from an *S*-nitrosated dextran derivative to eradicate bacteria in a nutrient rich media. This work is discussed in **Chapter 3**.

- Determine NO-releasing capabilities of S-nitrosated dextran cysteamine in nutrient broth media and compare with values reported in phosphate buffer saline (PBS) previously reported by our team.
- Investigate the amount of S-nitrosated dextran cystemaine required for maximum bactericidal activity – i.e. higher than 7-log reduction – over 24 h using *E.coli*, *A. baumanii* and *S. aureus*.

**Hypothesis 3:** NO-releasing polymers will allow for maintenance of cell function.

**Aim 3:** Determine cytotoxic threshold for NO released from materials using human cells involved in wound healing. This work is discussed in **Chapter 4**.

- Perform *in vitro* experiments using human dermal fibroblasts to assess the metabolic activity of the cells after exposure to the NO-releasing polymer
- Verify the metabolic activity of the cells after treatment using fluorescent cellular imaging techniques

**Hypothesis 4:** PLGH polymers can be processed into a fibrous scaffold while maintaining NO release capabilities.

**Aim 4:** Develop electrospinning processing parameters towards tailored polymer fiber morphology while maintaining NO release. This research is discussed in **Chapter 5**.

- Develop parameters under which uniform nanoscale fibers form using the electrospinning process.
- Demonstrate sustained release of NO over the timeframe of hours to days
- Maintain structure under physiological conditions

REFERENCES


1. Midwood, K. S.; Williams, L. V.; Schwarzbauer, J. E., Tissue repair and the dynamics of the extracellular matrix. *International Journal of Biochemistry & Cell Biology* **2004,** 36, (6), 1031-1037.

2. Martin, P., Wound healing - Aiming for perfect skin regeneration. *Science* **1997,** 276, (5309), 75-81.

3. Tschaikowsky, K.; Sittl, R.; Braun, G. G.; Hering, W.; Rugheimer, E., INCREASED FMET-LEU-PHE RECEPTOR EXPRESSION AND ALTERED SUPEROXIDE PRODUCTION OF NEUTROPHIL GRANULOCYTES IN SEPTIC AND POSTTRAUMATIC PATIENTS. *Clinical Investigator* **1993,** 72, (1), 18-25.

4. Singer, A. J.; Clark, R. A. F., Mechanisms of disease - Cutaneous wound healing. *New England Journal of Medicine* **1999,** 341, (10), 738-746.

5. Werner, S.; Grose, R., Regulation of wound healing by growth factors and cytokines. *Physiological Reviews* **2003,** 83, (3), 835-870.

6. Wulff, B. C.; Wilgus, T. A., Mast cell activity in the healing wound: more than meets the eye? *Experimental Dermatology* **2013,** 22, (8), 507-510.

7. Delavary, B. M.; van der Veer, W. M.; van Egmond, M.; Niessen, F. B.; Beelen, R. H. J., Macrophages in skin injury and repair. *Immunobiology* **2011,** 216, (7), 753-762.

8. Macri, L.; Clark, R. A. F., Tissue Engineering for Cutaneous Wounds: Selecting the Proper Time and Space for Growth Factors, Cells and the Extracellular Matrix. *Skin Pharmacology and Physiology* **2009,** 22, (2), 83-93.

9. Baum, C. L.; Arpey, C. J., Normal cutaneous wound healing: Clinical correlation with cellular and molecular events. *Dermatologic Surgery* **2005,** 31, (6), 674-686.

10. Yamaguchi, Y.; Yoshikawa, K., Cutaneous wound healing: An update. *Journal of Dermatology* **2001,** 28, (10), 521-534.

11. Li, J.; Chen, J.; Kirsner, R., Pathophysiology of acute wound healing. *Clinics in Dermatology* **2007,** 25, (1), 9-18.

12. Diegelmann, R. F.; Evans, M. C., Wound healing: An overview of acute, fibrotic and delayed healing. *Frontiers in Bioscience* **2004,** 9, 283-289.

13. Sen, C. K.; Gordillo, G. M.; Roy, S.; Kirsner, R.; Lambert, L.; Hunt, T. K.; Gottrup, F.; Gurtner, G. C.; Longaker, M. T., Human skin wounds: A major and snowballing threat to public health and the economy. *Wound Repair and Regeneration* **2009,** 17, (6), 763-771.

14. Gottrup, F., A specialized wound-healing center concept: importance of a multidisciplinary department structure and surgical treatment facilities in the treatment of chronic wounds. *American Journal of Surgery* **2004,** 187, (5A), 38S-43S.

15. Siddiqui, A. R.; Bernstein, J. M., Chronic wound infection: Facts and controversies. *Clinics in Dermatology* **2010,** 28, (5), 519-526.

16. Greer, N.; Foman, N.; Dorrian, J.; Fitzgerald, P.; MacDonald, R.; Rutks, I.; Wilt, T., Advanced Wound Care Therapies for Non-Healing Diabetic, Venous, and Arterial Ulcers: A Systematic Review. In VA-ESP, Ed. 2012.

17. Lazarus, G. S.; Cooper, D. M.; Knighton, D. R.; Margolis, D. J.; Pecoraro, R. E.; Rodeheaver, G.; Robson, M. C., DEFINITIONS AND GUIDELINES FOR ASSESSMENT OF WOUNDS AND EVALUATION OF HEALING. *Archives of Dermatology* **1994,** 130, (4), 489-493.

18. Demidova-Rice, T. N.; Hamblin, M. R.; Herman, I. M., Acute and Impaired Wound Healing: Pathophysiology and Current Methods for Drug Delivery, Part 2: Role of Growth Factors in Normal and Pathological Wound Healing: Therapeutic Potential and Methods of Delivery. *Advances in Skin & Wound Care* **2012,** 25, (8), 349-370.

19. Greaves, N. S.; Iqbal, S. A.; Baguneid, M.; Bayat, A., The role of skin substitutes in the management of chronic cutaneous wounds. *Wound Repair and Regeneration* **2013,** 21, (2), 194-210.

20. Guo, S.; DiPietro, L. A., Factors Affecting Wound Healing. *Journal of Dental Research* **2010,** 89, (3), 219-229.

21. Hall-Stoodley, L.; Costerton, J. W.; Stoodley, P., Bacterial biofilms: From the natural environment to infectious diseases. *Nature Reviews Microbiology* **2004,** 2, (2), 95-108.

22. Fonder, M. A.; Lazarus, G. S.; Cowan, D. A.; Aronson-Cook, B.; Kohli, A. R.; Mamelak, A. J., Treating the chronic wound: A practical approach to the care of nonhealing wounds and wound care dressings. *Journal of the American Academy of Dermatology* **2008,** 58, (2), 185-206.

23. Hatanaka, E.; Monteagudo, P. T.; Marrocos, M. S. M.; Campa, A., Neutrophils and monocytes as potentially important sources of proinflammatory cytokines in diabetes. *Clinical and Experimental Immunology* **2006,** 146, (3), 443-447.

24. Seth, A. K.; Geringer, M. R.; Hong, S. J.; Leung, K. P.; Mustoe, T. A.; Galiano, R. D., In vivo modeling of biofilm-infected wounds: A review. *Journal of Surgical Research* **2012,** 178, (1), 330-338.

25. Costerton, J. W.; Stewart, P. S.; Greenberg, E. P., Bacterial biofilms: A common cause of persistent infections. *Science* **1999,** 284, (5418), 1318-1322.

26. Hoiby, N.; Ciofu, O.; Johansen, H. K.; Song, Z.-j.; Moser, C.; Jensen, P. O.; Molin, S.; Givskov, M.; Tolker-Nielsen, T.; Bjarnsholt, T., The clinical impact of bacterial biofilms. *International Journal of Oral Science* **2011,** 3, (2), 55-65.

27. James, G. A.; Swogger, E.; Wolcott, R.; Pulcini, E. d.; Secor, P.; Sestrich, J.; Costerton, J. W.; Stewart, P. S., Biofilms in chronic wounds. *Wound Repair and Regeneration* **2008,** 16, (1), 37-44.

28. Gjødsbøl, K.; Christensen, J. J.; Karlsmark, T.; Jørgensen, B.; Klein, B. M.; Krogfelt, K. A., Multiple bacterial species reside in chronic wounds: a longitudinal study. *International Wound Journal* **2006,** 3, (3), 225-231.

29. Peleg, A. Y.; Seifert, H.; Paterson, D. L., Acinetobacter baumannii: Emergence of a successful pathogen. *Clinical Microbiology Reviews* **2008,** 21, (3), 538-582.

30. Maragakis, L. L.; Perl, T. M., Acinetobacter baumannii: Epidemiology, antimicrobial resistance, and treatment options. *Clinical Infectious Diseases* **2008,** 46, (8), 1254-1263.

31. Eveillard, M.; Joly-Guillou, M. L., Emerging Acinetobacter baumannii infections and factors favouring their occurrence. *Pathologie Biologie* **2012,** 60, (5), 314-319.

32. Berger, A.; Edelsberg, J.; Yu, H.; Oster, G., Clinical and Economic Consequences of Post-Operative Infections following Major Elective Surgery in US Hospitals. *Surgical Infections* **2014,** 15, (3), 322-327.

33. Hall-Stoodley, L.; Costerton, J. W.; Stoodley, P., Bacterial biofilms: from the Natural environment to infectious diseases. *Nat Rev Micro* **2004,** 2, (2), 95-108.

34. Stewart, P. S.; Costerton, J. W., Antibiotic resistance of bacteria in biofilms. *Lancet* **2001,** 358, (9276), 135-138.

35. Alberts, B., Molecular biology of the cell. **2002**.

36. Centers for Disease Control and Prevention Antibiotic Resistance Threats in the United States. http://www.cdc.gov/drugresistance/threat-report-2013/

37. Babaeijandaghi, F.; Shabani, I.; Seyedjafari, E.; Naraghi, Z. S.; Vasei, M.; Haddadi-Asl, V.; Hesari, K. K.; Soleimani, M., Accelerated Epidermal Regeneration and Improved Dermal Reconstruction Achieved by Polyethersulfone Nanofibers. *Tissue Engineering Part A* **2010,** 16, (11), 3527-3536.

38. Mayet, N.; Choonara, Y. E.; Kumar, P.; Tomar, L. K.; Tyagi, C.; Du Toit, L. C.; Pillay, V., A Comprehensive Review of Advanced Biopolymeric Wound Healing Systems. *Journal of Pharmaceutical Sciences* **2014,** 103, (8), 2211-2230.

39. Ozturk, F.; Ermertcan, A. T., Wound healing: a new approach to the topical wound care. *Cutaneous and Ocular Toxicology* **2011,** 30, (2), 92-99.

40. Broussard, K. C.; Powers, J. G., Wound Dressings: Selecting the Most Appropriate Type. *American Journal of Clinical Dermatology* **2013,** 14, (6), 449-459.

41. Khil, M. S.; Cha, D. I.; Kim, H. Y.; Kim, I. S.; Bhattarai, N., Electrospun nanofibrous polyurethane membrane as wound dressing. *Journal of Biomedical Materials Research Part B-Applied Biomaterials* **2003,** 67B, (2), 675-679.

42. Katti, D. S.; Robinson, K. W.; Ko, F. K.; Laurencin, C. T., Bioresorbable nanofiber-based systems for wound healing and drug delivery: Optimization of fabrication parameters. *Journal of Biomedical Materials Research Part B-Applied Biomaterials* **2004,** 70B, (2), 286-296.

43. Rho, K. S.; Jeong, L.; Lee, G.; Seo, B. M.; Park, Y. J.; Hong, S. D.; Roh, S.; Cho, J. J.; Park, W. H.; Min, B. M., Electrospinning of collagen nanofibers: Effects on the behavior of normal human keratinocytes and early-stage wound healing. *Biomaterials* **2006,** 27, (8), 1452-1461.

44. Chong, E. J.; Phan, T. T.; Lim, I. J.; Zhang, Y. Z.; Bay, B. H.; Ramakrishna, S.; Lim, C. T., Evaluation of electrospun PCL/gelatin nanofibrous scaffold for wound healing and layered dermal reconstitution. *Acta Biomaterialia* **2007,** 3, (3), 321-330.

45. Ojha, S. S.; Stevens, D. R.; Hoffman, T. J.; Stano, K.; Klossner, R.; Scott, M. C.; Krause, W.; Clarke, L. I.; Gorga, R. E., Fabrication and characterization of electrospun chitosan nanofibers formed via templating with polyethylene oxide. *Biomacromolecules* **2008,** 9, (9), 2523-2529.

46. Powell, H. M.; Supp, D. M.; Boyce, S. T., Influence of electrospun collagen on wound contraction of engineered skin substitutes. *Biomaterials* **2008,** 29, (7), 834-843.

47. Schneider, A.; Wang, X. Y.; Kaplan, D. L.; Garlick, J. A.; Egles, C., Biofunctionalized electrospun silk mats as a topical bioactive dressing for accelerated wound heating. *Acta Biomaterialia* **2009,** 5, (7), 2570-2578.

48. Liu, S. J.; Kau, Y. C.; Chou, C. Y.; Chen, J. K.; Wu, R. C.; Yeh, W. L., Electrospun PLGA/collagen nanofibrous membrane as early-stage wound dressing. *Journal of Membrane Science* **2010,** 355, (1-2), 53-59.

49. Zahedi, P.; Rezaeian, I.; Ranaei-Siadat, S. O.; Jafari, S. H.; Supaphol, P., A review on wound dressings with an emphasis on electrospun nanofibrous polymeric bandages. *Polymers for Advanced Technologies* **2010,** 21, (2), 77-95.

50. Zhong, W.; Xing, M. M. Q.; Maibach, H. I., Nanofibrous materials for wound care. *Cutaneous and Ocular Toxicology* **2010,** 29, (3), 143-152.

51. Rieger, K. A.; Birch, N. P.; Schiffman, J. D., Designing electrospun nanofiber mats to promote wound healing - a review. *Journal of Materials Chemistry B* **2013,** 1, (36), 4531-4541.

52. Sill, T. J.; von Recum, H. A., Electro spinning: Applications in drug delivery and tissue engineering. *Biomaterials* **2008,** 29, (13), 1989-2006.

53. Mogosanu, G. D.; Grumezescu, A. M., Natural and synthetic polymers for wounds and burns dressing. *International Journal of Pharmaceutics* **2014,** 463, (2), 127-136.

54. Pankey, G. A.; Sabath, L. D., Clinical relevance of bacteriostatic versus bactericidal mechanisms of action in the treatment of gram-positive bacterial infections. *Clinical Infectious Diseases* **2004,** 38, (6), 864-870.

55. Moriarty, T. F.; Grainger, D. W.; Richards, R. G., CHALLENGES IN LINKING PRECLINICAL ANTI-MICROBIAL RESEARCH STRATEGIES WITH CLINICAL OUTCOMES FOR DEVICE-ASSOCIATED INFECTIONS. *European Cells & Materials* **2014,** 28, 112-128.

56. Klasen, H. J., Historical review of the use of silver in the treatment of burns. I. Early uses. *Burns* **2000,** 26, (2), 117-130.

57. Maillard, J. Y.; Hartemann, P., Silver as an antimicrobial: facts and gaps in knowledge. *Critical Reviews in Microbiology* **2013,** 39, (4), 373-383.

58. Morones, J. R.; Elechiguerra, J. L.; Camacho, A.; Holt, K.; Kouri, J. B.; Ramirez, J. T.; Yacaman, M. J., The bactericidal effect of silver nanoparticles. *Nanotechnology* **2005,** 16, (10), 2346-2353.

59. Ahamed, M.; AlSalhi, M. S.; Siddiqui, M. K. J., Silver nanoparticle applications and human health. *Clinica Chimica Acta* **2010,** 411, (23-24), 1841-1848.

60. Rai, M.; Yadav, A.; Gade, A., Silver nanoparticles as a new generation of antimicrobials. *Biotechnology Advances* **2009,** 27, (1), 76-83.

61. Sondi, I.; Salopek-Sondi, B., Silver nanoparticles as antimicrobial agent: a case study on E-coli as a model for Gram-negative bacteria. *Journal of Colloid and Interface Science* **2004,** 275, (1), 177-182.

62. Hospenthal, D. R.; Murray, C. K.; Andersen, R. C.; Blice, J. P.; Calhoun, J. H.; Cancio, L. C.; Chung, K. K.; Conger, N. G.; Crouch, H. K.; D'Avignon, L. C.; Dunne, J. R.; Ficke, J. R.; Hale, R. G.; Hayes, D. K.; Hirsch, E. F.; Hsu, J. R.; Jenkins, D. H.; Keeling, J. J.; Martin, R. R.; Moores, L. E.; Petersen, K.; Saffle, J. R.; Solomkin, J. S.; Tasker, S. A.; Valadka, A. B.; Wiesen, A. R.; Wortmann, G. W.; Holcomb, J. B., Guidelines for the Prevention of Infection After Combat-Related Injuries. *The Journal of Trauma and Acute Care Surgery* **2008,** 64, (3).

63. Li, X. Z.; Nikaido, H.; Williams, K. E., Silver-resistant mutants of Escherichia coli display active efflux of Ag+ and are deficient in porins. *Journal of Bacteriology* **1997,** 179, (19), 6127-6132.

64. Bahar, A. A.; Ren, D., Antimicrobial Peptides. *Pharmaceuticals (Basel)* **2013,** 6, (12), 1543-1575.

65. Vreuls, C.; Zocchi, G.; Thierry, B.; Garitte, G.; Griesser, S. S.; Archambeau, C.; Van de Weerdt, C. V.; Martial, J.; Griesser, H., Prevention of bacterial biofilms by covalent immobilization of peptides onto plasma polymer functionalized substrates. *Journal of Materials Chemistry* **2010,** 20, (37), 8092-8098.

66. Contreras, D. L.; Robles, H. V.; Romo, E.; Rios, A.; Escalante, B., The role of nitric oxide in the post-ischemic revascularization process. *Pharmacology & Therapeutics* **2006,** 112, (2), 553-563.

67. Jones, M. L.; Ganopolsky, J. G.; Labbe, A.; Prakash, S., A novel nitric oxide producing probiotic patch and its antimicrobial efficacy: preparation and in vitro analysis. *Applied Microbiology and Biotechnology* **2010,** 87, (2), 509-516.

68. Joyner, M. J.; Dietz, N. M., Nitric oxide and vasodilation in human limbs. *Journal of Applied Physiology* **1997,** 83, (6), 1785-1796.

69. MacMicking, J.; Xie, Q. W.; Nathan, C., Nitric oxide and macrophage function. *Annual Review of Immunology* **1997,** 15, 323-350.

70. Fang, F. C.; Vazquez-Torres, A. S., Nitric oxide production by human macrophages: there's NO doubt about it. *American Journal of Physiology-Lung Cellular and Molecular Physiology* **2002,** 282, (5), L941-L943.

71. Moncada, S.; Higgs, A., MECHANISMS OF DISEASE - THE L-ARGININE NITRIC-OXIDE PATHWAY. *New England Journal of Medicine* **1993,** 329, (27), 2002-2012.

72. Witte, M. B.; Barbul, A., Role of nitric oxide in wound repair. *The American Journal of Surgery* **2002,** 183, 406-412.

73. Schwentker, A.; Vodovotz, Y.; Weller, R.; Billiar, T. R., Nitric oxide and wound repair: role of cytokines? *Nitric Oxide-Biology and Chemistry* **2002,** 7, (1), 1-10.

74. Schaffer, M. R.; Efron, P. A.; Thornton, F. J.; Klingel, K.; Gross, S. S.; Barbul, A., Nitric oxide, an autocrine regulator of wound fibroblast synthetic function. *Journal of Immunology* **1997,** 158, (5), 2375-2381.

75. Stallmeyer, B.; Kampfer, H.; Kolb, N.; Pfeilschifter, J.; Frank, S., The function of nitric oxide in wound repair: Inhibition of inducible nitric oxide-synthase severely impairs wound reepithelialization. *Journal of Investigative Dermatology* **1999,** 113, (6), 1090-1098.

76. Wink, D. A.; Mitchell, J. B., Chemical biology of nitric oxide: Insights into regulatory, cytotoxic, and cytoprotective mechanisms of nitric oxide. *Free Radical Biology and Medicine* **1998,** 25, (4-5), 434-456.

77. Delaney, S.; Delaney, J. C.; Essigmann, J. M., Chemical-biological fingerprinting: probing the properties of DNA lesions formed by peroxynitrite. *Chem Res Toxicol* **2007,** 20, (11), 1718-29.

78. Douki, T.; Cadet, J., Peroxynitrite Mediated Oxidation of Purine Bases of Nucleosides and Isolated DNA. *Free Radical Research* **1996,** 24, (5), 369-380.

79. Pacelli, R.; Wink, D. A.; Cook, J. A.; Krishna, M. C.; Degraff, W.; Friedman, N.; Tsokos, M.; Samuni, A.; Mitchell, J. B., NITRIC-OXIDE POTENTIATES HYDROGEN PEROXIDE-INDUCED KILLING OF ESCHERICHIA-COLI. *Journal of Experimental Medicine* **1995,** 182, (5), 1469-1479.

80. Juedes, M. J.; Wogan, G. N., Peroxynitrite-induced mutation spectra of pSP189 following replication in bacteria and in human cells. *Mutation Research-Fundamental and Molecular Mechanisms of Mutagenesis* **1996,** 349, (1), 51-61.

81. Jones, M. L.; Ganopolsky, J. G.; Labbe, A.; Wahl, C.; Prakash, S., Antimicrobial properties of nitric oxide and its application in antimicrobial formulations and medical devices. *Applied Microbiology and Biotechnology* **2010,** 88, (2), 401-407.

82. Schwarz, M. A.; Lazo, J. S.; Yalowich, J. C.; Allen, W. P.; Whitmore, M.; Bergonia, H. A.; Tzeng, E.; Billiar, T. R.; Robbins, P. D.; Lancaster, J. R.; Pitt, B. R., METALLOTHIONEIN PROTECTS AGAINST THE CYTOTOXIC AND DNA-DAMAGING EFFECTS OF NITRIC-OXIDE. *Proceedings of the National Academy of Sciences of the United States of America* **1995,** 92, (10), 4452-4456.

83. Hu, Z.; Zhang, C.; Tang, P.; Li, C.; Yao, Y.; Sun, S.; Zhang, L.; Huang, Y., Protection of cells from nitric oxide-mediated apoptotic death by glutathione C-60 derivative. *Cell Biology International* **2012,** 36, (7), 677-681.

84. Coneski, P. N.; Schoenfisch, M. H., Nitric oxide release: Part III. Measurement and reporting. *Chemical Society Reviews* **2012,** 41, (10), 3753-3758.

85. Fang, F. C., Mechanisms of nitric oxide-related antimicrobial activity. *Journal of Clinical Investigation* **1997,** 99, (12), 2818-2825.

86. Marletta, M. A.; Yoon, P. S.; Iyengar, R.; Leaf, C. D.; Wishnok, J. S., MACROPHAGE OXIDATION OF L-ARGININE TO NITRITE AND NITRATE - NITRIC-OXIDE IS AN INTERMEDIATE. *Biochemistry* **1988,** 27, (24), 8706-8711.

87. Shank, J. L.; Harper, R. H.; Silliker, J. H., EFFECT OF NITRIC OXIDE ON BACTERIA. *Applied Microbiology* **1962,** 10, (3), 185-&.

88. Privett, B. J.; Broadnax, A. D.; Bauman, S. J.; Riccio, D. A.; Schoenfisch, M. H., Examination of bacterial resistance to exogenous nitric oxide. *Nitric Oxide-Biology and Chemistry* **2012,** 26, (3), 169-173.

89. Ghaffari, A.; Jalili, R.; Ghaffari, M.; Miller, C.; Ghahary, A., Efficacy of gaseous nitric oxide in the treatment of skin and soft tissue infections. *Wound Repair and Regeneration* **2007,** 15, (3), 368-377.

90. Ghaffari, A.; Miller, C. C.; McMullin, B.; Ghahary, A., Potential application of gaseous nitric oxide as a topical antimicrobial agent. *Nitric Oxide-Biology and Chemistry* **2006,** 14, (1), 21-29.

91. Nablo, B. J.; Chen, T. Y.; Schoenfisch, M. H., Sol-gel derived nitric-oxide releasing materials that reduce bacterial adhesion. *Journal of the American Chemical Society* **2001,** 123, (39), 9712-9713.

92. Nablo, B. J.; Schoenfisch, M. H., Antibacterial properties of nitric oxide-releasing sol-gels. *Journal of Biomedical Materials Research Part A* **2003,** 67A, (4), 1276-1283.

93. Hetrick, E. M.; Shin, J. H.; Stasko, N. A.; Johnson, C. B.; Wespe, D. A.; Holmuhamedov, E.; Schoenfisch, M. H., Bactericidal efficacy of nitric oxide-releasing silica nanoparticles. *Acs Nano* **2008,** 2, (2), 235-246.

94. Hetrick, E. M.; Shin, J. H.; Paul, H. S.; Schoenfisch, M. H., Anti-biofilm efficacy of nitric oxide-releasing silica nanoparticles. *Biomaterials* **2009,** 30, (14), 2782-2789.

95. Carpenter, A. W.; Worley, B. V.; Slomberg, D. L.; Schoenfisch, M. H., Dual Action Antimicrobials: Nitric Oxide Release from Quaternary Ammonium-Functionalized Silica Nanoparticles. *Biomacromolecules* **2012,** 13, (10), 3334-3342.

96. Sun, B.; Slomberg, D. L.; Chudasama, S. L.; Lu, Y.; Schoenfisch, M. H., Nitric Oxide-Releasing Dendrimers as Antibacterial Agents. *Biomacromolecules* **2012,** 13, (10), 3343-3354.

97. Lu, Y.; Slomberg, D. L.; Shah, A.; Schoenfisch, M. H., Nitric Oxide-Releasing Amphiphilic Poly(amidoamine) (PAMAM) Dendrimers as Antibacterial Agents. *Biomacromolecules* **2013,** 14, (10), 3589-3598.

98. Worley, B. V.; Slomberg, D. L.; Schoenfisch, M. H., Nitric Oxide-Releasing Quaternary Ammonium-Modified Poly(amidoamine) Dendrimers as Dual Action Antibacterial Agents. *Bioconjugate Chemistry* **2014,** 25, (5), 918-927.

99. Neidrauer, M.; Ercan, U. K.; Bhattacharyya, A.; Samuels, J.; Sedlak, J.; Trikha, R.; Barbee, K. A.; Weingarten, M. S.; Joshi, S. G., Antimicrobial efficacy and wound-healing property of a topical ointment containing nitric-oxide-loaded zeolites. *Journal of Medical Microbiology* **2014,** 63, 203-209.

100. Riccio, D. A.; Schoenfisch, M. H., Nitric oxide release: Part I. Macromolecular scaffolds. *Chemical Society Reviews* **2012,** 41, (10), 3731-3741.

101. Carpenter, A. W.; Schoenfisch, M. H., Nitric oxide release: Part II. Therapeutic applications. *Chemical Society Reviews* **2012,** 41, (10), 3742-3752.

102. Carpenter, A. W.; Slomberg, D. L.; Rao, K. S.; Schoenfisch, M. H., Influence of Scaffold Size on Bactericidal Activity of Nitric Oxide-Releasing Silica Nanoparticles. *Acs Nano* **2011,** 5, (9), 7235-7244.

103. Lu, Y.; Slomberg, D. L.; Sun, B.; Schoenfisch, M. H., Shape- and Nitric Oxide Flux-Dependent Bactericidal Activity of Nitric Oxide-Releasing Silica Nanorods. *Small* **2013,** 9, (12), 2189-2198.

104. Nablo, B. J.; Rothrock, A. R.; Schoenfisch, M. H., Nitric oxide-releasing sol-gels as antibacterial coatings for orthopedic implants. *Biomaterials* **2005,** 26, (8), 917-924.

105. Lu, Y.; Slomberg, D. L.; Schoenfisch, M. H., Nitric oxide-releasing chitosan oligosaccharides as antibacterial agents. *Biomaterials* **2014,** 35, (5), 1716-1724.

106. Sulemankhil, I.; Ganopolsky, J. G.; Dieni, C. A.; Dan, A. F.; Jones, M. L.; Prakash, S., Prevention and Treatment of Virulent Bacterial Biofilms with an Enzymatic Nitric Oxide-Releasing Dressing. *Antimicrobial Agents and Chemotherapy* **2012,** 56, (12), 6095-6103.

107. Jones, M.; Ganopolsky, J. G.; Labbe, A.; Gilardino, M.; Wahl, C.; Martoni, C.; Prakash, S., Novel nitric oxide producing probiotic wound healing patch: preparation and in vivo analysis in a New Zealand white rabbit model of ischaemic and infected wounds. *International Wound Journal* **2012,** 9, (3), 330-343.

108. Han, G.; Martinez, L. R.; Mihu, M. R.; Friedman, A. J.; Friedman, J. M.; Nosanchuk, J. D., Nitric Oxide Releasing Nanoparticles Are Therapeutic for Staphylococcus aureus Abscesses in a Murine Model of Infection. *Plos One* **2009,** 4, (11).

109. Mihu, M. R.; Sandkovsky, U.; Han, G.; Friedman, J. M.; Nosanchuk, J. D.; Martinez, L. R., Nitric oxide releasing nanoparticles are therapeutic for Acinetobacter baumannii wound infections. *Virulence* **2010,** 1, (2), 62-67.

110. Martinez, L. R.; Han, G.; Chacko, M.; Mihu, M. R.; Jacobson, M.; Gialanella, P.; Friedman, A. J.; Nosanchuk, J. D.; Friedman, J. M., Antimicrobial and Healing Efficacy of Sustained Release Nitric Oxide Nanoparticles Against Staphylococcus Aureus Skin Infection. *Journal of Investigative Dermatology* **2009,** 129, (10), 2463-2469.

111. Bohls-Masters, K.; Leibovich, S.; Belem, P.; West, J.; Poole-Warren, L., The effects of nitric oxide releasing poly(vinyl alcohol) hydrogel dressings on dermal wound healing in diabetic mice. *Wound Rep Regen* **2002,** 10, 286-294.

# CHAPTER 2:

# SYNTHESIS AND CHARACTERIZATION OF NITRIC OXIDE RELEASING POLYMER SYSTEMS

A detailed description of the synthesis and characterization of two polymeric material systems, *S*-nitrosated PLGH and dextran derivatives are discussed. These materials will be utilized in chapters 3-5, so an in-depth understanding of their properties is necessary. I reproduced the synthesis and characterization of the *S*-nitrosated dextran-cysteamine polymers. Dr. Vinod Damodaran was responsible for the development of initial synthesis nitrosation methods for all PLGH and dextran derivatives.

Adapted from Damodaran, V.B.; Joslin, J.M.; Wold, K.A.; Lantvit, S.M.; Reynolds, M.M. *Journal of Materials Chemistry*, **2012**, 22(13), 5990-6001 with permission from The Royal Society of Chemistry

## 2.1 Introduction

The need for synthetic materials to aid in the repair and regeneration of tissues in prominent biomedical applications has resulted in a shift from the development of biostable to biodegradable materials over the last 20 years.[1-3] In fact, a wide variety of biodegradable polymers are currently being investigated for tissue engineering scaffolds and implants for orthopaedic and vascular applications.[4-13] However, many of these first generation materials cause localized cell death and work against cell regeneration processes. Furthermore, these materials still initiate the foreign body response and cause platelet activation. This lack of

integration with cells and tissues and the instigation of various bioresponses results in severe complications both initially and long-term. Taken together, the biological processes invoked by a synthetic material can ultimately lead to functional failure of implanted devices and significant health hazards to patients. In this regard, the development of biointeractive materials that control initial biological responses and degrade completely while promoting cell regeneration at the desired site is paramount.[14, 15]

Nitric oxide (NO) is a naturally occurring signaling agent responsible for maintaining a variety of important biological functions. Some of NO's vascular functions include modulating hemostasis, regulating vascular tone, promoting revascularization and fighting infection.[16-20] Moreover, NO is involved in other physiological processes such as anti-inflammatory responses[21-23] and wound-healing.[24, 25] Overall, compelling evidence suggests that biodegradable materials that release NO at tuneable levels may provide the ideal approach for creating a class of biointeractive materials that can modulate a variety of physiological processes without the limitations of biostable polymers. As shown schematically in Figure 2.1, the idea of a biodegradable polymer that promotes certain processes and inhibits others to treat a range of events is of the utmost importance.

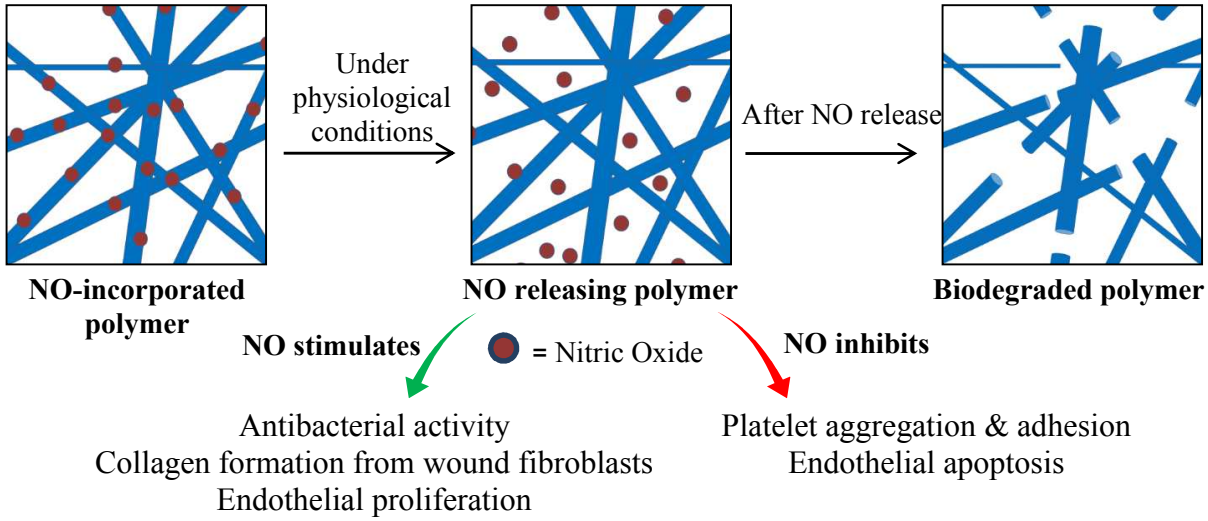


**Figure 2.1.** Schematic of intended biological effects of NO releasing biodegradable polymer systems

Because of its short half-life and high reactivity, NO must be stably stored within the material in the form of various donors such as nitrites, *S*-nitrosothiols and *N*-diazeniumdiolates.[26, 27] In the materials used throughout the studies detailed herein, the *S*-nitrosothiol (RSNO) moiety is employed for the storage and delivery of NO since RSNOs are endogenous NO donors *in vivo*, non-toxic and their decomposition is triggered through several mechanisms such as heat, light and exposure to aqueous conditions.[27-29] The variety of RSNO decomposition mechanisms makes such moieties advantageous for bioapplications as the NO release can be stimulated by the conditions present inside the body.

Extensive research exists on the development of biostable NO-releasing materials. This includes NO-releasing materials prepared from blends or covalent attachment of NO donor moieties to polymer backbones.[30-36] However, few reports have been published regarding biodegradable NO releasing materials. Coneski *et al.* synthesized degradable *S*-nitrosated polyesters.[37] The materials delivered a range of 0.04-2.28 μmol NO and the degradation rates of the non-nitrosated polymers ranged from 0-100% degradation within 10 weeks. The amount of

NO loaded into the polymer initially was assumed to be the amount of NO recovered, and no characterization of the *S*-nitrosation process was included. The assumption that the amount of NO loaded is equivalent to the NO recovered is common in the field of NO-releasing polymers and a thorough characterization of the extent of NO loading separate from the NO release data is important to understand the actual release behaviour of the polymer. Other reports of biodegradable NO releasing biomaterials use the NO donor diazeniumniolate to incorporate NO release into materials. The Ameer group developed two variations on diazeniumdiolated poly(diol-citrate) elastomers, another class of NO releasing biodegradable polyesters.[38, 39] The first report by Zaho *et al* describes the synthesis and characterization of films capable NO release over the period of 3 days and degradation rates of 20% over six weeks. In a second report, a photo-crosslinking method was employed to the polymer systems which increased the NO release time to 7 days while decreasing the degradation rate of the materials to between 26-32% over 6 months. The amount of NO released and the precise time period over which the materials are capable of releasing NO in these studies are unclear due to the method of NO analysis employed. NO release from the materials was measured daily via the Griess assay which does not provide real-time release results and relies on the indirect measurement of NO through the detection of nitrite, a by-product of NO oxidation.[40] In addition, a biodegradable NO releasing material based on the naturally derived polymer chitosan has been characterized.[41]

The studies to follow will describe the synthesis and characterization of two different biodegradable *S*-nitrosated polymers developed in the Reynolds lab. The polymers that constitute the backbone for the synthesis are both common in the biomaterials field. Poly(lactic-*co*-glycolic-*co*-hydroxymethyl propionic acid) or PLGH is a polymer based on poly(lactic-co-glycolic acid) (PLGA), a widely used polymer in FDA-approved medical devices.[42, 43] Dextran is

the base polymer for the second synthesis method discussed, and is a naturally occurring, bacteria-produced, water-soluble polymer currently used in antithrombitic applications.[44] In this chapter, the incorporation of thiols to modified PLGH and dextran polymers and their subsequent nitrosation conditions are described as well as the methods used to characterize the polymer systems.[45, 46] These material systems are the basis for the experiments performed in Chapters 3-6 of this thesis.

## 2.2 Synthesis of dextran derivatives

### 2.2.1 Materials

Reagents used in this work were obtained from commercial vendors and used without further purification: Dextran (from Leuconostoc spp., Molecular weigh 40000) from Sigma-Aldrich (St. Louis, MO, USA), spectra/por dialysis membrane (molecular weight cut off (MWCO) 8000) from Spectrum labs (Rancho Domingues, CA, USA), N-Hydroxysuccinimide (NHS) and *t*-butyl nitrite from Acros Organics (Morris Plains, NJ, USA). All other chemicals were procured from Sigma-Aldrich and used as received. Sodium chloride (99.8 % purity, MW 58.44) was obtained from Fisher Chemical.

### 2.2.2 S-nitrosated dextran-cysteamine synthesis

The synthesis of *S*-nitrosated dextran cysteamine from dextran is a multi-step process with two intermediate synthesis steps between dextran and the final product (Figure 2.2). The synthesis has been previously reported by the Reynolds group.[46] The first step involves the synthesis of carboxymethyl dextran (CM-dextran). Commercially available dextran was mixed with sodium hydroxide in an 80% 2-propanol (IPA) solution in Millipore water and stirred at 60 °C. When the solution was clear, a chloroacetic acid solution prepared in 80% IPA was added to

the mixture by an equilibrium addition funnel. The new mixture was maintained at 60 °C for 5 hours, cooled and pH adjusted to 5. The reaction was quenched with excess methanol and the precipitated product was re-dissolved in water and purified by dialyses using MWCO membranes. CM-dextran was used to obtain dextran cysteamine derivative product. NHS and N-(3-dimethylaminopropyl)-N-ethylcarbodiimide hydrochoride in Millipore water were used to pre-activate the carboxyl groups of CM-dextran. After 30 minutes stirring the solution, cysteamine hydrochloride was added to the mixture and the pH was adjusted to 5. The dextran-cysteamine was purified by dialysis using a MWCO membrane for several days. The solution was then treated with phosphine hydrochloride to reduce any disulfides and dialyzed for another week with intermediate changes of fresh Millipore filtered water to facilitate dialysis. As a final step, 4 mL methanol were added to 100 mg dextran-cysteamine in an EPA-certified amber vial (Fisher Scientific) and stirred, after which 0.4 mL *t*-butyl nitrate were added and stirred for 12 hours at room temperature. After nitrosation, the product was dried under vacuum to remove any excess methanol and *t*-butyl nitrate.

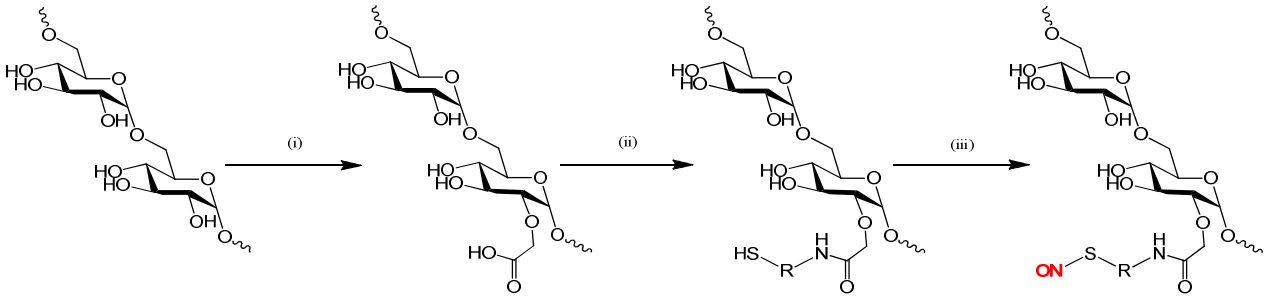


**Figure 2.2:** Scheme illustrating the synthesis of *S*-nitrosated dextran derivatives from dextran

## 2.3 Synthesis of PLGH derivatives

### 2.3.1 Materials

*N,N'*-dimethylformamide (DMF) and phosphate buffered saline (PBS) were purchased from EMD chemicals (Gibbstown, NJ, USA), and tertahydrofuran (THF) was purchased from Mallinckrodt chemicals (Phillipsburg, NJ, USA). *N*-hydroxysuccinimide (NHS) and *t*-butyl nitrite were purchased from Acros Organics (Morris Plains, NJ, USA). All other chemicals were procured from Sigma-Aldrich (St. Louis, MO, USA) and used as received.

### 2.3.2 S-nitrosated PLGH polymer synthesis

Thiolated and *S*-nitrosated PLGH derivatives were prepared in house following our earlier reported procedure and carried out by Dr. Vinod Damodaran.[47] In brief, a carboxyl functionalized polymer backbone (PLGH) was prepared from L-lactide (LA, 85% w/w) and glycolide (GL, 10% w/w) with 2,2'-bis(hydroxymethyl propionic acid) (HMPA, 5% w/w). The carboxyl groups were modified to thiol terminals by covalently conjugating a number of aminothiol derivatives such as cysteamine, cysteine and homocysteine through amide linkages using 1-ethyl-3-(3-dimethylaminopropyl) carbodiimide hydrochloride (EDC.HCl) and *N*-hydroxysuccinimide (NHS) in anhydrous DMF. The pendent thiol terminals were nitrosated with *t*-butyl nitrite (pre-treated with 10% w/v EDTA disodium salt) using a mixture of dichloromethane:methanol (1:2) to yield the corresponding *S*-nitrosated polymer derivatives. Due to the light sensitivity of the compound, the *S*-nitrosation was performed in an EPA-certified amber vial, free of metal ion contaminants that could result in premature *S*-nitrosothiol decomposition. The synthesis process is illustrated in Figure 2.3.

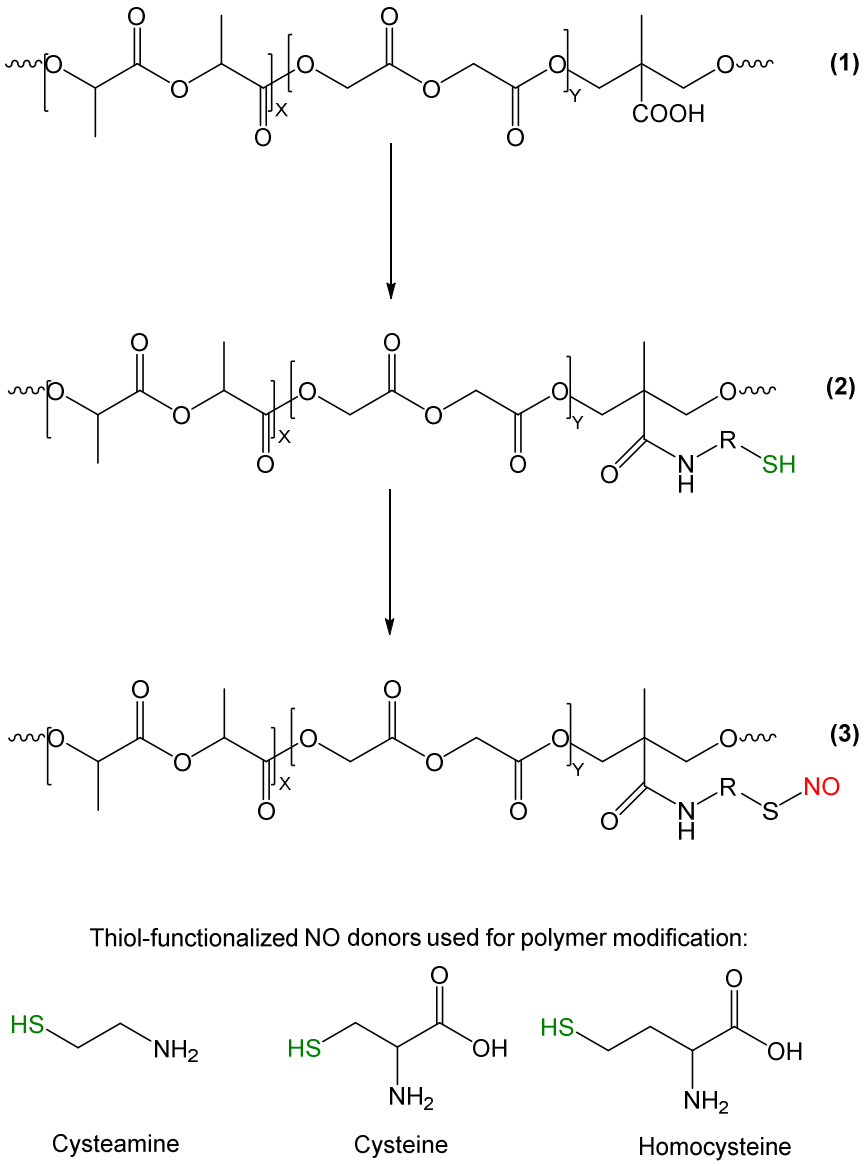


**Figure 1.3:** Scheme illustrating the synthesis of *S*-nitrosated PLGH derivatives. (1) PLGH, (2) incorporation of pendant thiol group and (3) *S*-nitrosation of thiol group to form an *S*-nitrosothiol. The three different thiols incorporated are shown below

## 2.4 Intermediate Product Characterization

Thiol incorporation was evaluated by Ellman's assay following a protocol described previously.[48, 49] Briefly, thiolated samples to be analyzed were prepared at 5 mg $mL^{-1}$ into phosphate buffer prepared by adding $NaH_2PO_4$ (100 mM, sodium phosphate, monobasic, anhydrous, molecular biology grade, BDH) to $Na_2HPO_4$ (100 mM, sodium phosphate, dibasic,

anhydrous, ACS grade, Mallinckrodt Chemicals) until pH 8 was reached. This polymer-buffer solution is referred to as the sample solution. In small glass vials, 100 μL sample solution was added to100 μL of 10 mM Ellman's reagent (5,5'-dithibis(2-nitrobenzoic acid or DTNB in 100 mM phosphate buffer). This mixture was then brought to a volume of 4 mL by the addition of 3.8 mL phosphate buffer. After shaking samples for 1 hour at room temperature, 200 μL aliquots were pipetted into a 96-well plate (Eppendorf, Hamburg, Germany) and absorbance values were recorded at 414 nm using a BioTek Synergy 2 plate reader (Biotek, Winooski, VT, USA). The recorded absorbance was used to assess the extent of the thiol incorporation. Cysteine was used to create a standard curve and the samples were prepared following the same protocol.

### 2.5 Nitric oxide characterization

#### 2.5.1 S-nitrosothiol characterization

UV absorption measurements of the *S*-nitrosated dextran were collected on a Nicolet Evolution 300 spectrophotometer (Thermo Electron Corporation) in order to quantify the RSNO content of the nitrosated polymers. Following previously reported methods, *S*-nitrosated samples were prepared in PBS at 0.75 mg $mL^{-1}$ and absorbance scans between 200-600 nm were collected in order to observe the absorbance feature around 335 nm corresponding to nitrosothiol product formation. Using the molar extinction coefficient of 766.0 ± 19.7, 882.9 ± 18.2, 652.1 ± 16.7 and 1115±42 $M^{-1}$ $cm^{-1}$, determined for *S*-nitrosated PLGH-cysteamine, PLGH-cysteine, PLGH-homocysteine and dextran-cysteamine respectively, along with the known concentration of polymer in solution, the moles of RSNO incorporated in the materials could be determined.[48] Thiolated polymer derivative solutions were used at the same concentration as the nitrosated analogues as baseline corrections.

### 2.5.2 Real-time NO analysis via chemiluminescence

Sievers chemiluminescence NO analyzers® (NOA 280i, GE Analytical, Boulder, CO, USA) were used to obtain the real-time NO release from *S*-nitrosated dextran cysteamine. To accurately measure NO in real time, NO released in solution is swept from the headspace of the NOA measurement cell into the reaction chamber located inside the NOA, where it reacts with ozone to form excited state nitrogen dioxide ($NO_2^*$). A photon between 600-850 nm is emitted when $NO_2^*$ decays to its ground state. This photon is measured by a photomultiplier tube within the NOA. This method allows for the instantaneous release of NO to be recorded in an analytical signal. Figure 2.4 provides a visual representation of the NOA cell set-up. For the NO release analysis of the polymers synthesized by the lab, a modified version of a previously described procedure was used.[48] In summary, the instruments were calibrated using nitrogen as the zero gas and also using a 45 ppm NO calibrant gas. 2 mL of a 0.75 mg $mL^{-1}$ solution containing *S*-nitrosated polymer sample in 10 mM PBS (pH 7.4) was injected into an NOA measurement cell. For general characterization studies reported in this chapter, the cell was maintained in a water bath at 37 °C and exposed to ambient light for the data collection period. Measurements were recorded in triplicate at a data interval of 5 s and a flow rate of 200 mL $min^{-1}$ with a cell pressure of 9.7 Torr and an oxygen pressure of 6 psi until NO release reached baseline.

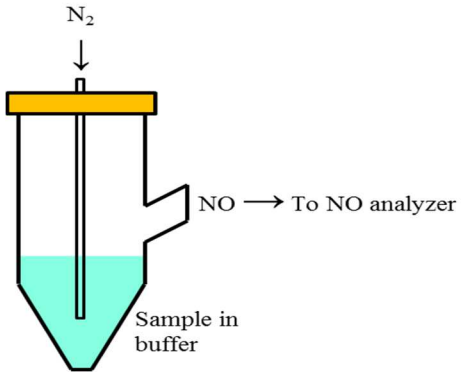


**Figure 2.4.** Diagram of NO analysis cell

## 2.6 *In vitro* polymer degradation

Polymer degradation was determined gravimetrically at seven different time points: initial and after 1, 2, 3, 4, 5, and 6 weeks of soaking in PBS. At the beginning of the study, 21 individual samples were prepared. Briefly, 150 mg sample was placed in 10 mL of 10 mM PBS (pH 7.4) at 37 °C. At the end of each week, 3 of the samples were separated from the buffer, washed with DI water and dried under vacuum to constant weight. The PBS buffer was replaced with fresh buffer for the remaining samples. This process was repeated each week until the completion of the study. The percent weight loss was determined gravimetrically. Each time point was performed in triplicate, with the average and standard deviation reported. Statistical differences were determined using the t-test.

## 2.7 Cytotoxicity

Cytotoxicity of the thiolated PLGH derivatives was evaluated according to approved International Organization for Standardization protocols (ISO-10993-5: Biological Evaluation of Medical Devices, Part 5: Tests for In Vitro Cytotoxicity) at NAMSA (Northwood, OH, USA).44 In brief, 60 $cm^2$ polymer samples along with positive (plasticized vinyl containing 10, 10′-oxybisphenoxarsine) and negative (high-density polyethylene) controls were extracted in Minimal Essential Medium (MEM) at 37 °C for 24 h. After which time, mouse LDL fibroblast cells were dosed with the extract and allowed to incubate for 48 h. A reagent control of the MEM was used to validate the stability of the extract vehicle. After incubation, cells were examined by microscope to analyze any abnormal cell morphological changes or cell lysis. The cells incubated with each material were assigned a reactivity score on a scale of 0–4.

## 2.8 Results and Discussion

### 2.8.1 S-nitrosated dextran derivatives

Using the Ellman's assay, incorporation of the thiol group cysteamine was determined to be 0.163±0.040 mmol thiol $g^{-1}$ (Table 2.1). Following nitrosation of the thiolated material, samples of 0.75 mg $mL^{-1}$ polymer dissolved in PBS were analyzed for NO release under ambient conditions (room temperature exposed to ambient light). The representative real-time NO release profile (Figure 2.5) shows, under these specific conditions, that the *S*-nitrosated dextran-cysteamine releases NO over a period of approximately 45 min. After reaching baseline, a total release of 0.036 ± 0.016 NO $g^{-1}$ was recorded (n>3).

UV-vis spectroscopy was employed to verify RSNO incorporation in the polymers both before and after NO release analysis. Representative spectra (Figure 2.6) show that after nitrosation the polymer exhibits a peak at approximately 335 nm characteristic of nitrosothiol product formation. After NO analysis of the polymer, the peak decays nearly completely indicating the nitrosation process is indeed nitrosating the thiol groups and the NO release observed is coming from decay of these groups.

Using these three techniques (Ellman's assay, NO analysis and UV-vis), reproducibility between batches can be assessed to control for the quality of the samples that are subsequently used for the studies described in the remainder of this dissertation.

**Table 2.1.** Thiol content obtained via Ellman's assay and NO recovery obtained via NOA associated with thiolated dextran-cysteamine. Measurements are reported as the average ± standard deviation of $n \geq 3$ trials.

| Thiol Group | Thiol content (mmol $mg^{-1}$) | NO recovery (mmol $g^{-1}$) | % NO recovery (vs. thiol content) |
|---|---|---|---|
| Cysteamine | 0.163 ± 0.040 | 0.034 ± 0.016 | 21% |

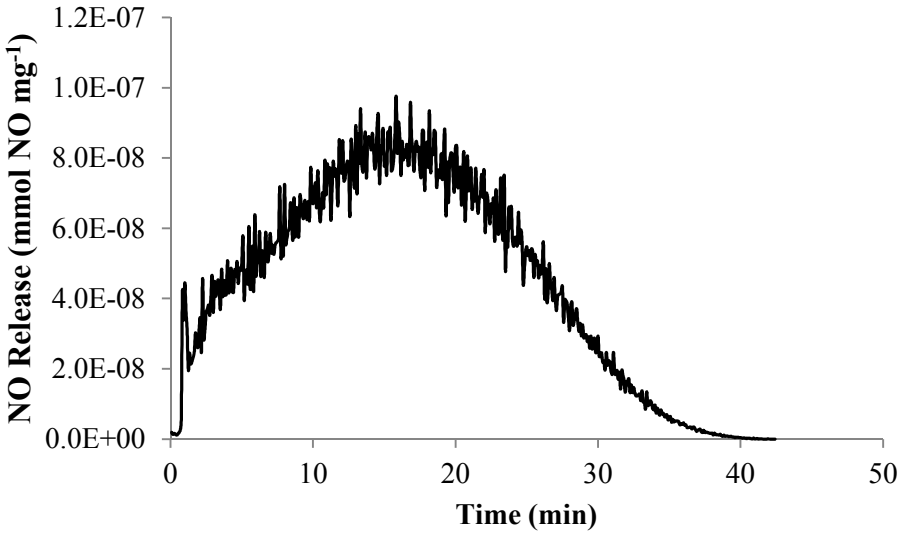


**Figure 2.5.** Representative real-time NO release profile of *S*-nitrosated dextran-cysteamine (0.75 mg $mL^{-1}$ polymer in PBS, pH 7.4, 37°C)

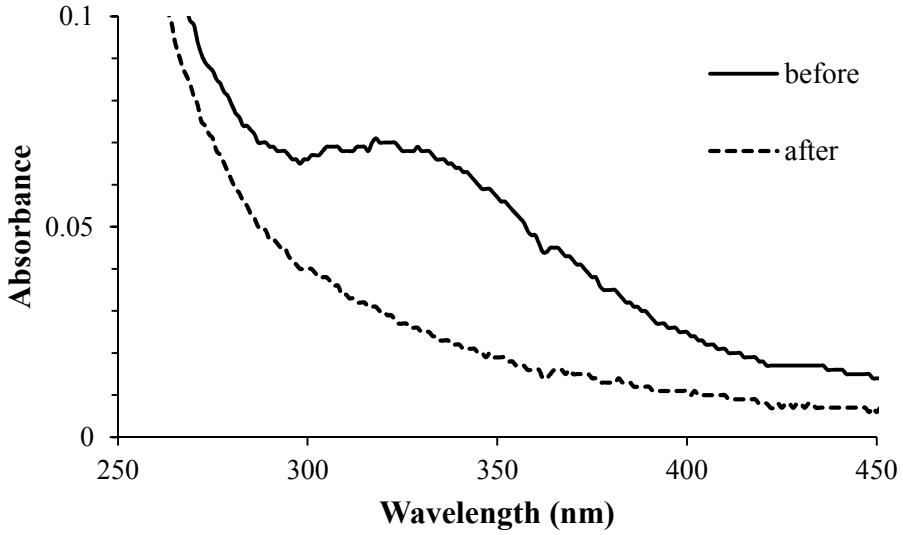


**Figure 2.6.** Representative UV-vis spectra for the *S*-nitrosated dextran-cysteamine derivative before and after NO analysis (0.75 mg $mL^{-1}$).

### 2.8.2 S-nitrosated PLGH derivatives

The synthesis and characterization of the thiolated and nitrosated PLGH polymer derivatives was reported in the publication describing the characterization of these materials.[47]

Thiol incorporation and NO recovery values are reproduced in Table 2.2 for the three different polymer derivatives. To record NO recovery from the *S*-nitrosated PLGH polymer derivatives polymer films (mass  4–6 mg, thickness  10 mm) were prepared on pre-cleaned glass slides by spin-coating the corresponding polymers dissolved in anhydrous dichloromethane and protected from light.

NO release profiles over 48 h, as well as the initial 5 h, are shown in Figure 2.7. For comparison, NO flux associated with the natural endothelium are included (EC, $0.5 \times 10^{-10}$ mol $cm^{-2}$ $min^{-1}$).[50] The homocysteine derivative NO release is characterized by a steady increase in the release of NO within the first hour, followed by a nearly steady decline in NO release to below that of the EC. The flux of homocysteine remains significantly lower than that of cysteine or cysteamine past the first hour of analysis, indicating a greater stability of the S-nitrosated homocysteine moiety. The behavior of the cysteine and cysteamine derivatives is significantly different from this trend as both polymers release an increasing NO flux for the first hour, followed by a gradual decay over the remaining 48 h. For both polymer derivatives, at nearly 25 h, the NO flux reaches below the EC. It is interesting to note that the cysteine derivative presented a characteristic exponential decay for over 70 h at a greater flux than cysteamine, indicating the S-nitrosated cysteine is the least stable RSNO form. The characteristic and controlled NO release profiles associated with the cysteine and cysteamine derivatives may be an added advantage in designing particular biomedical devices, where an initial set-state release is desirable.

**Table 2.2.** Thiol content obtained via Ellman's assay and NO recovery obtained via NOA associated with thiolated PLGH derivatives. Measurements are reported as an average ± standard deviation of $n \geq 3$ trials.

| Thiol Group | Thiol content [a] (mmol $mg^{-1}$) | NO recovery [a] (mmol $g^{-1}$) | % NO recovery (vs. thiol content) |
|---|---|---|---|
| Cysteamine | 0.57 ± 0.03 | 0.241 ± 0.004 | 42% |
| Cysteine | 0.39 ± 0.02 | 0.155 ± 0.009 | 29% |
| Homocysteine | 0.18 ± 0.05 | 0.033 ± 0.007 | 18% |

[a] previously published material [47]

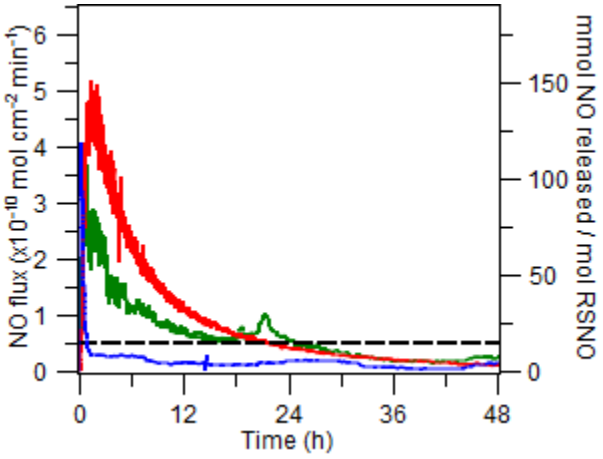


**Figure 2.7.** Representative real-time NO release profile from individual S-nitrosated polymers (homocysteine in blue, cysteine in red, and cysteamine in green; 10 mM PBS/pH 7.4/37 °C) over 48 h. For comparison, the lower-limit NO flux released by natural endothelial cells is indicated by the black dashed line.

### 2.8.3 Degradation

The biodegradation properties are important toward the final application of the material; therefore, it was necessary to investigate the effect of the thiol incorporation on the rate of degradation. In vitro polymer degradation proceeded via hydrolysis of the polymer linkages and degradation rates were evaluated gravimetrically during a PBS soak of the respective polymer (pH 7.4, 37 °C). Results of polymer degradation over 6 weeks are represented in Figure 2.8.

Linear extrapolation of the decomposition rate predicts complete degradation of the material over nearly 40 weeks for PLGH-cysteamine, 30 weeks for PLGH-cysteine, and 20 weeks for PLGH and PLGH-homocysteine polymer derivatives. This degradation profile will be an important prerequisite for using these materials for biomedical applications, which require a predictable and extended mechanical support without being a permanent implant.

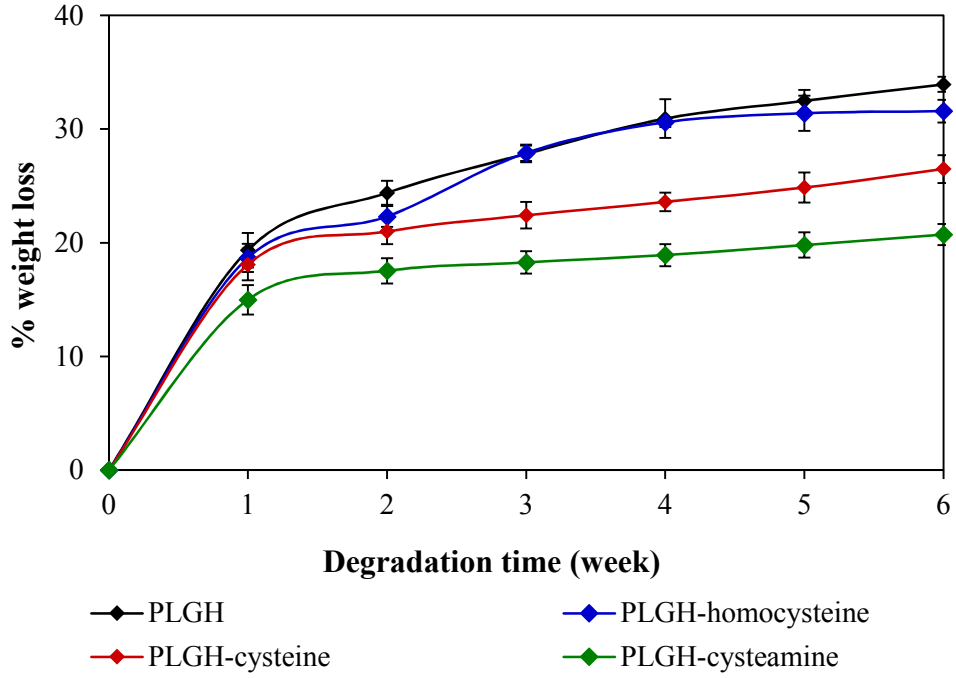


**Figure 2.8.** In vitro degradation profile of the thiol-modified PLGH polymers in 10 mM PBS (pH 7.4, 37 °C).

Degradation studies were performed under the same conditions for the S-nitrosated polymer derivatives. The percent weight loss after the first week was found to be 16 ± 1%, 17 ± 1%, and 19 ± 1% for S-nitrosated cysteamine, cysteine, and homocysteine derivatives, respectively. However, this extent of polymer degradation after the initial week was found to be not significantly different from that of the respective non-nitrosated thiolated polymers at a 95% confidence level. Moreover, because of the very short half-life of the NO moiety, as well as the periodic exchange of the buffer solution during the degradation, we come to the conclusion that

the remaining degradation profile of these polymers tends to follow the same pattern as that of the non-nitrosated parent thiol polymers.

### 2.8.4 Cytotoxicity

A preliminary biocompatibility evaluation of thiolated PLGH polymers was performed by NAMSA using the ISO 10993-5 cytotoxicity elution method. Following the extraction study, the degree of cell lysis for each polymer sample was evaluated on a scale of 0 to 4, where a score of 0 corresponded to 0% cell lysis and a score of 4 corresponded to complete destruction of the cellular layers. In these tests, all thiolated PLGH polymers received a score of 0, which corresponds to no cytotoxicity, cell lysis or reduction of cell growth associated with the polymer material. By comparison, the negative control polymer received a score of 0 and the positive control polymer received a score of 4. This preliminary cytotoxicity evaluation suggested the absence of observed cytotoxicity associated with the degradation products of the thiolated PLGH polymers, a critical requirement for use of polymer materials in the body.

## 2.9 Conclusion

This chapter detailed the synthesis and extensive characterization involved in the development of the two *S*-nitrosated biodegradable polymer systems used throughout the experiments in the chapters to follow. The close monitoring of NO release characteristics from these polymers is crucial to understanding the biological effects seen when exposing them at various concentrations to cells and bacteria. All *S*-nitrosated polymer derivatives exhibit high levels of initial NO release, followed by a taper to lower, sustained release. These profile characteristics are analogous to the observed NO production by cells in a healthy wound

environment, indicating promise for the incorporation of these material systems in wound treatment and management systems.

REFERENCES


1. Ulery, B. D.; Nair, L. S.; Laurencin, C. T., Biomedical applications of biodegradable polymers. *Journal of Polymer Science Part B: Polymer Physics* **2011,** 49, (12), 832-864.

2. Kroeze, R.; Helder, M.; Govaert, L.; Smit, T., Biodegradable Polymers in Bone Tissue Engineering. *Materials* **2009,** 2, (3), 833-856.

3. Navarro, M.; Michiardi, A.; Castaño, O.; Planell, J. A., Biomaterials in orthopaedics. *Journal of The Royal Society Interface* **2008,** 5, (27), 1137-1158.

4. Coulembier, O.; Degée, P.; Hedrick, J. L.; Dubois, P., From controlled ring-opening polymerization to biodegradable aliphatic polyester: Especially poly([beta]-malic acid) derivatives. *Progress in Polymer Science* **2006,** 31, (8), 723-747.

5. Kumbar, S. G.; Nukavarapu, S. P.; James, R.; Nair, L. S.; Laurencin, C. T., Electrospun poly(lactic acid-co-glycolic acid) scaffolds for skin tissue engineering. *Biomaterials* **2008,** 29, (30), 4100-4107.

6. Nair, L. S.; Bhattacharyya, S.; Bender, J. D.; Greish, Y. E.; Brown, P. W.; Allcock, H. R.; Laurencin, C. T., Fabrication and Optimization of Methylphenoxy Substituted Polyphosphazene Nanofibers for Biomedical Applications. *Biomacromolecules* **2004,** 5, (6), 2212-2220.

7. Nukavarapu, S. P.; Kumbar, S. G.; Brown, J. L.; Krogman, N. R.; Weikel, A. L.; Hindenlang, M. D.; Nair, L. S.; Allcock, H. R.; Laurencin, C. T., Polyphosphazene/Nano-Hydroxyapatite Composite Microsphere Scaffolds for Bone Tissue Engineering. *Biomacromolecules* **2008,** 9, (7), 1818-1825.

8. Su, Q.; Zhao, A.; Peng, H.; Zhou, S., Preparation and Characterization of Biodegradable Electrospun Polyanhydride Nano/Microfibers. *Journal of Nanoscience and Nanotechnology* **2010,** 10, (10), 6369-6375.

9. Betz, M. W.; Modi, P. C.; Caccamese, J. F.; Coletti, D. P.; Sauk, J. J.; Fisher, J. P., Cyclic acetal hydrogel system for bone marrow stromal cell encapsulation and osteodifferentiation. *Journal of Biomedical Materials Research Part A* **2008,** 86A, (3), 662-670.

10. Welle, A.; Kröger, M.; Döring, M.; Niederer, K.; Pindel, E.; Chronakis, I. S., Electrospun aliphatic polycarbonates as tailored tissue scaffold materials. *Biomaterials* **2007,** 28, (13), 2211-2219.

11. Macario, D. K.; Entersz, I.; Bolikal, D.; Kohn, J.; Nackman, G. B., Iodine inhibits antiadhesive effect of PEG: Implications for tissue engineering. *Journal of Biomedical Materials Research Part B: Applied Biomaterials* **2008,** 86B, (1), 237-244.

12. Asai, T.; Lee, M.-H.; Arrecubieta, C.; von Bayern, M. P.; Cespedes, C. A.; Baron, H. M.; Cadeiras, M.; Sakaguchi, T.; Marboe, C. C.; Naka, Y.; Deng, M. C.; Lowy, F. D., Cellular coating of the left ventricular assist device textured polyurethane membrane reduces adhesion of Staphylococcus aureus. *The Journal of Thoracic and Cardiovascular Surgery* **2007,** 133, (5), 1147-1153.

13. Uttayarat, P.; Perets, A.; Li, M.; Pimton, P.; Stachelek, S. J.; Alferiev, I.; Composto, R. J.; Levy, R. J.; Lelkes, P. I., Micropatterning of three-dimensional electrospun polyurethane vascular grafts. *Acta Biomaterialia* **2010,** 6, (11), 4229-4237.

14. Smith, B. S.; Yoriya, S.; Grissom, L.; Grimes, C. A.; Popat, K. C., Hemocompatibility of titania nanotube arrays. *Journal of Biomedical Materials Research Part A* **2010,** 95A, (2), 350-360.

15. Stevens, M. M., Biomaterials for bone tissue engineering. *Materials Today* **2008,** 11, (5), 18-25.

16. Furchgott, R. F., Endothelium-Derived Relaxing Factor: Discovery, Early Studies, and Identifcation as Nitric Oxide (Nobel Lecture). *Angewandte Chemie International Edition* **1999,** 38, (13-14), 1870-1880.

17. Ignarro, L. J.; Buga, G. M.; Wood, K. S.; Byrns, R. E.; Chaudhuri, G., Endothelium-derived relaxing factor produced and released from artery and vein is nitric oxide. *Proceedings of the National Academy of Sciences of the United States of America* **1987,** 84, (24), 9265-9269.

18. Luque Contreras, D.; Vargas Robles, H.; Romo, E.; Rios, A.; Escalante, B., The role of nitric oxide in the post-ischemic revascularization process. *Pharmacology & Therapeutics* **2006,** 112, (2), 553-563.

19. Gallo, O.; Fini-Storchi, I.; Vergari, W. A.; Masini, E.; Morbidelli, L.; Ziche, M.; Franchi, A., Role of Nitric Oxide in Angiogenesis and Tumor Progression in Head and Neck Cancer. *Journal of the National Cancer Institute* **1998,** 90, (8), 587-596.

20. Isenberg, J. S.; Ridnour, L. A.; Espey, M. G.; Wink, D. A.; Roberts, D. D., Nitric oxide in wound-healing. *Microsurgery* **2005,** 25, (5), 442-451.

21. Hill, B. G.; Dranka, B. P.; Bailey, S. M.; Lancaster, J. R.; Darley-Usmar, V. M., What Part of NO Don't You Understand? Some Answers to the Cardinal Questions in Nitric Oxide Biology. *Journal of Biological Chemistry* **2010,** 285, (26), 19699-19704.

22. Massion, P. B.; Feron, O.; Dessy, C.; Balligand, J.-L., Nitric Oxide and Cardiac Function: Ten Years After, and Continuing. *Circulation Research* **2003,** 93, (5), 388-398.

23. Radomski, M. W., Nitric Oxide: Biological Mediator, Modulator and Effector. *Annals of Medicine* **1995,** 27, (3), 321-329.

24. Isenberg, J. S.; Ridnour, L. A.; Espey, M. G.; Wink, D. A.; Roberts, D. A., Nitric oxide in wound-healing. *Microsurgery* **2005,** 25, (5), 442-451.

25. Rizk, M.; Witte, M. B.; Barbul, A., Nitric Oxide and Wound Healing. *World Journal of Surgery* **2004,** 28, (3), 301-306.

26. Wang, P. G.; Xian, M.; Tang, X.; Wu, X.; Wen, Z.; Cai, T.; Janczuk, A. J., Nitric Oxide Donors: Chemical Activities and Biological Applications. *Chemical Reviews* **2002,** 102, (4), 1091-1134.

27. Al-Sa'doni, H.; Ferro, A., S-Nitrosothiols: a class of nitric oxide-donor drugs. *Clinical Science* **2000,** 98, 507-520.

28. Szaciłowski, K.; Stasicka, Z., S-NITROSOTHIOLS: MATERIALS, REACTIVITY AND MECHANISMS. *Progress in Reaction Kinetics and Mechanism* **2001,** 26, 1-58.

29. Williams, D. L. H., The Chemistry of S-Nitrosothiols. *Accounts of Chemical Research* **1999,** 32, (10), 869-876.

30. Mowery, K. A.; H. Schoenfisch, M.; Saavedra, J. E.; Keefer, L. K.; Meyerhoff, M. E., Preparation and characterization of hydrophobic polymeric films that are thromboresistant via nitric oxide release. *Biomaterials* **2000,** 21, (1), 9-21.

31. Coneski, P. N.; Schoenfisch, M. H., Synthesis of nitric oxide-releasing polyurethanes with S-nitrosothiol-containing hard and soft segments. *Polymer Chemistry* **2011,** 2, (4), 906-913.

32. Zhao, H.; Serrano, M. C.; Popowich, D. A.; Kibbe, M. R.; Ameer, G. A., Biodegradable nitric oxide-releasing poly(diol citrate) elastomers. *Journal of Biomedical Materials Research Part A* **2010,** 93A, (1), 356-363.

33. Parzuchowski, P. G.; Frost, M. C.; Meyerhoff, M. E., Synthesis and Characterization of Polymethacrylate-Based Nitric Oxide Donors. *Journal of the American Chemical Society* **2002,** 124, (41), 12182-12191.

34. Smith, D. J.; Chakravarthy, D.; Pulfer, S.; Simmons, M. L.; Hrabie, J. A.; Citro, M. L.; Saavedra, J. E.; Davies, K. M.; Hutsell, T. C.; Mooradian, D. L.; Hanson, S. R.; Keefer, L. K., Nitric Oxide-Releasing Polymers Containing the [N(O)NO]- Group. *Journal of Medicinal Chemistry* **1996,** 39, (5), 1148-1156.

35. Seabra, A. B.; Martins, D.; Simões, M. M.; Da Silva, R.; Brocchi, M.; De Oliveira, M. G., Antibacterial Nitric Oxide-Releasing Polyester for the Coating of Blood-Contacting Artificial Materials. *Artificial Organs* **2010,** 34, (7), E204-E214.

36. Jun, H.-W.; Taite, L. J.; West, J. L., Nitric Oxide-Producing Polyurethanes. *Biomacromolecules* **2005,** 6, (2), 838-844.

37. Coneski, P. N.; Rao, K. S.; Schoenfisch, M. H., Degradable Nitric Oxide-Releasing Biomaterials via Post-Polymerization Functionalization of Cross-Linked Polyesters. *Biomacromolecules* **2010,** 11, (11), 3208-3215.

38. Zhao, H. C.; Serrano, M. C.; Popowich, D. A.; Kibbe, M. R.; Ameer, G. A., Biodegradable nitric oxide-releasing poly(diol citrate) elastomers. *Journal of Biomedical Materials Research Part A* **2010,** 93A, (1), 356-363.

39. Wang, Y.; Kibbe, M. R.; Ameer, G. A., Photo-crosslinked biodegradable elastomers for controlled nitric oxide delivery. *Biomaterials Science* **2013,** 1, (6), 625-632.

40. Coneski, P. N.; Schoenfisch, M. H., Nitric oxide release: Part III. Measurement and reporting. *Chemical Society Reviews* **2012,** 41, (10), 3753-3758.

41. Lu, Y.; Slomberg, D. L.; Schoenfisch, M. H., Nitric oxide-releasing chitosan oligosaccharides as antibacterial agents. *Biomaterials* **2014,** 35, (5), 1716-1724.

42. Gentile, P.; Chiono, V.; Carmagnola, I.; Hatton, P. V., An Overview of Poly(lactic-co-glycolic) Acid (PLGA)-Based Biomaterials for Bone Tissue Engineering. *International Journal of Molecular Sciences* **2014,** 15, (3), 3640-3659.

43. Danhier, F.; Ansorena, E.; Silva, J. M.; Coco, R.; Le Breton, A.; Preat, V., PLGA-based nanoparticles: An overview of biomedical applications. *Journal of Controlled Release* **2012,** 161, (2), 505-522.

44. Ratner, B. D.; Hoffman, A. S.; Schoen, F. J.; Lemons, J. E., Biomaterials Science - An Introduction to Materials in Medicine (2nd Edition). In Elsevier.

45. Damodaran, V. B.; Reynolds, M. M., Biodegradable S-nitrosothiol tethered multiblock polymer for nitric oxide delivery. *Journal of Materials Chemistry* **2011,** 21, (16), 5870-5872.

46. Damodaran, V. B.; Place, L. W.; Kipper, M. J.; Reynolds, M. M., Enzymatically degradable nitric oxide releasing S-nitrosated dextran thiomers for biomedical applications. *Journal of Materials Chemistry* **2012,** 22, (43), 23038-23048.

47. Damodaran, V. B.; Joslin, J. M.; Wold, K. A.; Lantvit, S. M.; Reynolds, M. M., S-Nitrosated biodegradable polymers for biomedical applications: synthesis, characterization and impact of thiol structure on the physicochemical properties. *Journal of Materials Chemistry* **2012,** 22, (13), 5990-6001.

48. Joslin, J. M.; Damodaran, V. B.; Reynolds, M. M., Selective nitrosation of modified dextran polymers. *Rsc Advances* **2013,** 3, (35), 15035-15043.

49. Ellman, G. L., TISSUE SULFHYDRYL GROUPS. *Archives of Biochemistry and Biophysics* **1959,** 82, (1), 70-77.

50. Vaughn, M. W.; Kuo, L.; Liao, J. C., Estimation of nitric oxide production and reaction rates in tissue by use of a mathematical model. *American Journal of Physiology-Heart and Circulatory Physiology* **1998,** 274, (6), H2163-H2176.

# CHAPTER 3:

# BACTERICIDAL ACTIVITY OF MACROMOLECULAR NITRIC OXIDE RELEASING POLYMERS

Health-care associated infections (HAIs) are a costly and a persistent problem worldwide.[1] Although the number of HAIs has been reduced by using improved sterilization protocols, the costs related to HAIs are still quantified in billions of dollars.[2, 3] The quest for new methods to eradicate bacterial infection is, therefore, increasingly important in antimicrobial, drug delivery and biomaterials research. Herein, the antibacterial properties of an NO releasing *S*-nitrosated dextran-cysteamine polymer against *Escherichia coli, Acinetobacter baumannii,* and *Staphylococcus aureus* and the polymer's NO release characteristics in broth media were evaluated. Under these experimental conditions, the minimum dosage required to induce over 7-log reductions over 24 h for the three bacteria strains varied between 7.5 to 20 mg $mL^{-1}$, indicating the need of tuning dosages depending on the strains present on the infected area. The over 7-log reduction in bacterial survival over 24 h presented here is among the highest reduction reported to date using a NO delivery system. In addition, no recovery of bacteria activity was observed in that period of time suggesting that this delivery system is a promising route for further reduction of HAIs. I developed protocol for and carried out the bactericidal assays described herein in addition to synthesizing and characterizing the *S*-nitrosated dextran-cysteamine polymer and its derivatives.

Results intended for publication as Wold, K.A.; Pegalajar-Jurado, D.; Joslin, J.M.; Arabea, K.; Suazo, L.A; McDaniel, S.L.; Bowen, R.; Reynolds, M.M. 7-log bacterial reduction using a nitric oxide-releasing polysaccharide derivative. *Molecular Pharmaceutics*

## 3.1 Introduction

In 2009, the estimated cost of all health-care associated infections (HAIs) in the U.S. was $45 billion which corresponded to 1,737,125 cases.[4] The most recent report for HAIs showed an estimated 722,000 events for 2011.[5] Although a reduction of approximately 60% has been observed over that time span, the number of patients affected remains significant with an annual cost on the order of billions of dollars. The quest for new methods to eradicate bacterial infection is, therefore, crucial in antimicrobial, drug delivery and biomaterials research. Recent approaches for developing biocidal agents and materials have found inspiration in nature. For instance, peptides are being widely exploited for their bactericidal properties.[6-8] Both natural and synthetic versions can kill bacteria with reductions as high as 6-log,[9] and can be effective against drug resistant bacteria such as methicillin-resistant *Staphylococcus aureus* (MRSA).[10, 11] Alternatively, nitric oxide (NO) has also captured the attention of the scientific community as a potent and non-specific antibacterial agent as it is a natural broad-spectrum antimicrobial agent. In addition, the development of bacterial resistance to NO is unlikely as the molecule is involved in natural mammalian immune defense.[12] However NO can be difficult to deliver to infection sites, therefore material systems have been devised to store and deliver localized NO.[13-22] NO release from these materials has been shown to be effective against gram-positive and gram-negative bacteria in planktonic and biofilm forms. Despite efforts toward developing effective antimicrobial materials, only a few polymeric biomaterials to date have exhibited bacterial reductions greater than 6-log.[23] NO releasing materials, however, have shown recent promise in their potential to achieve high levels of bactericidal activity, with high log reductions achieved *in vitro*.[24] Neidrauer *et al*. recorded high kill rates using an NO-releasing zinc-exchanged zeolite emulsified in ointment, albeit using a high concentration of 100 mg NO-releasing ointment per

mL bacteria medium. This leaves room for further research into other NO-releasing material systems capable of similar kill rates at lower dosages.

Herein, we evaluate the activity of water soluble *S*-nitrosated dextran-cysteamine against planktonic gram-negative *Escherichia coli* (*E. coli*) and *Acinetobacter baumannii* (*A. baumannii*) as well as gram-positive *Staphylococcus aureus* (*S. aureus*) over 24 h. Bactericidal results were determined using a time kill-rate approach. Positive bacteria, dextran and non-nitrosated dextran-cysteamine polymers were used as controls to verify the impact of NO release independent of the material system on bactericidal activity. In addition, the NO release capability of the material system in broth media was evaluated to link the log reduction observed to the NO delivery.

## 3.2 Experimental

### 3.2.1 S-nitrosated dextran-cysteamine derivative

The synthesis of *S*-nitrosated dextran cysteamine has been previously reported.[25, 26] Briefly, dextran was modified with a carboxymethyl group using monochloroacetic acid. The resulting carboxymethylated dextran (CM-dextran) was conjugated with the amine group cysteamine to create the thiolated derivative dextran-cysteamine. As a final step, the cysteamine group was nitrosated using *t*-butyl nitrate to yield the *S*-nitrosated dextran-cysteamine derivative. Structural and morphological properties of the intermediate and finished products were characterized using $^{1}$H NMR and compared with our previous published results (Varian NMR Systems, Palo Alto, CA, USA).[26] Thiol content was determined using the Ellman's assay (BioTek Synergy 2 plate reader Biotek, Winooski, VT, USA). The *S*-nitrosothiol content was analyzed via UV-vis spectroscopy (Nicolet Evolution 300 spectrometer, Thermo Electron Corporation, Madison, WI, USA) for material dissolved in phosphate buffer at 0.75 mg mL$^{-1}$ to ensure reproducibility

between different material batches. The molar extinction coefficient was used to determine the *S*-nitrosothiol content, as described elsewhere.[25]

### 3.2.2 Real-time NO analysis

Sievers chemiluminescence NO analyzers® (NOA 280i, GE Analytical, Boulder, CO, USA) were used to obtain the real-time NO release from *S*-nitrosated dextran-cysteamine. A modified version of a previously described procedure was used.[27] In summary, NO release was measured over 24 h by shielding the samples from direct exposure to light in nutrient broth (pH 7.4) at 37 °C. Measurements were recorded in triplicate.

### 3.2.3 Bacteria preparation

*Escherichia coli* (*E. coli*, ATCC 25922) and *Staphylococcus aureus* (*S. aureus,* ATCC 29213) were purchased from American Type Culture Collection (ATCC, USA). The *Acinetobacter baumannii* (*A. baumannii*) used is a clinical isolate provided by Herbert Schweizer. Lyophilized bacteria were reconstituted in Oxoid Nutrient Broth (OXCM0001B) and grown overnight with shaking at 37 °C and 100 rpm. The overnight culture was diluted 1:1 using a glycerol solution (30 % v $v^{-1}$) and stored at -80 °C. Prior to each experiment, a tube of bacteria was thawed and centrifuged at 4500 rpm for 20 min to collect a pellet. The pellet was re-suspended in nutrient broth and incubated overnight. The overnight culture was diluted with fresh warm nutrient broth to $O.D_{600nm}$ ~ 0.1 and incubated (37 ºC at 100 rpm) until it reached the logarithmic growth phase ($O.D_{600nm}$ ~ 0.3). The bacteria solution was used in the bacterial assays.

### 3.2.4 Time-kill bactericidal assay

The bactericidal activity of the *S*-nitrosated dextran-cysteamine was assessed according to a modified method based on National Committee for Clinical Laboratory Standards guidelines described previously.[28, 29] All antibacterial activity assays were performed in nutrient broth in

order to better reproduce *in vivo* conditions compared to using phosphate buffered saline (PBS), or other low-nutrient systems, which provide stagnant conditions for bacteria survival but not growth.

Aliquots of the bacterial solution ($O.D._{600nm}$ ~0.3) were added to 20 mL amber EPA vials (EnviroWare, Fisher Scientific, Fair Lawn, NJ, USA) containing polymer samples. Bacteria were added at concentrations necessary for diluting the polymer samples to the necessary concentration, between 7.5 and 20 mg polymer per mL bacterial culture. Four different sample groups were studied: (1) bacteria + dextran, (2) bacteria + dextran-cysteamine, (3) bacteria + *S*-nitrosated dextran-cysteamine and (4) positive control (bacteria in the absence of polymer). Vials were vortexed for 20 s to disperse the polymer and incubated in a shaking incubator at 37 ºC and 100 rpm. At 2, 4 and 24 h, 100 µL aliquots of the samples were removed for the assessment of colony forming units per mL (CFU $mL^{-1}$). CFU $mL^{-1}$ was calculated by performing between zero and seven 10-fold serial dilutions on the sample aliquot and plating 50 µL of diluted solution onto agar plates prepared with Oxoid Nutrient Agar (OXCM0003B). Plates were incubated in static conditions overnight and CFUs were counted the next day. CFU $mL^{-1}$ was calculated using Equation 1. For plates containing no CFUs, the number of CFUs was estimated as 0.5 in order to perform the calculations. As 50 µL of each undiluted sample was plated, the minimum detectible level of bacteria is 10 CFU $mL^{-1}$.

$$CFU\ mL^{-1} = \frac{\#\ CFU}{dilution\ factor * volume\ plated} \qquad (1)$$

### 3.2.5 Bactericidal Calculations

The CFU $mL^{-1}$ for the positive control was used to determine the log reduction of viable cells in each sample at each time point. The fraction of bacteria surviving and log reduction in the

polymer-containing samples were calculated using Equation (2) and (3). All experiments were performed in triplicate (n ≥ 9). Data are reported as mean ± standard deviation.

$$Survival\ fraction = \frac{CFU\ mL^{-1}\ after\ treatment}{CFU\ mL^{-1}\ in\ control\ sample} \quad (2)$$

$$Log\ reduction\ =\ log_{10}\ (1 * survival\ fraction^{-1}) \quad (3)$$

### 3.3 Results

The purpose of this study was to assess the bactericidal potential of a polysaccharides derivate, *S*-nitrosated dextran-cysteamine, and determine minimum dosages necessary to exhibit industrially relevant bactericidal reduction (7-log or higher) against gram-positive and gram-negative bacteria. In addition, we aim to correlate the bactericidal effect achieved to the amount of NO delivered under experimental conditions which strive to mimic more closely the physiological environment. Synthesis and characterization of the *S*-nitrosated dextran-cysteamine derivative has been previously reported by our team[26] however the potential bactericidal activity of the material was not assessed at that time.

#### 3.3.1 Nitric oxide release in broth media

To correlate the exact amount of NO release under biological experimental conditions (i.e. nutrient broth), the NO release profile of the polysaccharide derivative, *S*-nitrosated dextran-cysteamine, was obtained in the presence of nutrient broth. For this study, the NO release profile of *S*-nitrosated dextran-cysteamine was evaluated in nutrient broth at a concentration of 15 mg $mL^{-1}$. Results are shown in Figure 1a. NO was rapidly released from the polymer, exhibiting maximum instantaneous release 29.9 ± 2.4 nmol $mL^{-1}$, and the NO profiles shows that the majority of NO was released after 10 h. Over 24 h, the polysaccharide derivative released 49.5 ±

5.0 μmol $g^{-1}$ NO (Figure 1b), after which time the NO release capabilities of the material were completely extinguished by allowing the instrument to return to baseline (Figure 1b).

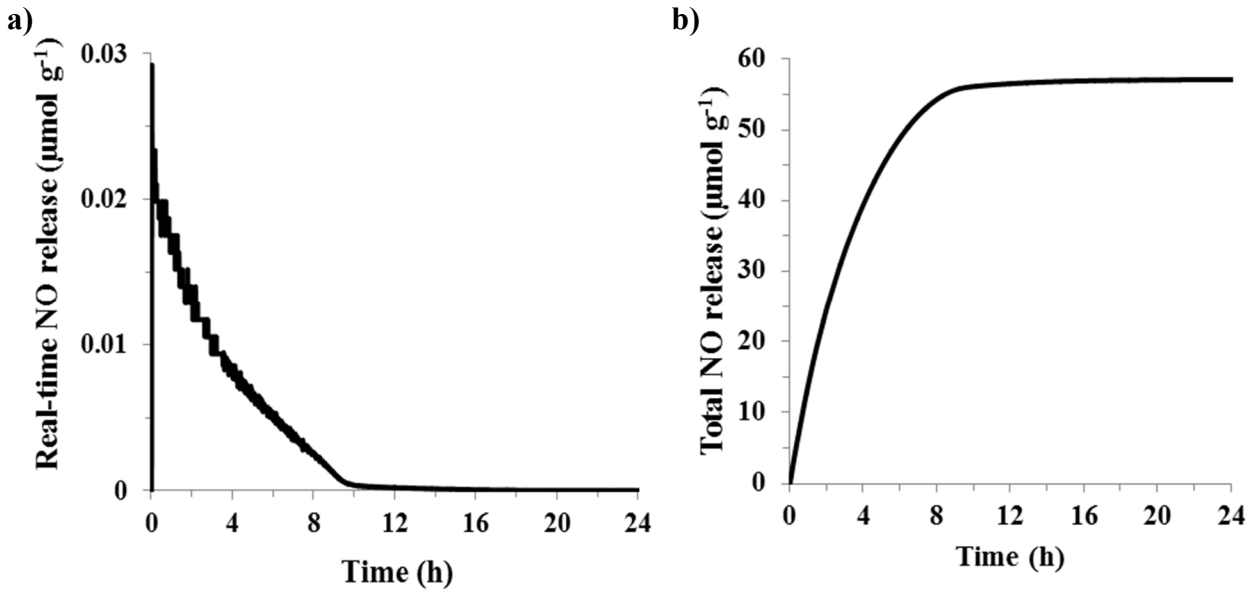


**Figure 1.** (a) Representative real-time NO release profile and (b) cumulative NO release from 15 mg $mL^{-1}$ *S*-nitrosated dextran-cysteamine in broth media (37 °C) over 24 h.

### 3.3.2 Time-kill bactericidal assays

The biocidal activity of the polysaccharide derivative was tested against Gram-negative *E. coli* and *A. baumannii,* and gram-positive *S. aureus* and data are presented in Figure 2. Log reductions of bacteria were calculated to represent the difference between NO-treated and control bacteria after 24 h of growth and are shown in Table 1. To isolate the effect of the NO released versus any leachables from intermediate materials on bacterial survival, bacteria were also exposed to dextran and dextran-cysteamine as control experiments. Both control experiments performed using dextran and dextran-cysteamine demonstrated no change in growth characteristics from the positive control sample (*E. coli),* indicating that intermediate materials do not alter *E. coli* bacterial growth. Based on these observations we can infer that dextran and

dextran-cysteamine will neither affect *A. baumannii* nor *S. aureus* bacterial growth. Independently of the bacteria strain tested, each experiment started with $10^8$ CFU $mL^{-1}$ and, in the positive control samples, bacteria grew to a maximum of $10^9$ CFU $mL^{-1}$ over 24 h.

Figure 2a represents the CFU $mL^{-1}$ for *E. coli* exposed to 7.5 mg $mL^{-1}$ and the correspondent positive control. At 2 and 4 h, bacteria reductions were only 1 and 2-log respectively. After 24h of incubation, the number of viable bacterial for samples exposed to NO reached the limit of detection of the technique. The reduction in viable cells observed in comparison to the positive control was a 7-log reduction (Table 1). A similar study was performed using 15 mg $mL^{-1}$ of NO-releasing polymer (Figure 2b); in this case an initial significant reduction in bacterial count was observed after 4h and corresponded to a 6-log reduction. The reduction continued over 24 h reaching an 8-log reduction in viable E. coli when samples were exposed to 15 mg $mL^{-1}$ (Table 1).

The same study was performed using *A. baumannii*, the bacterial solution was exposed to 15 and 20 mg $mL^{-1}$ of NO-releasing polymer (Figure 2c and Figure 2d respectively) showing significant decrease in viable cells after 24 h. A 7-log reduction in viable *A. baumannii* was observed when using 20 mg $mL^{-1}$ after 24 h (Table 1). In terms of *S. aureus*, 15 mg $mL^{-1}$ was needed to reach the limit of detection (Figure 2e) over 24 h which is equivalent to a 7-log reduction (Table 1).

a)

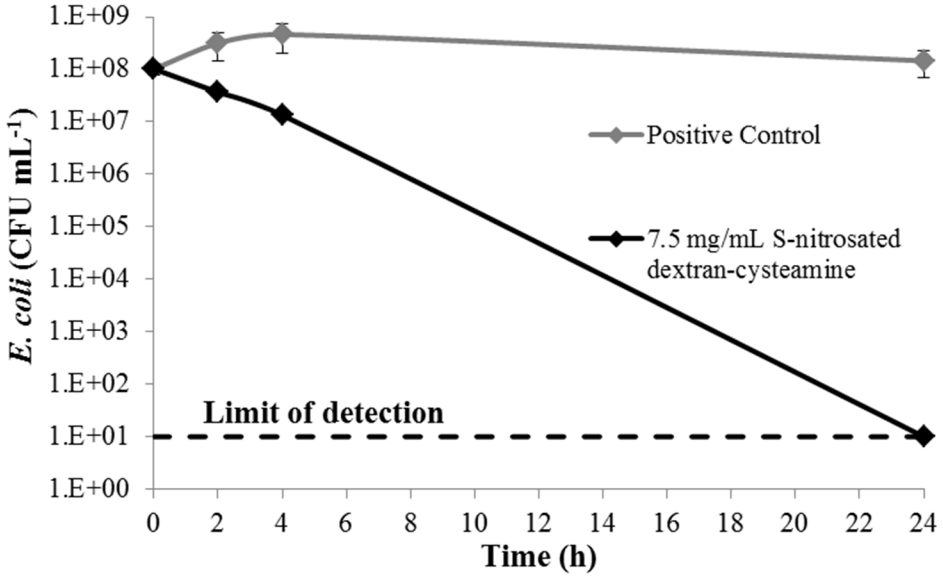
1.E+09
1.E+08
1.E+07
1.E+06
1.E+05
1.E+04
1.E+03
1.E+02
1.E+01
1.E+00
E. coli (CFU mL-1)
Positive Control
7.5 mg/mL S-nitrosated dextran-cysteamine
Limit of detection
0 2 4 6 8 10 12 14 16 18 20 22 24
Time (h)

b)

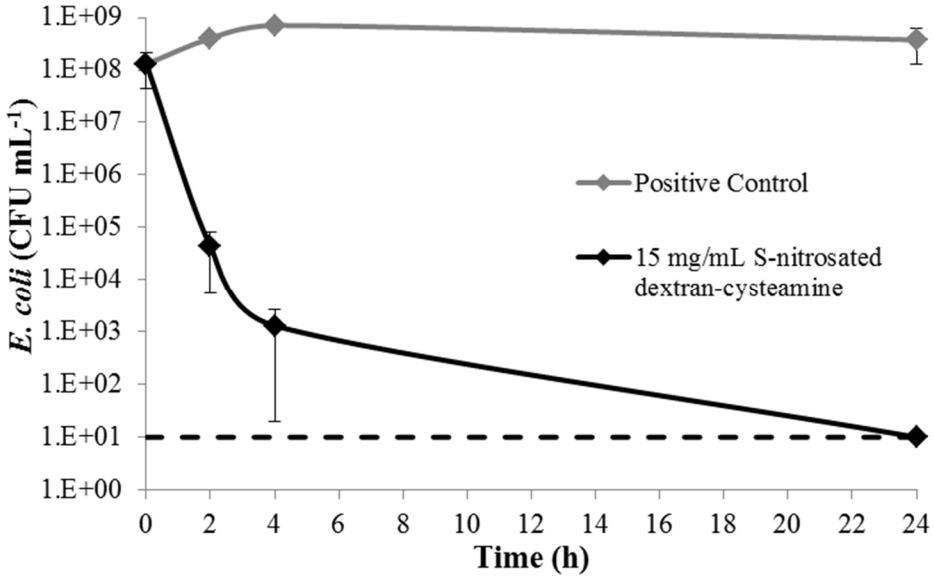
1.E+09
1.E+08
1.E+07
1.E+06
1.E+05
1.E+04
1.E+03
1.E+02
1.E+01
1.E+00
E. coli (CFU mL-1)
Positive Control
15 mg/mL S-nitrosated dextran-cysteamine
0 2 4 6 8 10 12 14 16 18 20 22 24
Time (h)

**c)**

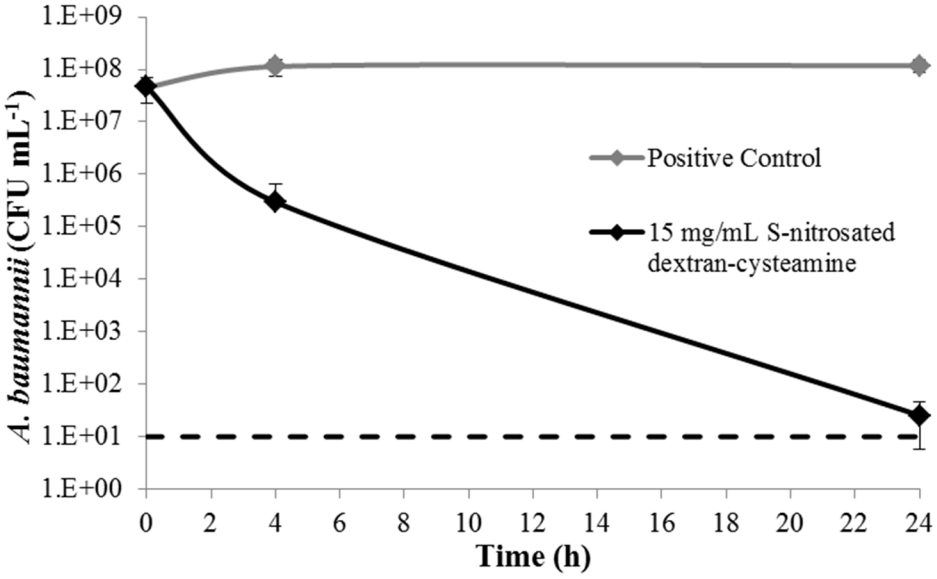
1.E+09
1.E+08
1.E+07
1.E+06
1.E+05
1.E+04
1.E+03
1.E+02
1.E+01
1.E+00
A. baumannii (CFU mL-1)
0
2
4
6
8
10
12
14
16
18
20
22
24
Time (h)
Positive Control
15 mg/mL S-nitrosated dextran-cysteamine

**d)**

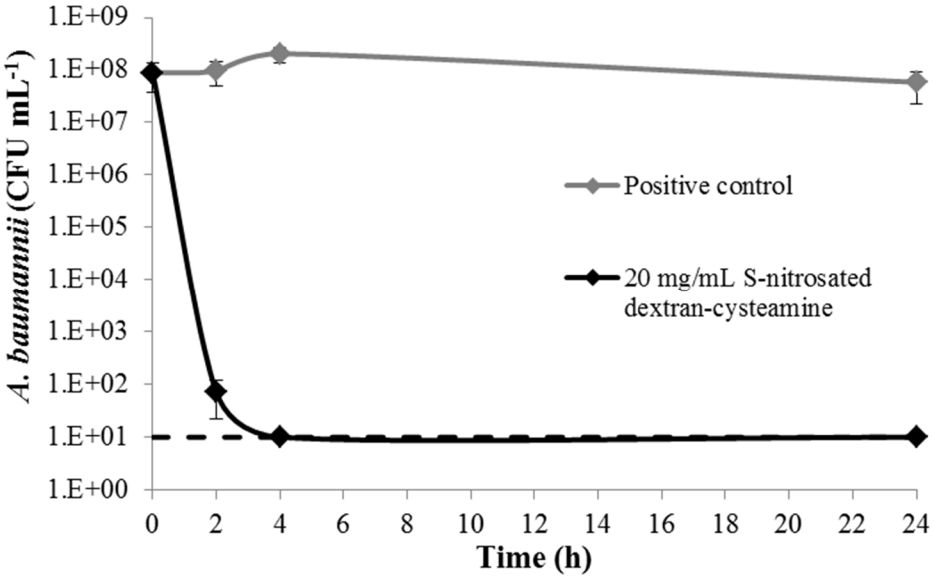
1.E+09
1.E+08
1.E+07
1.E+06
1.E+05
1.E+04
1.E+03
1.E+02
1.E+01
1.E+00
A. baumannii (CFU mL-1)
0
2
4
6
8
10
12
14
16
18
20
22
24
Time (h)
Positive control
20 mg/mL S-nitrosated dextran-cysteamine

e)

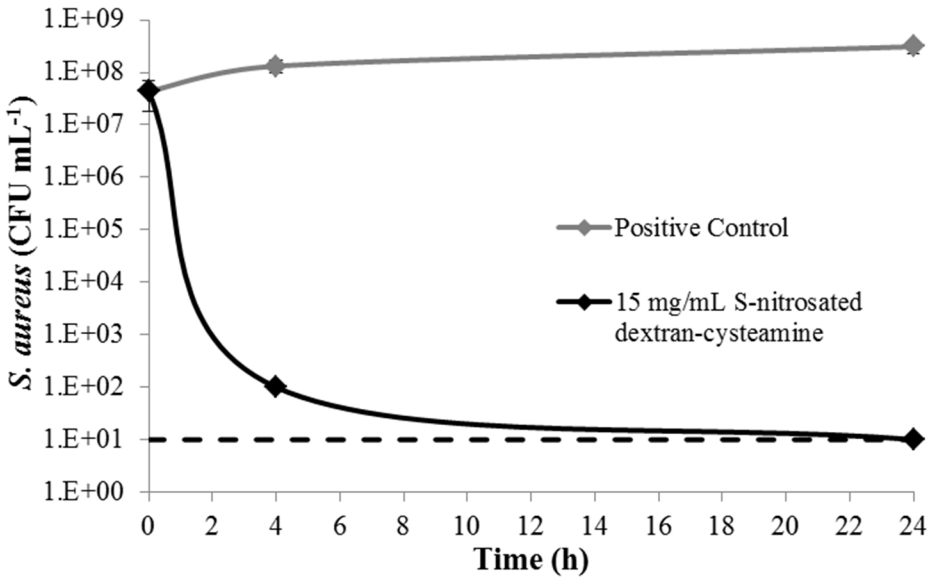


**Figure 2.** Bacterial CFU $mL^{-1}$ over 24 h as determined by time-kill studies for *Escherichia coli* (*E. coli*) (a and b), *Acinetobacter baumannii* (*A. baumannii*) (c and d) and *Staphylococcus aureus* (*S. aureus)* (e); dashed line, lowest detectable limit (10 CFU $mL^{-1}$)

**Table 1.** Log reduction in bacterial colonies after exposure to different concentrations of *S*-nitrosated dextran-cysteamine for 24 h

| Organism | Polymer Concentration (mg $mL^{-1}$) | Log Reduction |
|---|---|---|
| *Escherichia coli* | 15 | 8 |
| *Escherichia coli* | 7.5 | 7 |
| *Acinetobacter baumannii* | 15 | 6 |
| *Acinetobacter baumannii* | 20 | 7 |
| *Staphylococcus aureus* | 15 | 8 |

### 3.4 Discussion

The study reported here highlights the bactericidal potential of a polysaccharide derivate, *S*-nitrosated dextran-cysteamine, and correlated the minimum NO dosages necessary to achieve a 7-log or higher reduction in viable *E. coli*, *A. baumannii,* and *S. aureus*. The experimental design reported here permitted observation of a larger bacterial kill rate compared to other studies performed in static low- or no-nutrient environments as performing the kill-rate experiments in nutrient broth allows bacteria to grow during the experiment.[19-21, 30, 31]

### 3.4.1 Nitric oxide release in broth media

Recent work in the Reynolds and Schoenfisch groups demonstrated the potential for NO scavenging in cell media solution.[21, 32] Thus, when experiments are performed in cell media or nutrient broth in the case of bacteria experiments, it is possible not all NO released is available for uptake by cells or bacteria. Although cell media presents a more complex composition than nutrient broth, assessment of the NO releasing capabilities under the specific experimental conditions is necessary to gain a more comprehensive understanding of the results as *in vivo* environments involve exposure to complex fluids. In this study, the amount of NO delivered over 24h can be easily estimated by using the following conversion factor 49.5 ± 5.0 μmol $g^{-1}$ NO (Figure 1b).

### 3.4.2 Time-kill bactericidal assays

To achieve a 7-log or higher reduction in viable bacteria, the concentration of *S*-nitrosated dextran-cysteamine (7.5 to 20 mg $mL^{-1}$) needed is dependent on the bacteria strain tested. Gram-negative *E. coli* was most susceptible to *S*-nitrosated dextran-cysteamine; at dosages of 7.5 mg $mL^{-1}$ (0.371 ± 0.039 μmol $mL^{-1}$ of NO) a 7-log reduction was achieved after 24 h while only 4 h were needed for the same level of reduction for 15 mg $mL^{-1}$ dosages (0.742 ± 0.077 μmol $mL^{-1}$ of NO). These findings indicate that we have the ability to tune the dosage of NO releasing material required for the severity of the *E. coli* bacterial infection. Gram-negative *A. baumannii* was more resilient to being eradicated by exposure to *S*-nitrosated dextran-cysteamine, unsurprisingly as *A. baumannii* is well known for how difficult is to eradicate.[33] A concentration of 20 mg $mL^{-1}$ (0.989 ± 0.103 μmol $mL^{-1}$of NO) was required to achieve a 7-log reduction in viable bacteria after 4 hours of exposure. Gram-positive *S. aureus* exhibited a 6-log reduction

after 2h of exposure to 15 mg $mL^{-1}$ of *S*-nitrosated dextran-cysteamine (0.742 ± 0.077 μmol $mL^{-1}$ of NO).

The reduction of *E. coli, A. baumannii* and *S. aureus* in response to NO treatment is consistent with other reported data on NO-releasing systems, and it highlights that NO induces broad range antimicrobial effects.[31, 34] Although *E. coli* and *A. baumannii* are both gram-negative bacteria, *A. baumannii* required dosages nearly three times greater than *E. coli* for reducing bacteria burden to the experimental limit of detection after 24 h. These differences indicate the greater resilience of *A. baumannii* and the need to tune treatment dosages based upon the bacteria strains present in an infected wound to achieve effective treatment.

Reported bactericidal doses for other NO releasing macromolecular vehicles vary based on the material delivery system, experimental set up and delivery time. Therefore, a direct comparison across the literature is a difficult task. In understanding this, the total concentration of NO released into the bacterial solution over the experimental time frame is reported in μmol $mL^{-1}$ for comparison. Schoenfisch and coworkers have reported NO dosage range of 0.002-1.254 μmol $mL^{-1}$ over 2 h period from NO releasing dendrimers to result in a 3-log reduction of another gram-negative bacteria, *P. aeruginosa*.[19] The same kill rate for *P. aeruginosa* was achieved over 24 h with an NO dose between 0.090-0.125 μmol $mL^{-1}$ using NO releasing silica particles.[30] Alternatively, Neidrauer *et al.* demonstrated 5 to 8 log reductions in bacteria over 8 h with NO-release dosages between 1.7-3.5 μmol $mL^{-1}$ released over 3 h.[24] As a comparison, *S*-nitrosated dextran-cysteamine released a total of 0.989 ± 0.103 μmol $mL^{-1}$, 0.742 ± 0.077 μmol $mL^{-1}$ and 0.371 ± 0.039 μmol $mL^{-1}$ for dosages of 20, 15 and 7.5 mg $mL^{-1}$ respectively over 24 h, which falls within the lower range of previous values. It is important to highlight the differences in experimental time between the reported studies and our work, the majority of the mentioned

studies indicated that they achieved the bacterial reduction over 2-4 h. However, no follow up experiments were performed after 24h to confirm that the bacteria did not recover after being exposed to the biocidal. In our case, the extended experimental time used, 24 h versus the widely-used 2-4 h corroborates the relatively long-term effectiveness of this material as no recovery of the bacteria was recorded over time. The continuity of the bactericidal effectiveness is important as several authors have reported that surviving bacteria are capable of recovery within 24 h after exposure to biocidal agents.[28, 35] Consequently, these results also suggest *S*-nitrosated dextran-cysteamine will likely prevent biofilm formation for 24 h as there are not viable bacteria available for colonizing the wound area.

Along with Neidrauer *et al.*, we were capable of reporting the largest log reductions reported to date by performing kill rate experiments in nutrient-rich media, however our reduction was maintained for a longer period of time than the data reported by Neidrauer *et al.* Even though these tests do not represent the complex *in vivo* environment, they strive to improve upon traditional minimum inhibitory concentration studies where materials are assessed under static conditions and lower log reductions are accepted.[21, 31] To our knowledge, this in conjunction with the data reported by Neidrauer *et al.* represents the highest log reduction of bacteria reported to date by an NO releasing system.

### 3.5 Conclusion

*S*-nitrosated dextran-cysteamine was tested for its broad range antibacterial activity against *E. coli, A. baumannii* and *S. aureus* in nutrient broth solution over 24 h. NO-release profiles, performed in nutrient broth at 15 mg $mL^{-1}$ to control for possible scavenging, demonstrate NO release of 49.5 ± 5.0 μmol $g^{-1}$. To achieve over 7-log bacterial reductions (reducing bacteria

burden to the experimental limit of detection) the concentration of *S*-nitrosated dextran-cysteamine vary by bacteria strain and range from 7.5 to 20 mg $mL^{-1}$. These results show the ability of *S*-nitrosated dextran-cysteamine to induce clinically relevant bactericidal activity in planktonic bacteria, demonstrating the potential for this water-soluble polymer as a treatment for *in vivo* infection.

REFERENCES


1. Rosenthal, V. D.; Maki, D. G.; Jamulitrat, S.; Medeiros, E. A.; Todi, S. K.; Yepes Gomez, D.; Leblebicioglu, H.; Abu Khader, I.; Miranda Novales, M. G.; Berba, R.; Ramirez Wong, F. M.; Barkat, A.; Requejo Pino, O.; Duenas, L.; Mitrev, Z.; Hu, B.; Gurskis, V.; Kanj, S. S.; Mapp, T.; Fernandez Hidalgo, R.; Ben Jaballah, N.; Raka, L.; Gikas, A.; Ahmed, A.; Le Thi Anh, T.; Guzman Siritt, M. E.; Members, I., International Nosocomial Infection Control Consortium (INICC) report, data summary for 2003-2008, issued June 2009. *American Journal of Infection Control* **2010,** 38, (2), 95-U31.

2. Zimlichman, E.; Henderson, D.; Tamir, O.; Franz, C.; Song, P.; Yamin, C. K.; Keohane, C.; Denham, C. R.; Bates, D. W., Health Care-Associated Infections A Meta-analysis of Costs and Financial Impact on the US Health Care System. *Jama Internal Medicine* **2013,** 173, (22), 2039-2046.

3. Magill, S. S.; Edwards, J. R.; Bamberg, W.; Beldavs, Z. G.; Dumyati, G.; Kainer, M. A.; Lynfield, R.; Maloney, M.; McAllister-Hollod, L.; Nadle, J.; Ray, S. M.; Thompson, D. L.; Wilson, L. E.; Fridkin, S. K.; Emerging Infect Program, H., Multistate Point-Prevalence Survey of Health Care- Associated Infections. *New England Journal of Medicine* **2014,** 370, (13), 1198-1208.

4. Scott, R. D., *The direct medical costs of healthcare-associated infections in US hospitals and the benefits of prevention*. In 2009

5. Magill, S. S.; Edwards, J. R.; Bamberg, W.; Beldavs, Z. G.; Dumyati, G.; Kainer, M. A.; Lynfield, R.; Maloney, M.; McAllister-Hollod, L.; Nadle, J., Multistate Point-Prevalence Survey of Health Care–Associated Infections. *New England Journal of Medicine* **2014,** 370, (13), 1198-1208.

6. Hancock, R. E. W., Peptide antibiotics. *Lancet* **1997,** 349, (9049), 418-422.

7. Mintzer, M. A.; Dane, E. L.; O'Toole, G. A.; Grinstaff, M. W., Exploiting Dendrimer Multivalency To Combat Emerging and Re-Emerging Infectious Diseases. *Molecular Pharmaceutics* **2012,** 9, (3), 342-354.

8. Rapsch, K.; Bier, F. F.; von Nickisch-Rosenegk, M., Rational Design of Artificial beta-Strand-Forming Antimicrobial Peptides with Biocompatible Properties. *Molecular Pharmaceutics* **2014,** 11, (10), 3492-3502.

9. Vreuls, C.; Zocchi, G.; Thierry, B.; Garitte, G.; Griesser, S. S.; Archambeau, C.; Van de Weerdt, C. V.; Martial, J.; Griesser, H., Prevention of bacterial biofilms by covalent immobilization of peptides onto plasma polymer functionalized substrates. *Journal of Materials Chemistry* **2010,** 20, (37), 8092-8098.

10. Santoro, D.; Maddox, C. W., Canine antimicrobial peptides are effective against resistant bacteria and yeasts. *Veterinary Dermatology* **2014,** 25, (1), 35-+.

11. Oh, D.; Sun, J.; Shirazi, A. N.; LaPlante, K. L.; Rowley, D. C.; Parang, K., Antibacterial Activities of Amphiphilic Cyclic Cell-Penetrating Peptides against Multidrug-Resistant Pathogens. *Molecular Pharmaceutics* **2014,** 11, (10), 3528-3536.

12. Privett, B. J.; Broadnax, A. D.; Bauman, S. J.; Riccio, D. A.; Schoenfisch, M. H., Examination of bacterial resistance to exogenous nitric oxide. *Nitric Oxide-Biology and Chemistry* **2012,** 26, (3), 169-173.

13. Jones, M. L.; Ganopolsky, J. G.; Labbe, A.; Prakash, S., A novel nitric oxide producing probiotic patch and its antimicrobial efficacy: preparation and in vitro analysis. *Applied Microbiology and Biotechnology* **2010,** 87, (2), 509-516.

14. Nablo, B. J.; Chen, T. Y.; Schoenfisch, M. H., Sol-gel derived nitric-oxide releasing materials that reduce bacterial adhesion. *Journal of the American Chemical Society* **2001,** 123, (39), 9712-9713.

15. Hetrick, E. M.; Shin, J. H.; Stasko, N. A.; Johnson, C. B.; Wespe, D. A.; Holmuhamedov, E.; Schoenfisch, M. H., Bactericidal efficacy of nitric oxide-releasing silica nanoparticles. *Acs Nano* **2008,** 2, (2), 235-246.

16. Riccio, D. A.; Dobmeier, K. P.; Hetrick, E. M.; Privett, B. J.; Paul, H. S.; Schoenfisch, M. H., Nitric oxide-releasing S-nitrosothiol-modified xerogels. *Biomaterials* **2009,** 30, (27), 4494-4502.

17. Carpenter, A. W.; Slomberg, D. L.; Rao, K. S.; Schoenfisch, M. H., Influence of Scaffold Size on Bactericidal Activity of Nitric Oxide-Releasing Silica Nanoparticles. *Acs Nano* **2011,** 5, (9), 7235-7244.

18. Naghavi, N.; de Mel, A.; Alavijeh, O. S.; Cousins, B. G.; Seifalian, A. M., Nitric Oxide Donors for Cardiovascular Implant Applications. *Small* **2013,** 9, (1), 22-35.

19. Sun, B.; Slomberg, D. L.; Chudasama, S. L.; Lu, Y.; Schoenfisch, M. H., Nitric Oxide-Releasing Dendrimers as Antibacterial Agents. *Biomacromolecules* **2012,** 13, (10), 3343-3354.

20. Lu, Y.; Slomberg, D. L.; Shah, A.; Schoenfisch, M. H., Nitric Oxide-Releasing Amphiphilic Poly(amidoamine) (PAMAM) Dendrimers as Antibacterial Agents. *Biomacromolecules* **2013,** 14, (10), 3589-3598.

21. Lu, Y.; Slomberg, D. L.; Sun, B.; Schoenfisch, M. H., Shape- and Nitric Oxide Flux-Dependent Bactericidal Activity of Nitric Oxide-Releasing Silica Nanorods. *Small* **2013,** 9, (12), 2189-2198.

22. Storm, W. L.; Youn, J.; Reighard, K. P.; Worley, B. V.; Lodaya, H. M.; Shin, J. H.; Schoenfisch, M. H., Superhydrophobic nitric oxide-releasing xerogels. *Acta Biomaterialia* **2014,** 10, (8), 3442-3448.

23. Amitai, G.; Andersen, J.; Wargo, S.; Asche, G.; Chir, J.; Koepsel, R.; Russell, A. J., Polyurethane-based leukocyte-inspired biocidal materials. *Biomaterials* **2009,** 30, (33), 6522-6529.

24. Neidrauer, M.; Ercan, U. K.; Bhattacharyya, A.; Samuels, J.; Sedlak, J.; Trikha, R.; Barbee, K. A.; Weingarten, M. S.; Joshi, S. G., Antimicrobial efficacy and wound-healing property of a topical ointment containing nitric-oxide-loaded zeolites. *Journal of Medical Microbiology* **2014,** 63, 203-209.

25. Joslin, J. M.; Damodaran, V. B.; Reynolds, M. M., Selective nitrosation of modified dextran polymers. *Rsc Advances* **2013,** 3, (35), 15035-15043.

26. Damodaran, V. B.; Place, L. W.; Kipper, M. J.; Reynolds, M. M., Enzymatically degradable nitric oxide releasing S-nitrosated dextran thiomers for biomedical applications. *Journal of Materials Chemistry* **2012,** 22, (43), 23038-23048.

27. Reynolds, M. M.; Hrabie, J. A.; Oh, B. K.; Politis, J. K.; Citro, M. L.; Keefer, L. K.; Meyerhoff, M. E., Nitric oxide releasing polyurethanes with covalently linked diazeniumdiolated secondary amines. *Biomacromolecules* **2006,** 7, (3), 987-94.

28. Pegalajar-Jurado, A.; Easton, C. D.; Styan, K. E.; McArthur, S. L., Antibacterial activity studies of plasma polymerised cineole films. *Journal of Materials Chemistry B* **2014**.

29. Barry, A. L.; Craig, W. A.; Nadler, H.; Reller, L. B.; Sanders, C. C.; Swenson, J. M., *Methods for determining bactericidal activity of antimicrobial agents: approved guideline*. National Committee for Clinical Laboratory Standards: 1999.

30. Slomberg, D. L.; Lu, Y.; Broadnax, A. D.; Hunter, R. A.; Carpenter, A. W.; Schoenfisch, M. H., Role of Size and Shape on Biofilm Eradication for Nitric Oxide-Releasing Silica Nanoparticles. *Acs Applied Materials & Interfaces* **2013,** 5, (19), 9322-9329.

31. Carpenter, A. W.; Worley, B. V.; Slomberg, D. L.; Schoenfisch, M. H., Dual Action Antimicrobials: Nitric Oxide Release from Quaternary Ammonium-Functionalized Silica Nanoparticles. *Biomacromolecules* **2012,** 13, (10), 3334-3342.

32. Harding, J. L.; Reynods, M. M., Accurate Nitric Oxide Measurements from Donors in Cell Media: Identification of Scavenging Agents. *Analytical Chemistry* **2014,** 86, (4), 2025-2032.

33. Dijkshoorn, L.; Nemec, A.; Seifert, H., An increasing threat in hospitals: multidrug-resistant Acinetobacter baumannii. *Nature Reviews Microbiology* **2007,** 5, (12), 939-951.

34. Sulemankhil, I.; Ganopolsky, J. G.; Dieni, C. A.; Dan, A. F.; Jones, M. L.; Prakash, S., Prevention and Treatment of Virulent Bacterial Biofilms with an Enzymatic Nitric Oxide-Releasing Dressing. *Antimicrobial Agents and Chemotherapy* **2012,** 56, (12), 6095-6103.

35. May, J.; Chan, C. H.; King, A.; Williams, L.; French, G. L., Time-kill studies of tea tree oils on clinical isolates. *Journal of Antimicrobial Chemotherapy* **2000,** 45, (5), 639-643.

# CHAPTER 4:

# *IN VITRO* CELL FUNCTION UNDER EXPOSURE TO NO RELEASING POLYMERS

The cytotoxicity of PLGH and dextran-cysteamine polymer derivatives is determined *in vitro* using assays to examine cell viability and cell morphology. Dr. Vinod Damodaran synthesized PLGH and dextran polymers and their derivatives. I developed protocol and carried out the cell viability and morphology assays.

Results intended for publication as Wold, K.A.; Pegalajar-Jurado, D.; Arabea, K.; Suazo, L.A; McDaniel, S.L.; Bowen, R.A..; Reynolds, M.M. *S*-nitrosated dextran polymers as antibacterial agents. *Journal of Materials Chemistry B.*

## 4.1 Introduction

Nitric oxide plays a vital, concentration-dependent role in a variety of biological processes.[1] At lower levels, NO promotes cell growth and proliferation but begins to exhibit negative effects, including cell death, at higher levels.[2] The literature suggests instantaneous biological concentrations of NO above 400 nM are considered important for antibacterial effects, but levels exceeding 1 μM can stimulate apoptotic effects that could be potentially harmful to cells of healthy tissue.[1] When exploring the use of NO releasing materials to achieve biological responses, it is important to understand how the material systems will interact at the cellular level at the site of intended application. Equally important is the understanding of the material NO release properties to discern whether observed cellular effects are a result of this release or an artifact of the material system independent of NO incorporation. There is a general understanding of how much NO is produced naturally by the body under varying biological

situations, yet ideal levels of NO release for implants and synthetic materials for enhancing cell growth in wound healing are currently not well established.

The initial step to determining cellular biocompatibility is generally accomplished through *in vitro* eukaryotic cell viability assays. Fibroblasts are commonly used to assess biocompatibility and potential wound healing efficacy of new materials *in vitro*.[3] In these studies, the activity of *S*-nitrosated polymers PLGH and dextran, introduced in Chapter 2, were exposed directly to cultured fibroblasts and cell viability was evaluated with assays measuring cell viability and morphology. Thiolated polymers and untreated cells were used as controls.

## 4.2 Experimental

### 4.2.1 Cell culture

Human dermal fibroblast cells (HDF, Clonetics) were stored frozen in cryovials in 1 mL aliquots of $10^6$ cells $mL^{-1}$ at -80°C. Prior to culture, they were thawed at room temperature and warmed to 37°C in a water bath. HDF cells were grown in Medium 106 supplemented with low serum growth supplement (LSGS) and gentamicin/amphotericin (Cascade Biologics). Media was warmed to 37°C in a water bath prior to use. Cells were suspended in 15 mL fortified cell culture media and incubated in 75 $cm^2$ culture flasks at 37 °C and 5% $CO_2$. The first media change took place approximately 24 h after initial culture, after which media was changed every other day until cells were ~ 70 - 90% confluent. Cells were viewed under a light microscope to ensure attachment to the flask bottom had occurred. Cells were removed from culture flasks by aspirating cell media and rinsing with 1 mL trypsin digestion (0.025% trypsin/EDTA for HDF, 0.05% for HEK) to remove any unattached cells. Cells were then incubated with 3 mL trypsin digestion for 5 min. Following cell-surface detachment, 6 mL trypsin neutralizer (0.5% fetal

bovine serum in PBS) was added to arrest the trypsin reaction. The contents of the flask were transferred to a 15 mL centrifuge tube and a cell pellet was formed by centrifugation at 180 × *g* for 7 min. Supernatant was aspirated and HDF cells re-suspended in culture medium. The cell density was determined using a hemocytometer. Cells were then either prepared for use in viability experiments or seeded into new culture flasks and grown for future use. The experiments for this study were performed using cells of passage 3 through 10.

**4.2.2 MTT Assay**

Cells grown to confluence in 75 $cm^2$ culture flasks were trypsinized and the centrifuged cell pellet was re-suspended in cell media to a concentration of 2 x $10^4$ cells $mL^{-1}$. This cell solution was seeded into well plates at volumes of 500 µL per well for 24-well plates or 200 µL per well for 96-well plates. Cell-free culture media was used to represent negative controls. Well plates were placed in the incubator overnight to allow for cell attachment. The following day, wells were viewed under a light microscope to confirm cell attachment to the well plate and media was aspirated. Nitrosated and non-nitrosated polymers to be tested were dissolved in fresh cell media at known concentrations ranging from 0.1 to 2 mg $mL^{-1}$, gently shaken, and pipetted into the cell-containing wells, five wells for each concentration. Unaltered cell media was added to five cell-containing wells as positive controls and cell media was changed in five wells containing no cells, representing negative controls. Plates were then returned to the incubator for either 24 h or 5 days.

Cell viability was assessed using a commercially available methylthiazol tetrazolium (MTT) assay kit (*In vitro* toxicology assay kit (Tox-1), Sigma). After incubation with polymer-doped cell media, samples were moved from the incubator to a biosafety cabinet. As the cell culture media used for growing HDF cells contains phenol red, a component that can decrease

sensitivity of the MTT assay, cell media was aspirated from the samples. Sample wells were carefully rinsed twice with PBS. A vial of lyophilized MTT was reconstituted with 3 mL PBS in accordance with manufacturer recommendations. Ten percent MTT was mixed in PBS to a volume sufficient for the number of samples in the experiment. MTT solution was prepared so volumes added covered the bottom of each well (500 µL for 24-well plates, 120 µL for 96-well plates). Once MTT was added to each sample, the plate was placed back in the incubator for exactly 3 hours. After this incubation period, the plate was removed and MTT solubilization solution was added to each well in equivalent volumes to the amount of MTT added previously. Crystals formed on the bottom of the well were scraped with a pipette tip and mixed by pipetting up and down until they were solubilized in solution. Two 200 µL aliquots from each sample well were pipetted into separate wells in a new 96-well plate. The plate was inserted into a plate reader. Background absorbance was read at 690 nm and absorbance was read at 570 nm. The measurement values at 690 nm were subtracted from the values at 570 nm to obtain the final absorbance. Absorbance values were normalized to the value the positive control. Viabilities < 70% of the control were considered to exhibit cytotoxic potential according to ISO 10993-5:2009.

### 4.2.3 Fluorescent staining

Cells grown to confluence in 75 $cm^2$ culture flasks were trypsinized and the centrifuged cell pellet was re-suspended in cell media to a concentration of 2 x $10^4$ cells $mL^{-1}$. 500 µL of cell solution was seeded onto tissue cultured polystyrene discs placed at the bottom of 24-well plates. Cell-free culture media was also used in additional wells to represent negative controls. Well plates were placed in the incubator overnight to allow for cell attachment. The following day, wells were viewed under a light microscope to confirm cell attachment to the well plate and

media was aspirated. Nitrosated and non-nitrosated polymers to be tested were dissolved in fresh cell media at known concentrations ranging from 0.1 to 2 mg $mL^{-1}$, gently shaken, and pipetted onto the cell-seeded polystyrene discs. Three discs were treated for each polymer concentration. Cell media was added to three cell-seeded discs as positive controls and cell media was changed on three discs containing no cells, representing negative controls. Plates were then returned to the incubator for either 24 h or 5 days.

All staining protocol was conducted in a biosafety cabinet. Cell culture media was aspirated from sample wells, washed twice with PBS and polystyrene discs moved to a new 24-well plate. Fixative was prepared consisting of 3.7% formaldehyde in PBS. Fixative was added to each sample well in volumes large enough to completely cover samples, incubated for 15 min at room temperature and aspirated. Samples were then washed twice with PBS. Permeablizer prepared of 1% Triton-X in PBS was then added to each sample in volumes large enough to cover each slide and incubated for 3 min at room temperature. Permeablizer was then aspirated and samples rinsed twice with PBS, allowing PBS to incubate for ~ 3 min during each wash. The samples were then considered ready for staining.

Rhodamine phalloidin was used as the actin cytoskeleton stain. The stain was received from the manufacturer as a lyophilized powder, reconstituted with 500 µL methanol and stored at -20 °C. This reconstituted rhodamine is referred to as the stock solution. To dilute to working concentrations, the concentration used for staining, the stock solution was diluted 1:200 in PBS. DAPI (AnaSpec) was received from the manufacturer as 25 mg of powder and reconstituted with 25 mL DI water per manufacturer recommendations. This is referred to as the stock solution and stored at -20 °C in 5 mL aliquots. To prepare the working solution, storage solution was diluted

1:1000 in PBS to bring to a concentration of 1 μg $mL^{-1}$. To use for staining samples, the working solution is diluted 105:1000 in PBS to bring to a final concentration of 105 ng $mL^{-1}$.

To stain fixed samples, 600 μL working concentration of rhodamine phalloidin was added to each sample and control well. The plate was then incubated at room temperature for 25 min protected from light. Next, 100 uL DAPI nuclear stain was added to each well and incubated for 5 min at room temperature protected from light. After the incubation period, the stain was aspirated from the wells and samples were washed twice with PBS to remove excess stain. Fluorescently stained samples were imaged using an upright fluorescent microscope (Zeiss) with a DAPI BP 445/50 blue filter and HQ Texas Red BP 560/40 red filter.

### 4.2.4 Statistics

All experiments, unless stated otherwise, were performed on three different cell populations, with at least five samples for each cell population for the MTT assay ($n \geq 15$) and at least three samples for fluorescent staining assays ($n \geq 9$). Quantitative data are reported as a mean ± standard deviation. Significance was considered at $p < 0.05$ and calculated using an analysis of variance (ANOVA).

## 4.3 Results and Discussion

Biocompatibility of NO releasing material systems on human tissue is a concern that must be considered from both a material and therapeutic release standpoint. In this work, varying concentrations of *S*-nitrosated PLGH and dextran polymers were exposed to human dermal fibroblasts *in vitro* and examined for their viability, adhesion and morphological properties. Non-nitrosated polymers were used along with untreated positive controls to determine whether any effect on the cells are a result of the NO release or simply the exposure of the polymer to the

cells in general. Detailed description of polymer synthesis and NO release determination are found in Chapter 2.

Prior cytotoxicity studies of thiolated PLGH derivatives indicate degradation products of the polymer induced no cytotoxic effect on mouse fibroblast cells,[4] while dextran is in itself considered to be nontoxic.[5] These properties warrant further studies quantifying how direct exposure of varying levels of the polymer systems might affect cell growth and proliferation to human cells *in vitro*.

### 4.3.1 NO release

The total cumulative dosage of NO released from the polymer systems over the time course of the experiment is presented in Table 4.1 in μmol $mL^{-1}$, a common unit of measurement in biological NO release reporting for particulate materials.[6] These values represent cumulative NO release of the materials and are consistent with dosages of other recently reported NO releasing materials intended for biological applications.[6, 7] One major drawback in the NO release data reported is NO analysis was performed in PBS, while the cell culture experiments are conducted in cell culture media. Cell culture media has been proven capable of scavenging NO from the system, meaning not all NO released by the polymers is exposed to the cells.[8, 9] Future studies will be directed at determining NO release under specific cell culture media environments used in this experiment in order to more accurately understand the relationship between NO release from the polymers and cell survival.

| Material and dosage | NO release (μmol $mL^{-1}$) |
|---|---|
| PLGH-cysteamine 1 mg/mL | 0.241±0.0040 |
| PLGH-cysteamine 2 mg/mL | 0.482±0.0080 |
| Dextran-cysteamine 0.1 mg/mL | 0.013±0.0004 |
| Dextran-cysteamine 1 mg/mL | 0.125±0.0040 |
| Dextran-cysteamine 2 mg/mL | 0.250±0.0080 |

**Table 4.1.** NO release from *S*-nitrosated PLGH and dextran polymers at different concentrations of polymer in solution. NO release recorded at 37°C and pH 7.4 in PBS.

### 4.3.2 Cytotoxicity studies

The effect of NO release from the material systems on cell viability was evaluated by examining metabolic activity using the MTT assay and cell morphology using fluorescent staining. The MTT assay is used to determine the metabolic activity of cells by reducing yellow methylthiazol tetrazolium to an insoluble purple formazan, a reaction that only occurs in the mitochondria of living cells. Viability is determined colorimetrically by measuring the absorbance of the solution. To attain this data, the changes in MTT absorbance of cells cultured with the addition of varying concentrations of NO and non-NO releasing polymer to cell media were observed and cell viability was assessed after 24 h of polymer-exposed cell growth. These results were compared to positive controls.

HDF viability after exposure to concentrations of 1 and 2 mg $mL^{-1}$ PLGH-cysteamine and *S*-nitrosated PLGH-cysteamine was assessed using the MTT assay. Cell viability normalized to positive controls is shown in Figure 4.1. Due to the water-insoluble nature of the material, 1 and 2 mg polymer samples were individually weighed and directly transferred into 1 mL of cell media in the appropriate wells of the 24-well plate containing attached cells. As potential for inaccuracies using this method were large, the data reported herein represents five different polymer samples observed using one cell population (n = 5). The results suggest concentrations of PLGH-cysteamine powder of 1 mg $mL^{-1}$ induces cytotoxicity *in vitro* as the cell viability normalized to untreated cells is 58.3 ± 13.9%, and doubling the polymer concentration in cell

media to 2 mg $mL^{-1}$ resulted in lesser cell viability (13.1 ± 5.1%). ISO 10993-5 standards for MTT assay indicate viability below 70% is suggestive of cytotoxic potential of the material, and each of these samples fall below this value. The *S*-nitrosated PLGH-cysteamine at 1 mg $mL^{-1}$ and 2 mg $mL^{-1}$ resulted in nearly 0% cell viability suggesting the incorporation of NO release to the polymer further negatively influences fibroblast viability.

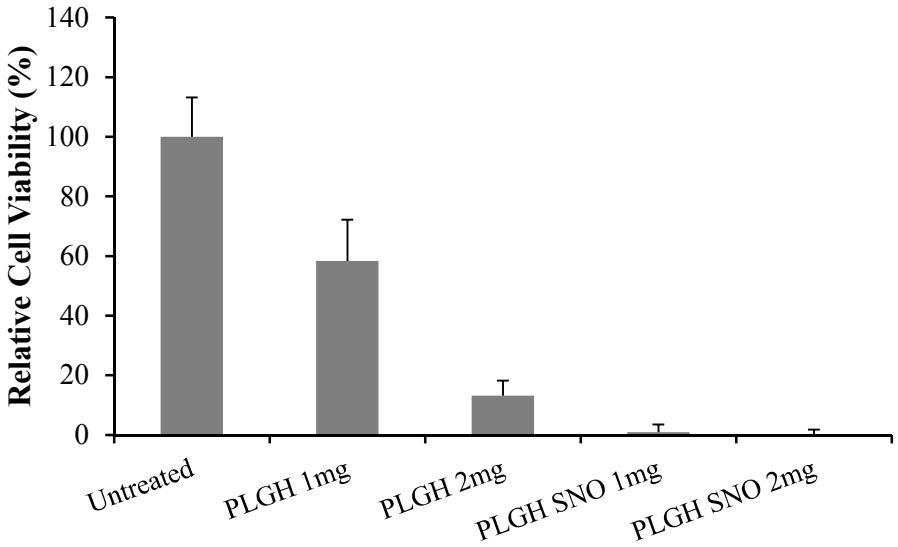


**Figure 4.1.** 24 h viability of human dermal fibroblasts exposed to unmodified and *S*-nitrosated PLGH-cysteamine with unmodified growth conditions as the control. Studies consist of five samples (n = 5) with error bars representing standard deviation.

Using the aforementioned methods for determining the effect of NO release from *S*-nitrosated materials on fibroblasts, PLGH was not an ideal polymer system to work with due to its insolubility in the cell media. Dextran-cysteaine polymer systems synthesized by the lab exhibited solubility in cell media. This was a more favorable polymer system for use in these experiments as the solubility of dextran-cysteamine allowed it to be dissolved in large volumes of media and pipetted into the polystyrene well plates, achieving more reliable polymer concentrations in cell media. This also allowed for the use of smaller well plates (96- instead of

24-well plates) and, in turn, smaller volumes of media and polymer per experiment, crucial as polymer synthesis times are long and batch sizes are small.

Dextran-cysteamine exhibited greater HDF viability when compared with PLGH-cysteamine. (Figure 4.2). Over 24 h, cell viability in wells exposed to 1 mg $mL^{-1}$ dextran-cysteamine was 85.9 ± 13.3% that of untreated cells, fulfilling the 70% metabolic activity benchmark indicating low cytotoxic potential. However, 2 mg $mL^{-1}$ concentrations exhibited a decreased viability of 58.5 ± 15.1%. The addition of *S*-nitrosated polymers to the cell media proved detrimental to the growth of fibroblasts, with the NO releasing material exhibiting poor cell viability (24.8 ± 18.9% and 5.8 ± 8.6% for 1 mg $mL^{-1}$ and 2 mg $mL^{-1}$). To determine whether cell viability would recover with increased exposure after NO release from the polymer was complete, MTT assays were repeated at day 5 in culture and results are represented in Figure 4.3. Relative cell viability decreased in all four samples when compared to the 24 h time point. Fluorescent staining of the cells in each group at day 5 confirmed the MTT findings (Figure 4.4). The control fibroblasts grew to near confluence by day 5 and exhibited fibrous cytoskeletal extensions as observed from the red phalloidin stain. Fibroblast cell density is decreased from that of the control when exposed to 1 mg $mL^{-1}$ dextran-cysteamine, yet the present cells still exhibit healthy morphologies. For the remainder of the samples, fibroblast growth is significantly inhibited as there is little cytoskeleton growth. Fluorescent staining was not performed on cell samples at the 24 h time point as cell densities were not high enough and characteristic morphologies seen in confluent cells were not observable.

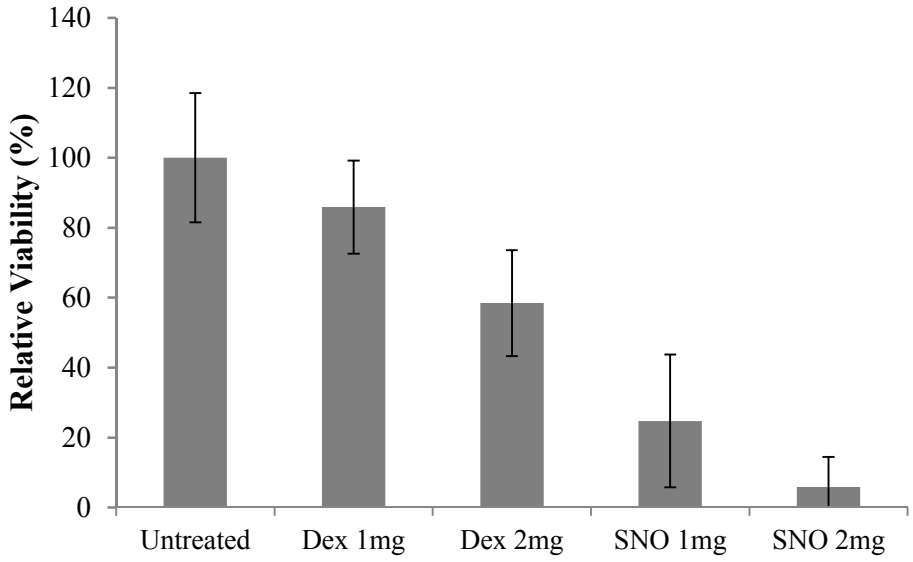


**Figure 4.2.** 24 h viability of human dermal fibroblasts exposed to unmodified and *S*-nitrosated dextran-cysteamine with unmodified growth conditions as the control. Studies consist of at least three experiments of five samples ($n \geq 15$) with error bars representing standard deviation.

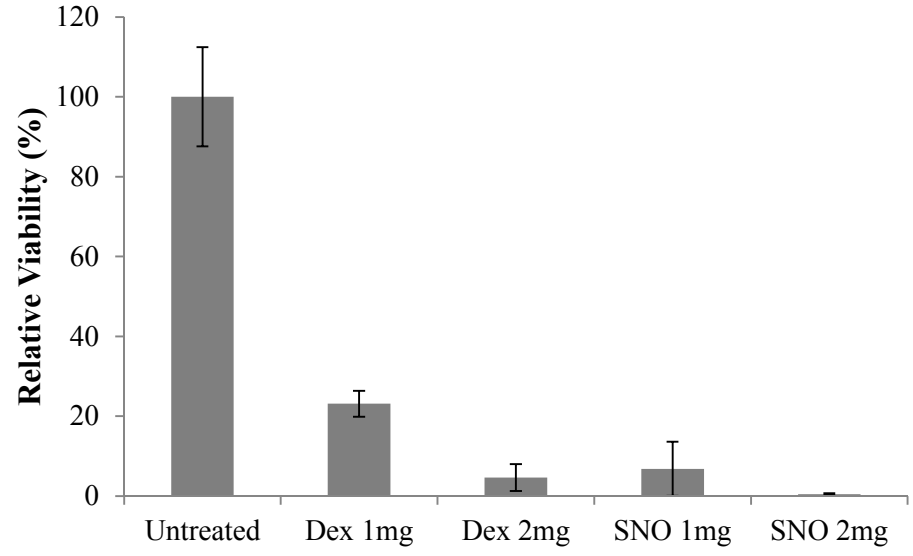


**Figure 4.3.** 5 day viability of human dermal fibroblasts exposed to unmodified and *S*-nitrosated dextran-cysteamine with unmodified growth conditions as the control. Studies consist of at least three experiments of five samples ($n = 15$) with error bars representing standard deviation.

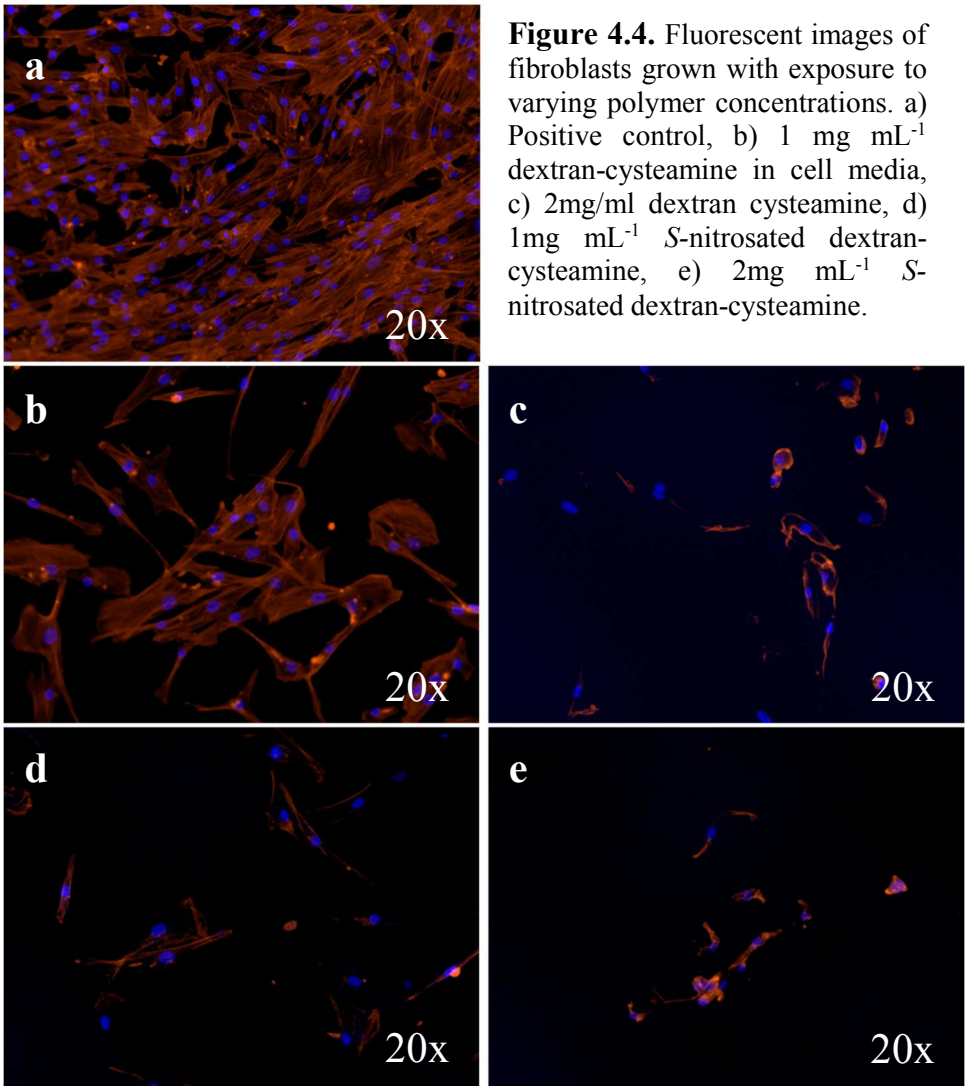


**Figure 4.4.** Fluorescent images of fibroblasts grown with exposure to varying polymer concentrations. a) Positive control, b) 1 mg $mL^{-1}$ dextran-cysteamine in cell media, c) 2mg/ml dextran cysteamine, d) 1mg $mL^{-1}$ *S*-nitrosated dextran-cysteamine, e) 2mg $mL^{-1}$ *S*-nitrosated dextran-cysteamine.

As the *S*-nitrosated polymers exhibited poor cell viability in comparison to the positive control and dextran-cysteamine at 1 and 2 mg $mL^{-1}$, polymer concentration was reduced in the subsequent experiments, thereby reducing the total NO release as well as the amount of material in each well. 1mg and 0.1mg polymer per mL cell media were tested against the control in a similar method as the last experiments. The results of this experiment showed the reduced concentration of polymer resulted in improved cell viability (Figure 4.5). 1 mg $mL^{-1}$ dextran-cysteamine had previously been shown to exhibit greater than 70% viability. Similarly, 0.1 mg $mL^{-1}$ sample exhibits viability statistically similar to that of the control. Non-cytotoxic potential

was demonstrated for *S*-nitrosated dextran-cysteamine at the 0.1 mg $mL^{-1}$ concentration, exhibiting metabolic activity statistically similar to that of fibroblasts exposed to 1 mg $mL^{-1}$ dextran-cysteamine. The results in these lower concentrations are most likely due to the reduced presence of material present in the cell media rather than indicating an ideal level of NO release for cell survival has been achieved.

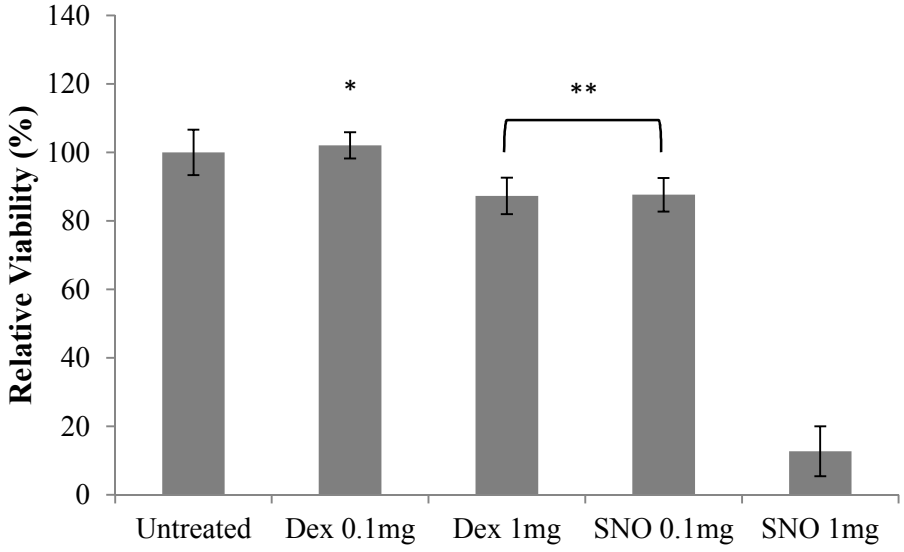


**Figure 4.5.** 24 h viability of human dermal fibroblasts exposed to unmodified and *S*-nitrosated dextran-cysteamine with unmodified growth conditions as the control. Studies consist of five samples (n = 5) with error bars representing standard deviation. * indicates statistically similar values to control. ** indicate samples are statistically similar to one another ($p < 0.05$).

Other NO releasing material systems have also exhibited low *in vitro* fibroblast viabilities. Schoenfisch *et al* also witnessed poor fibroblast viability in the presence of NO releasing silica nanoparticles and sol-gel derived materials.[10-12] Although fibroblast viability is commonly used as a preliminary indicator of cytotoxicity for materials investigated for their wound healing potential, results may represent more severe cytotoxic action than would be realized in an actual *in vivo* environment as significant *in vitro* fibroblast toxicity has been reported in clinically used topical antibacterial treatments. For example, povidone-iodine, a clinically used topical antimicrobial agent, resulted in high cytotoxicity in *in vitro* fibroblast

viability after one week at a concentration ten times more dilute than what is used clinically.[13] Additionally, viability of < 25% was recorded over 24 h for several silver-based antibacterial wound care products.[14] In another study, similar dressings were shown to exhibit low cell viability in both fibroblasts and keratinocytes under two dimensional cell culture models, similar to those described here, while viability in three dimensional tissue culture models demonstrated improved cell viability.[15] It was believed that the more complex cellular system was a better representation of *in vivo* cellular responses. These observations highlight the difficulty in comparing *in vitro* to *in vivo* results, yet suggest *in vivo* cell viability will likely be improved from the results of the *in vitro* cell culture viability reported due to the more complex nature of the system.

### 4.4 Conclusion

The goal of these experiments was to determine a polymer concentration threshold detrimental to cell growth, and an NO release level suitable for sustaining or promoting the growth of these cells. What can be concluded is the ideal material/NO release properties suitable for promoting the growth of fibroblasts have not yet been determined. The data suggest the effects on cultured cells for the particulate form of these materials in solution range from inhibitory to cytotoxic. Further viability studies must be conducted using live/dead staining and a larger range of polymer concentrations in media to better understand the impact these polymers have upon cell viability *in vitro*. More detailed NO release profiles also need to be conducted in order to determine the extent of NO scavenging occurring in the cell media.

REFERENCES


1. Coneski, P. N.; Schoenfisch, M. H., Nitric oxide release: Part III. Measurement and reporting. *Chemical Society Reviews* **2012,** 41, (10), 3753-3758.

2. Cooke, J. P.; Losordo, D. W., Nitric oxide and angiogenesis. *Circulation* **2002,** 105, (18), 2133-2135.

3. Thelestam, M.; Mollby, R., CULTURED HUMAN-FIBROBLASTS AS A MODEL FOR EVALUATION OF POTENTIAL INVIVO TOXICITY OF MEMBRANE DAMAGING ANTIBIOTICS. *Chemico-Biological Interactions* **1980,** 29, (3), 315-325.

4. Damodaran, V. B.; Joslin, J. M.; Wold, K. A.; Lantvit, S. M.; Reynolds, M. M., S-Nitrosated biodegradable polymers for biomedical applications: synthesis, characterization and impact of thiol structure on the physicochemical properties. *Journal of Materials Chemistry* **2012,** 22, (13), 5990-6001.

5. Naessens, M.; Cerdobbel, A.; Soetaert, W.; Vandamme, E. J., Leuconostoc dextransucrase and dextran: production, properties and applications. *Journal of Chemical Technology and Biotechnology* **2005,** 80, (8), 845-860.

6. Lu, Y.; Slomberg, D. L.; Schoenfisch, M. H., Nitric oxide-releasing chitosan oligosaccharides as antibacterial agents. *Biomaterials* **2014,** 35, (5), 1716-1724.

7. Slomberg, D. L.; Lu, Y.; Broadnax, A. D.; Hunter, R. A.; Carpenter, A. W.; Schoenfisch, M. H., Role of Size and Shape on Biofilm Eradication for Nitric Oxide-Releasing Silica Nanoparticles. *Acs Applied Materials & Interfaces* **2013,** 5, (19), 9322-9329.

8. Harding, J. L.; Reynods, M. M., Accurate Nitric Oxide Measurements from Donors in Cell Media: Identification of Scavenging Agents. *Analytical Chemistry* **2014,** 86, (4), 2025-2032.

9. Hunter, R. A.; Storm, W. L.; Coneski, P. N.; Schoenfisch, M. H., Inaccuracies of Nitric Oxide Measurement Methods in Biological Media. *Analytical Chemistry* **2013,** 85, (3), 1957-1963.

10. Carpenter, A. W.; Worley, B. V.; Slomberg, D. L.; Schoenfisch, M. H., Dual Action Antimicrobials: Nitric Oxide Release from Quaternary Ammonium-Functionalized Silica Nanoparticles. *Biomacromolecules* **2012,** 13, (10), 3334-3342.

11. Hetrick, E. M.; Shin, J. H.; Paul, H. S.; Schoenfisch, M. H., Anti-biofilm efficacy of nitric oxide-releasing silica nanoparticles. *Biomaterials* **2009,** 30, (14), 2782-2789.

12. Nablo, B. J.; Schoenfisch, M. H., In vitro cytotoxicity of nitric oxide-releasing sol-gel derived materials. *Biomaterials* **2005,** 26, (21), 4405-4415.

13. Balin, A. K.; Pratt, L., Dilute povidone-iodine solutions inhibit human skin fibroblast growth. *Dermatologic Surgery* **2002,** 28, (3), 210-214.

14. Burd, A.; Kwok, C. H.; Hung, S. C.; Chan, H. S.; Gu, H.; Lam, W. K.; Huang, L., A comparative study of the cytotoxicity of silver-based dressings in monolayer cell, tissue explant, and animal models. *Wound Repair and Regeneration* **2007,** 15, (1), 94-104.

15. Poon, V. K. M.; Burd, A., In vitro cytotoxity of silver: implication for clinical wound care. *Burns* **2004,** 30, (2), 140-147.

# CHAPTER 5:

# *S*-NITROSATED POLYMER MICRO- AND NANO-FIBERS BY ELECTROSPINNING

This chapter presents a method for the development of NO releasing nonwoven fibers exhibiting nanoscale diameters from *S*-nitrosated polymer materials. The synthesis and of PLGH and dextran derivatives was performed by Dr. Vinod Damodaran. Using these polymers, I developed protocol and found parameters for processing electrospun fibers from the *S*-nitrosated polymers and their derivatives. In addition, I performed all characterization of fiber morphology using SEM. I characterized NO release from the electrospun polymers and I designed and performed experiments to test their degradation properties under aqueous conditions. Additionally, I measured the viscosities and conductivities of electrospinning solutions.

Adapted with permission from: Wold, K.A.; Damodaran, V.B.; Suazo, L.A.; Bowen, R.A.; Reynolds, M.M. *ACS Applied Materials and Interfaces,* **2013**, 4(6), 3022-3030. 

## 5.1 Introduction

The structure of polymeric biomaterials is crucial to their performance, and it can be tailored with a specific application in mind. For polymers to function optimally as wound healing materials, the structure should promote cell growth and proliferation while retaining bactericidal properties. Electrospun nanofibers have been extensively studied as a versatile polymer processing method for biomedical device materials, including those involved in wound healing. This is due to their large surface area, tunable mechanical properties, and ability to mimic the ECM.[1, 2] Although not currently in clinical use, several natural and synthetic polymer

formulations have been developed into nanofibers and investigated as materials to aid in the repair and healing of skin.[3-5] These studies demonstrate the promise biodegradable electrospun polymer materials have in supporting cell growth and accelerating the wound healing process. Others have shown that electrospun blends of poly-L-lactide (PLLA) and poly(D,L)-lactide-*co*-glycolide (PLGA) allow complete cell migration into the scaffold material during wound healing[3] and electrospun fibers consisting of a blend of PLGA and collagen accelerate early stage wound healing.[5]

The incorporation of NO release capability into a biodegradable nanofibrous scaffold would provide a two-fold healing potential and have significant advantages over current material platforms. Tailored NO release would provide a natural therapeutic toward adverse bacterial responses whereas a fibrous matrix would mimic the natural ECM and serve to support cell attachment. Fibers developed from polymers blended with NO donors have been reported previously in the literature. Coneski et al. developed microfibers by blending PROLI/NO, a discrete NO donor, with polymer solutions of Tecoflex™ polyurethane and poly(vinyl chloride).[6] Lopez-Jaramillo et al. developed a multi-layer NO releasing transdermal patch where NO donor was encapsulated in Tecophilic polymer nanofibers.[7] Bohlender *et al.* also utilized a blended system in creating light triggered NO release from electrospun nanofibers with NO releasing ligands and poly(lactic acid). In all three of these cases, the fibers created were biostable. Similarly, the development of nanofibers using degradable polymers blended with NO donors has also been reported.[8, 9] While different methods have been used to demonstrate NO release from these materials, the NO release rates are rapid (extinguished within about 1 h) or not well characterized in terms of quantity of NO released or the time interval of release.[6] One electrospun polymer system that has achieved long term NO release was reported by Koh *et al*.

They developed biostable polyurethane electrospun fibers doped with macromolecular NO-releasing silica nanoparticles capable of NO release from hours to days, depending on the system.[10] A concern in using donor blended systems for use in localized NO delivery is donor leaching. If donors are leaching from the polymer materials, NO release can occur in areas other than the intended release site. Also, some NO donors, namely *N*-diazeniumdiolates, have the potential to degrade into toxic byproducts, which should not be released into the body.[11, 12] Consequently, a stable incorporation of the NO donor as well as its specific release conditions and controlled, quantified release capability are ideal requirements to provide a long-term therapeutic effect.

In this chapter, an electrospinning process developed to prepare NO releasing nanofibers from the thiol- and NO-incorporated derivatives of poly(lactic-*co*-glycolic-*co*-hydroxymethyl propionic acid) (PLGH) will be introduced. The morphology of the fibers, NO release characteristics, and effects of short-term aqueous exposure to the morphology of the fibers will be evaluated.

## 5.2 Experimental

Thiolated and *S*-nitrosated PLGH and dextran derivatives used in these experiments were prepared following synthesis methods developed by the group and discussed in detail in Chapter 2.2 and 2.3.[13]

### 5.2.1 Electrospinning

Conditions where PLGH, its thiolated derivatives, and the *S*-nitrosated derivatives were electrospun were deduced by following electrospinning conditions reported previously, and altering parameters until uniform fiber morphology was obtained.[14] For all polymers electrospun,

a 1 mL syringe with a 22 G blunt tip needle was loaded with polymer solution and inserted into a variable speed syringe pump (Kent Scientific Corp., Torrington, CT, USA) with a flow rate of 0.2 mL $h^{-1}$. Various potentials were applied via a high-voltage power supply (Gamma High Voltage Research, Ormond Beach, FL, USA). Fibers were collected on either aluminum foil (for SEM imaging and NO release studies) or glass slides (for degradation studies) attached to a grounded copper plate. The electrospinning process was performed inside a Plexiglas box vented into a fume hood. The temperature of the electrospinning environment was approximately 25°C with 15% humidity. As light can induce decomposition of *S*-nitrosothiols, the nitrosated polymers were electrospun with the syringe guarded from light exposure in a darkened room.

### 5.2.2 Viscosity measurements

Viscosity of polymer solutions at concentrations used for electrospinning were recorded using a stress-controlled AR-G2 rheometer in Pa s at 25°C under sheer rates ranging from 10 to 100 $s^{-1}$. (TA Instruments, New Castle, Delaware) equipped with at 40mm, 2° steel cone. Sample sizes of approximately 600 μL of 10% PLGH-cysteamine, 20% PLGH-cysteine, 40% PLGH-homocysteine, and 20% of each *S*-nitrosated PLGH-cysteamine, -cysteine, and -homocysteine were used, and viscosities for each material were measured in triplicate.

### 5.2.3 Conductivity measurements

Conductivity of polymer solutions was measured using an Accumet XL50 dual channel pH/ion/conductivity meter (Fisher Scientific). The conductivity probe was placed in a glass vial containing 1 mL polymer solution, and measurements were recorded in μS/cm.

### 5.2.4 Fiber morphological stability under physiological conditions

*S*-nitrosated polymer fibers spun onto glass slides were submersed in 10 mL PBS (pH 7.4) in separate glass vials. Vials were covered with a rubber septum and nitrogen was bubbled

into the system. Temperature was maintained at 37 °C. After a period of 48 h, samples were removed and rinsed with deionized (DI) water.

### 5.2.5 Fiber analysis

Scanning electron microscopy (JEOL JSM-6500F, JEOL USA, Peabody, MA, USA) was used to visualize fiber morphology. Images were acquired using an accelerating voltage of 15 kV. Fibers were electrospun onto a sheet of aluminum foil for a time interval long enough to where a thin layer of visible polymer deposition could be seen. A small sample of foil was cut to the size of a SEM sample stub and attached with carbon tape and grounded with gold tape. Before analysis, samples were sputter coated with 10 nm gold. The average diameter of the polymer fibers were measured from the original SEM micrographs at 10,000x magnification using Adobe Photoshop CS5 software as described previously from Duan *et al*.[15] The diameter of 25 fibers from three different SEM micrograph frames was recorded, for a total of 75 measured fibers for each polymer system. The number of measurements recorded was 75 based on previously published work.[6]

### 5.2.6 Nitric Oxide Release

Real-time NO release from polymer fibers was determined using a modification of methods published previously and described in detail in Chapter 2.5.2[16] For these studies, fibers were electrospun until multiple layers were deposited on aluminum foil and small tissue-like samples could be peeled off. Approximately 5 mg *S*-nitrosated electrospun polymer sample was removed from the aluminum foil, weighed and inserted into an NOA measurement cell, containing 30 mL deoxygenated 10 mM phosphate buffered saline (PBS, pH 7.4) submersed in a water bath to maintain system temperature at 37 °C and shielded from direct exposure to light using aluminum foil.

### 5.2.7 Statistical Analysis

All experiments were performed in triplicate. Data is expressed as a mean ± standard deviation. Statistical analysis was performed using the t-test and significance was considered at $p \leq 0.05$.

## 5.3 Results and Discussion

### 5.3.1 Nanofiber formation and morphology

In this study, an electrospinning method was developed to create a porous scaffold structure with preserved NO release function from PLGH and its thiolated and nitrosated polymer derivatives. Previous groups have studied the use of unmodified PLGA nanofibers or blends of unmodified PLGA with other polymers for applications in biomedical devices, especially those related to wound healing.[5, 14] As PLGA is a commercial polymer with structural similarities to PLGH it was predicted electrospinning conditions for the two polymers would be similar. Using these parameters as a starting point, the applied voltage, polymer flow rate through the syringe, and polymer concentration in solution were varied until uniform nanofibers were achieved.[17, 18] To begin, the unmodified PLGH polymer was prepared for electrospinning according to the optimized conditions published by Katti *et al.*[14] Following these reported optimized conditions, PLGH polymer was dissolved in a 75:25 w/w solution of THF and DMF to achieve a polymer concentration of 20% w/w polymer to solvent. The distance between the nozzle and collecting plate were maintained at a constant 15 cm and flow rate was set at 0.2 mL $h^{-1}$. With these conditions set, voltage was varied between 8 and 15 kV in order to find the condition where the polymer was pulled most evenly from the syringe without sputtering and fiber morphology was most consistent. A voltage of 10 kV was found to be ideal for forming

uniform, bead free fibers under these conditions as confirmed by SEM micrographs (Figure 5.1). Next, the PLGH thiol derivatives were electrospun under the optimized conditions for forming fibers from PLGH to see if the thiol incorporation affected the ability of the polymer to be electrospun. Under these parameters, the PLGH-cysteine derivative formed uniform fibers while PLGH-cysteamine and PLGH-homocysteine exhibited many bead defects (Figure 5.2). When changes to voltage and flow rate did not improve fiber morphology, the concentration of polymer in solution was altered. The usual practice to rid fibers of bead defects is to increase the viscosity of solution by increasing the concentration of polymer. Solutions of 25, 30, 35 and 40% were prepared for both polymers. The PLGH-homocysteine derivative responded to this increase of polymer concentration as was expected, with bead defects becoming less prominent as concentration was increased until uniform fiber morphologies were achieved at 40% (Figure 5.3). This was not the case for PLGH-cysteamine, where few fibers were formed as the concentration was increased and instead amorphous bead-like morphologies were observed under SEM. In response, polymer concentrations were reduced from the initial 20% concentration to see whether that resulted in more uniform fiber morphologies. While bead defects were still present in 15% solutions, a 10% solution produced uniform fibers (Figure 5.4).

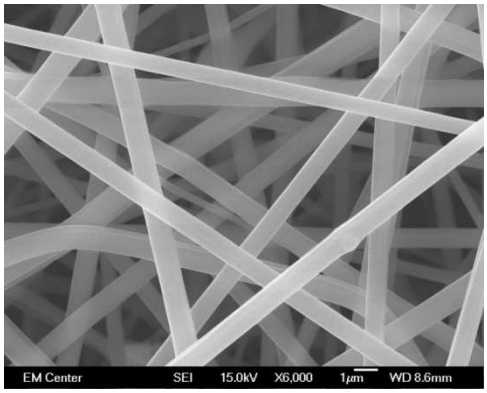


**Figure 5.1.** Representative SEM micrograph (6000x magnification) depicting the fibrous morphology of electrospun PLGH.

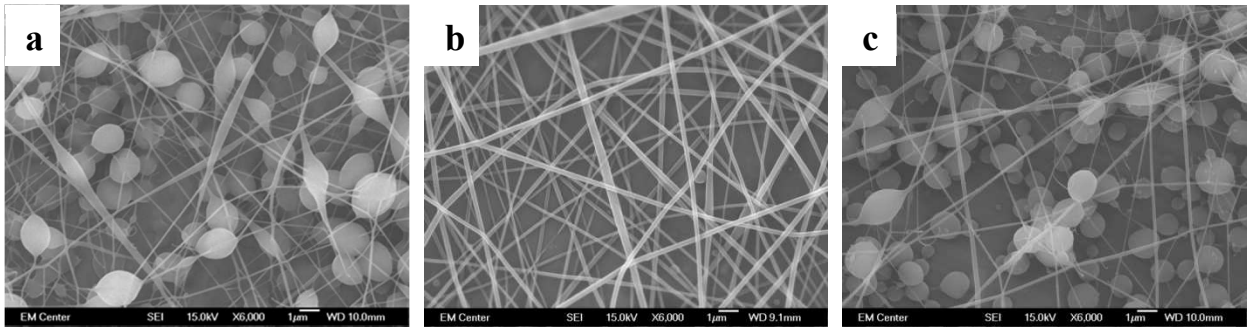


**Figure 5.2.** Representative SEM images (6000x magnification) of a) PLGH cysteamine, b) cysteine and c) homocysteine electrospun at 20% w/w polymer to solvent. PLGH-cysteine (b) exhibits ideal fiber morphology while bead defects in the fibers are abundant in PLGH-cysteamine and -homocysteine fibers. Bead defects indicate electrospinning parameters must further be optimized.

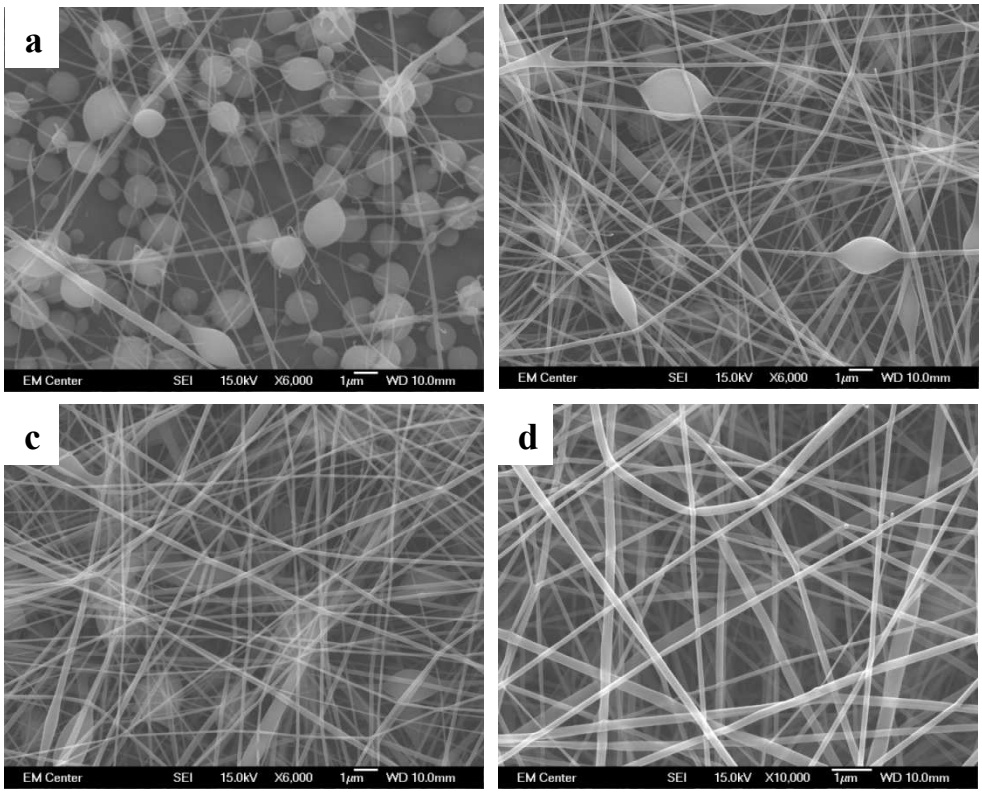


**Figure 5.3.** SEM images of PLGH-homocysteine electrospun at a) 25, b) 30, c) 35 and d) 40% w/w solutions. Bead defects in the 25% w/w fibers (a) are abundant, and present to a lesser extend as polymer concentration increases to 30 and 35% w/w (b and c) indicating an increase in polymer concentration in this polymer aids in reducing bead defects. Ideal electrospun fiber morphology lacking bead defects was finally achieved with a 40% w/w solution. Magnification of 6000x for (a-c) and 10000x for (d).

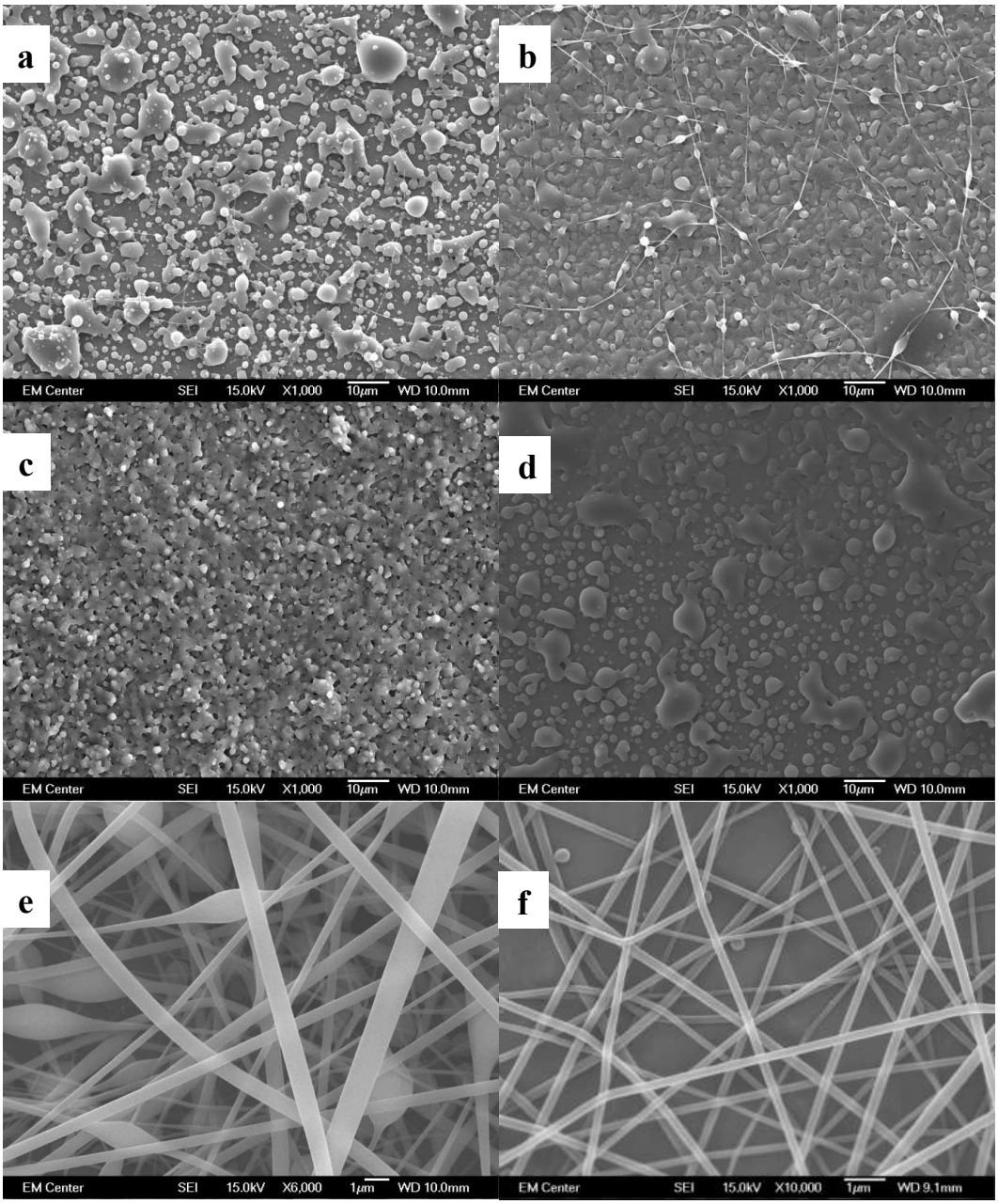


**Figure 5.4.** SEM images of PLGH-cysteamine electrospun in solutions of a) 25, b) 30, c) 35, d) 40, e) 15 and f) 10% w/w. Increasing the polymer concentration from the 20% solution that exhibited beaded fibers (in Fig. 5.2) did not result in fewer bead defects as it did in the PLGH-homocysteine derivative. Decreasing the polymer concentration in solution from 20% decreased the presence of bead defects and resulted in more uniform fiber formation. Suitable fiber morphologies were achieved with a 10% polymer solution (f). Magnification of 1000x for (a – d), 6000x for (e) and 10000x for (f).

*S*-nitrosated versions of the three thiolated PLGH derivatives were then synthesized and attempts at electrospinning were initiated. To begin, all derivatives were electrospun using the initial electrospinning conditions for unmodified PLGH (20% w/w polymer in solution). These conditions turned out to be ideal for forming uniform fibers for all three derivatives (Figure 5.5). At their optimized electrospinning conditions, briefly overviewed in Table 5.1, thiolated and nitrosated electrospun polymers exhibited highly porous structures with interconnected pores distributed throughout the fibrous structure. All fibers exhibited a random orientation. The overall shape, orientation, and pore size of the fibers are similar regardless of the identity of the thiol (i.e., cysteine, cysteamine, and homocysteine) or the subsequent nitrosation. Further, the scaffolds were similar to that of unmodified PLGH. The fiber morphology exhibits high surface-to-volume area and high porosity in a three-dimensional structure. This is important as the nanofiber structure mimics that of the natural ECM thereby capable of supporting cellular attachment.[19]

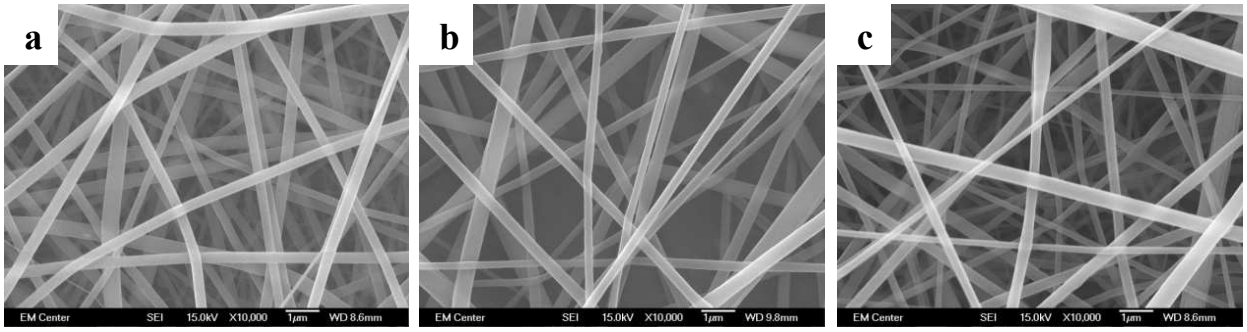


**Figure 5.5.** Representative SEM images (10000x) of a) S-nitrosated PLGH-cysteamine, b) cysteine and c) homocysteine electrospun at optimized conditions.

**Table 5.1.** Summary of optimized electrospinning conditions

| Parameter Variables | Optimized Conditions |
|---|---|
| Polymer concentration | 10 to 40% |
| Applied voltage | 10 kV |
| Flow rate | 0.2 mL $h^{-1}$ |
| Solvent system | THF/DMF (75:25 w/w) |
| Distance between the nozzle and collector | 15 cm |
| Electrospinning time | 30 min |

The fiber diameter obtained for the unmodified PLGH polymer (803 ± 205 nm) was found to be comparable to that reported for other electrospun fibers prepared with PLGA of similar composition (760 ± 210 nm).[17, 20] The fiber diameters of this unmodified PLGH materials were found to be almost twice to four times larger than the fibers electrospun from the thiolated and *S*-nitrosated polymer analogs (Table 3.2). Fiber diameters ranged from an average of 200 to 330 nm for the thiolated PLGH polymers and 250 to 410 nm for the *S*-nitrosated polymers. However, no trend in fiber diameter was observed for the thiolated or *S*-nitrosated materials regardless of the specific thiol system used. The mean values for the thiolated and *S*-nitrosated polymers are similar (roughly between 200 and 400 nm) and are within one standard deviation of each other. Although the standard deviations are large for all samples, subsequent analysis of the measured diameters from each SEM image (n = 75) did not reveal a trend with regards to a) the diameter size, b) the location on the image, or c) whether each of the polymer samples had fiber diameters with significant outliers (Figure 5.6). Taken together, the images as well as the measured fiber diameters suggest that the resulting diameters are randomly dispersed but fall within relative ranges of each other. The fiber diameters within the natural ECM are also random and range from several tens to hundreds of nanometers.[21] This makes these nanofibers an ideal representation of the natural ECM environment.

**Table 5.2.** Average fiber diameters for electrospun PLGH polymers.

| Polymer | Fiber diameter (nm) |
|---|---|
| PLGH | 803 ± 205 |
| PLGH-cysteamine | 330 ± 78 |
| PLGH-cysteine | 200 ± 205 |
| PLGH-homocysteine | 216 ± 116 |
| PLGH-cysteamine SNO | 250 ± 93 |
| PLGH-cysteine SNO | 410 ± 145 |
| PLGH-homocysteine SNO | 281 ± 116 |

n = 75

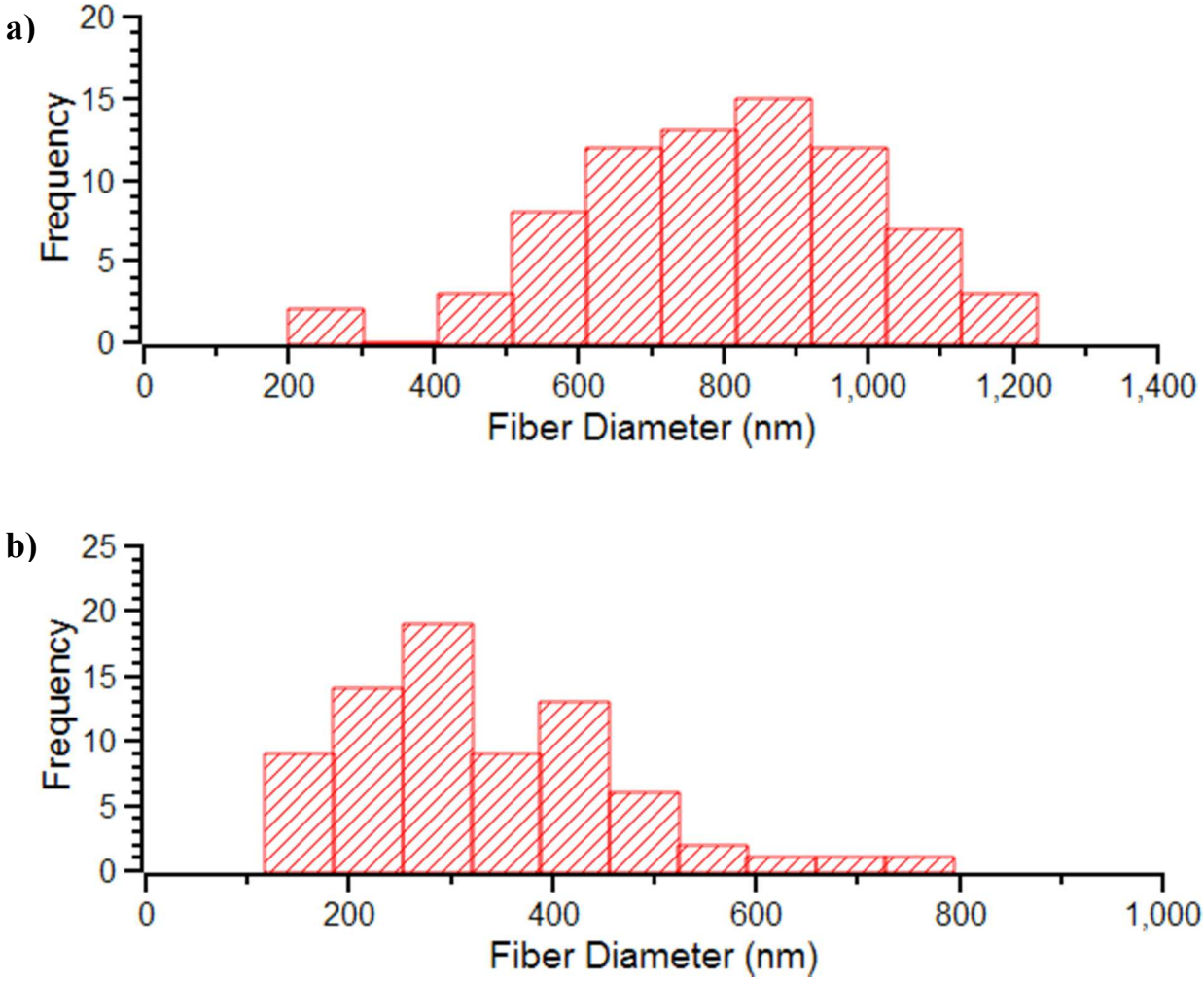

**c)**

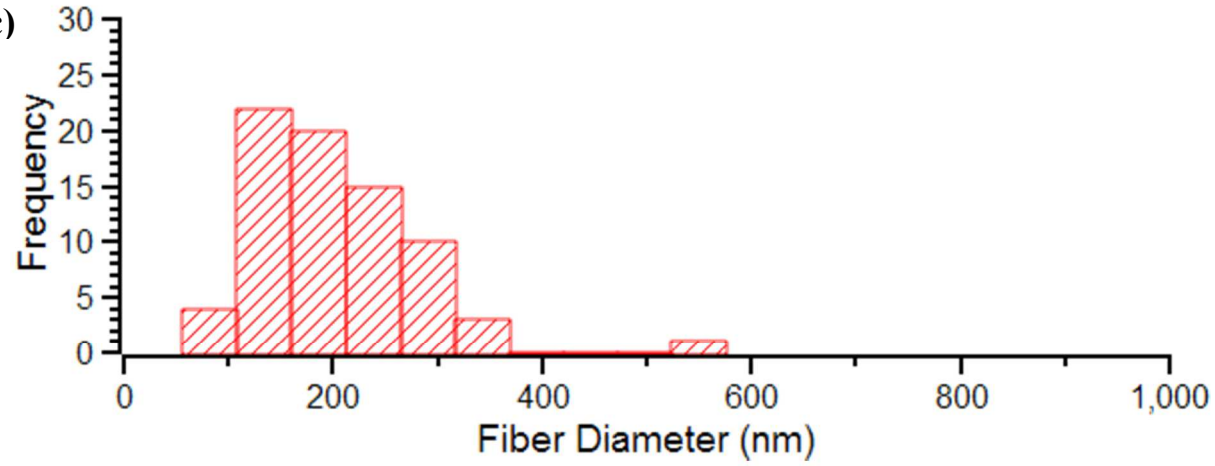
Frequency
0
5
10
15
20
25
30
0
200
400
600
800
1,000
Fiber Diameter (nm)

**d)**

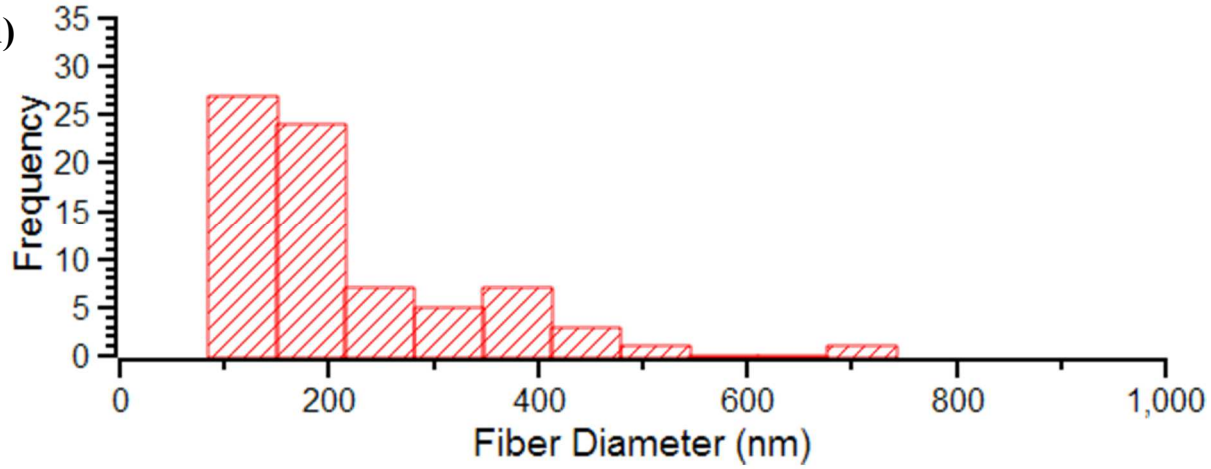
Frequency
0
5
10
15
20
25
30
35
0
200
400
600
800
1,000
Fiber Diameter (nm)

**e)**

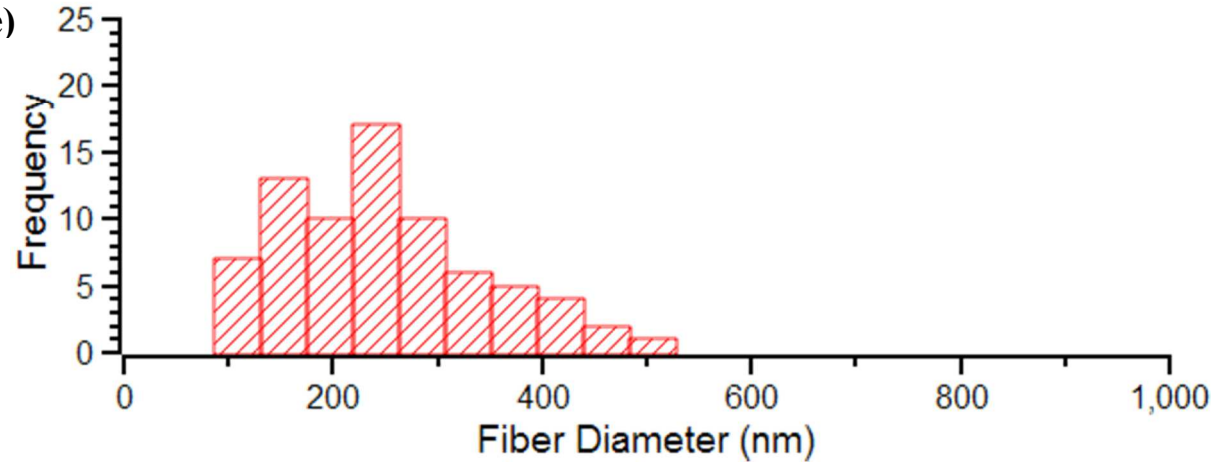
Frequency
0
5
10
15
20
25
0
200
400
600
800
1,000
Fiber Diameter (nm)

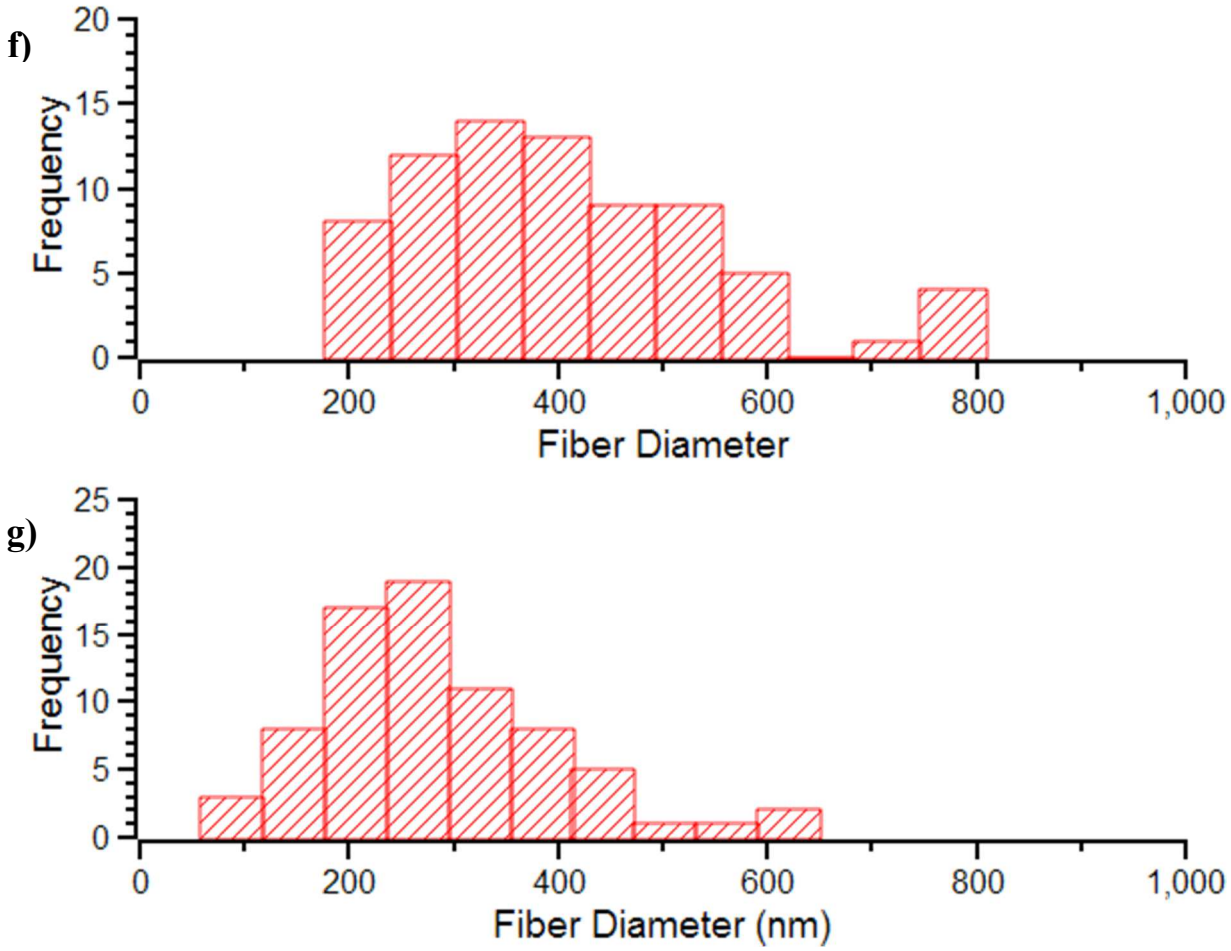


**Figure 5.6.** Fiber diameter distribution for electrospun a) PLGH, b) PLGH-cysteamine, c) PLGH-cysteine, d) PLGH-homocysteine, e) *S*-nitrosated PLGH-cysteamine, f) *S*-nitrosated PLGH-cysteine and g) *S*-nitrosated PLGH-homocysteine. Bars represent actual recorded values and therefore no error values are presented.

Although polymer concentration seemingly had the most significant influence on the ability to form nanofibers, fiber morphology is also known to be influenced by solution viscosity and conductivity. In order to determine the contribution of viscosity and conductivity on the ability to form NO releasing nanofibers, additional experiments were performed. Viscosity measurements were performed for all thiolated and nitrosated PLGH polymers at the concentrations that successfully produced the electrospun fibers. All polymer derivatives exhibited Newtonian viscosity across sheer stresses ranging from 10-100 $s^{-1}$. As a result, final

viscosity measurements were determined by averaging the values over this sheer range. As shown in Table 5.3, the differences in viscosity were significant for the thiol-modified PLGH polymers, with the 10% PLGH-cysteamine solution exhibiting the lowest viscosity (0.0020 Pa s) and the 40% PLGH-homocysteine solution exhibiting the highest viscosity (0.0364 Pa s). The nitrosated polymers (all in solutions of 20% w/w %) were also all statistically different from each other. The measured viscosities ranged from 0.0032 Pa s for *S*-nitrosated PLGH-cysteamine solution to 0.0089 Pa s for *S*-nitrosated PLGH-cysteine solution. The PLGH-cysteine derivative was the only solution where the same polymer concentration was used to produce electrospun fibers from both thiolated and *S*-nitrosated materials. This shows that at the same concentration, viscosity of the polymer solutions are altered by the nitrosation process as the thiolated and *S*-nitrosated PLGH-cysteine polymers exhibit statistically different viscosities. Taken together, these results show no apparent relationship between polymer concentrations and viscosity under fiber-forming concentrations of the polymers. Even the *S*-nitrosated polymers, which were all electrospun at the same concentration, exhibit different viscosities.

**Table 5.3.** Viscosities of PLGH polymer solutions

| **Polymer** | **Thiol** | | **SNO** | |
|---|---|---|---|---|
| | Polymer concentration | Viscosity (Pa s) | Polymer concentration | Viscosity (Pa s) |
| PLGH-cysteamine | 10% | 0.00201 ± 0.00008 | 20% | 0.00319 ± 0.00038 |
| PLGH-cysteine | 20% | 0.00762 ± 0.00045 | 20% | 0.00886 ± 0.00092 |
| PLGH-homocysteine | 40% | 0.03637 ± 0.00491 | 20% | 0.00795 ± 0.00056 |

Another factor known to influence fiber formation is solution conductivity. It has been reported that thinner and more uniform fibers with fewer bead defects can be achieved by increasing the solution conductivity,[22] as more highly conductive solutions are better able to

accept the applied electrical charge.[23] To explore whether solution conductivity had any effect on these materials, we measured the conductivity of the thiolated (40 wt. %) and nitrosated (20 wt. %) PLGH-homocysteine polymer solutions that produced bead free fibers. We found that functionalization with a nitroso group significantly decreased the solution conductivity, from approximately 1.5 μS/cm in the thiolated polymer solution to 0.2 μS/cm in the nitrosated polymer solution. The reason for this observed changed in solution conductivity may be due to the conversion of the more conductive amine sites on the thiolated polymer to less conductive NO sites.

Based on these experiments, we have determined neither viscosity nor conductivity provide adequate explanations for the variations in thiolated polymer concentrations necessary for forming nanofibers. The effect of polymer concentration on nanofiber formation however may be best explained by analyzing the thiol content of each polymer derivative. All of the polymer solutions had the same amount of thiol present (i.e. ~0.07 mmol $g^{-1}$), where, as reported previously[13], each of the thiol modified PLGH polymers had different loadings of the respective thiol groups cysteamine (0.57 ± 0.03 mmol $g^{-1}$), cysteine (0.39 ± 0.02 mmol $g^{-1}$), or homocysteine (0.18 ± 0.05 mmol $g^{-1}$). When each polymer solution was normalized for thiol content (mmol $g^{-1}$) in the electrospinning solution, the thiol content in solution was found to be similar across polymer derivatives (Table 5.4). This correlation between thiol content and solution concentration suggests that the extent of thiol in solution may have the greatest influence on fiber formation for these materials. This observed behavior may arise from the extensive cross-linking of the polymer chains through disulfide linkages under the given applied voltage. Consequently, to prevent this disulfide bond formation, a lower polymer concentration for higher thiol content polymers was required to produce bead free nanofibers. This explanation

is also consistent with the observation that all of the nitrosated polymers (cysteamine, homocysteine, and cysteine PLGH derivatives) were successfully electrospun at a solution concentration of 20 wt %. After nitrosation, far fewer thiol groups exist, thus eliminating the possibility of disulfide bond formation. As an example, in PLGH-homocysteine, 96% of thiol sites are converted to *S*-nitrosothiol sites after the nitrosation process while PLGH-cysteamine has a 93% conversion. In contrast, PLGH-cysteamine demonstrates only a 43% conversion.[13]

**Table 5.4.** Thiol content of polymers normalized for concentration in electrospinning solution.

| **Polymer** | **Electrospinning process** | |
|---|---|---|
| | Polymer concentration in solution (% w/w) | Net thiol content in polymer solution (mmol $g^{-1}$) |
| PLGH-cysteamine | 10 | 0.06 |
| PLGH-cysteine | 20 | 0.08 |
| PLGH-homocysteine | 40 | 0.07 |

As no correlations were found to exist between solution conductivity, viscosity, and nanofiber formation, we hypothesize that the difference in diameter size can be explained by considering the lattice structures of the unmodified and modified polymers. Incorporation of the thiol functionalities onto the polymer backbone increases the randomness in the polymer lattice. This, in turn, increases the self-repulsion interactions between the polymer chains. Consequently, these repulsive forces enhance the stretching force of the polymer jet under the applied field[24] and result in comparably smaller fiber diameters for the thiolated and *S*-nitrosated PLGH derivatives compared to unmodified PLGH.

To see if the optimized thiol concentration in solution for electrospinning PLGH polymers was consistent across different polymer systems, conditions for electrospinning

thiolated dextran derivative dextran-cysteamine was examined. (The dextran polymer derivative synthesis is explained in detail in Chapter 2). Because of polymer solubility differences, dextran polymer derivatives were electrospun using a 50/50 blend of dimethyl sulfoxide (DMSO) and dimethylformamide (DMF) under a 15 kV applied voltage and 17 cm distance between needle and collector. The unmodified dextran and thiol modified dextran-cysteamine derivative were dissolved in the DMSO/DMF solution at a concentration of 60% w/w. *S*-nitrosated dextran-cysteamine has not yet been successfully electrospun as the polymer swells but does not dissolve in solution resulting in highly beaded morphology (Figure 5.7). As the dextran-cysteamine derivative has a thiol content of 0.27 ± 0.07 mmol $g^{-1}$, the thiol content in the electrospinning solution is 0.15 mmol $g^{-1}$. This is roughly double the average thiol concentration seen in the optimized electrospun PLGH polymers. So, like with other electrospinning parameters, the thiol content necessary for forming electrospun fibers is not the same across polymer types. By finding electrospinning parameters for other thiolated dextran derivatives we could determine whether thiol is indeed a key determinant in fiber formation ability of this polymer system as well by comparing thiol concentrations in solution across the different derivatives.

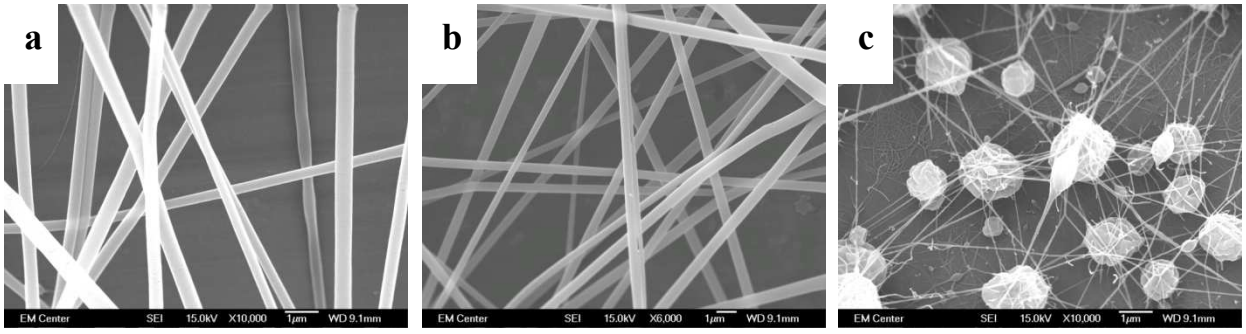


**Figure 5.7.** Representative SEM images of the electrospun morphology of a) dextran, b) dextran-cysteamine and c) *S*-nitrosated dextran-cysteamine. Both dextran and dextran-cysteamine exhibited uniform fibrous morphology while the *S*-nitrosated dextran-cysteamine exhibits large bead defects as this polymer derivative swelled but did not dissolve in the solvent system used.

### 5.3.2 Nitric oxide release

The ability of the electrospun fibers to maintain their NO release capabilities after fabrication is important if the resulting material is to be practically useful for the treatment of bacterial infections. Thus, our primary aim was to demonstrate that nanofibers could be formed from *S*-nitrosated PLGH derivatives without diminishing their capability of releasing NO. We also wanted to investigate the effect of the different thiols on NO release profiles of the resulting polymers. In this regard, we evaluated the extent of NO release from nanofibers under physiological pH and temperature in PBS buffer using a highly specific, real-time chemiluminescence NO analyzer. NO release results from the nanofibers are presented in terms of 1) comparison to thin-films and 2) comparison to the various thiol analogs.

### 5.3.3 Comparison between thin films and nanofibers

Figure 5.8 shows the representative real-time NO release profiles normalized for the weight of each polymer analog as a function of fabrication method: electrospun nanofibers and polymer films. The shapes of the curves and relative magnitude of release demonstrate that the high voltages applied to the polymer solution during the electrospinning process do not alter the NO storage capabilities or release kinetics of the material compared with other processing methods. While the total amount of NO released from the electrospun *S*-nitrosated PLGH-homocysteine ($0.026 \pm 0.004$ mmol $g^{-1}$) was found to be statistically similar to the spin-coated films ($0.033 \pm 0.007$ mmol $g^{-1}$), the electrospun *S*-nitrosated PLGH-cysteine and -cysteamine materials exhibited statistically significant differences ($p \leq 0.05$) in the total moles of NO released after 48 h (Table 3.5). For these materials, however, no trend in the loss of NO release capability was observed. Thin film *S*-nitrosated PLGH-cysteine exhibited an NO release of $0.155 \pm 0.009$ mmol $g^{-1}$, which was statistically greater than the amount of NO released from the

electrospun material (0.110 ± 0.007 mmol $g^{-1}$). In contrast, the electrospun *S*-nitrosated PLGH-cysteamine demonstrated a greater NO release over 48 h when compared to the same polymer processed as a thin film (0.281 ± 0.016 mmol $g^{-1}$as compared to 0.241 ± 0.004 mmol $g^{-1}$). While these differences were statistically determined to be significantly different from one another, the differences in NO release after processing are considered to be small and can be attributed to the relative stability of the *S*-nitrosothiol materials and not the fabrication process itself, with *S*-nitrosated PLGH-homocysteine exhibiting a greater stability for NO retention than the other two derivatives.

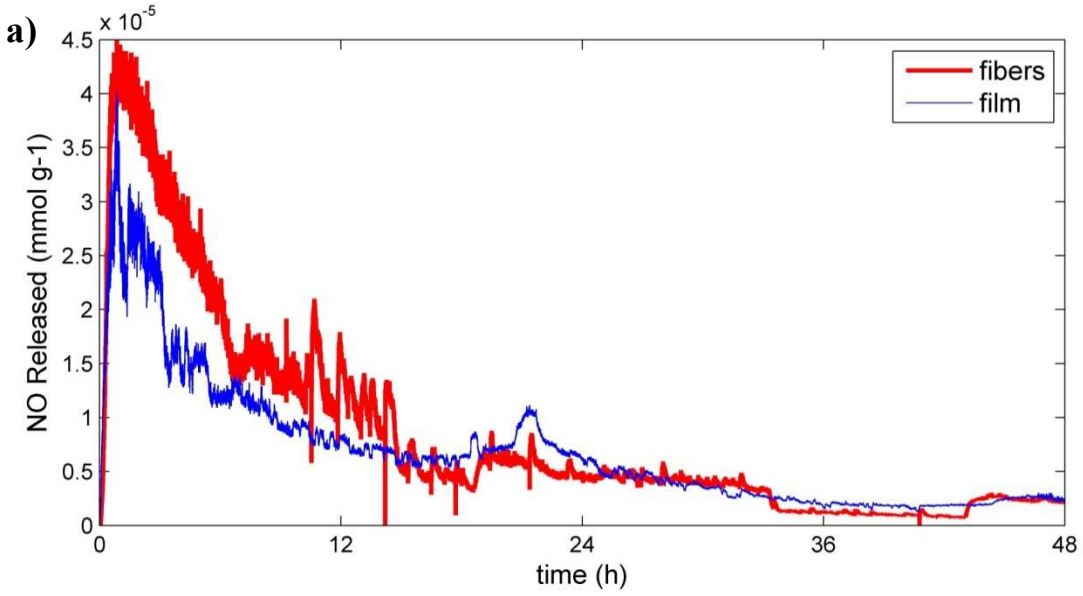

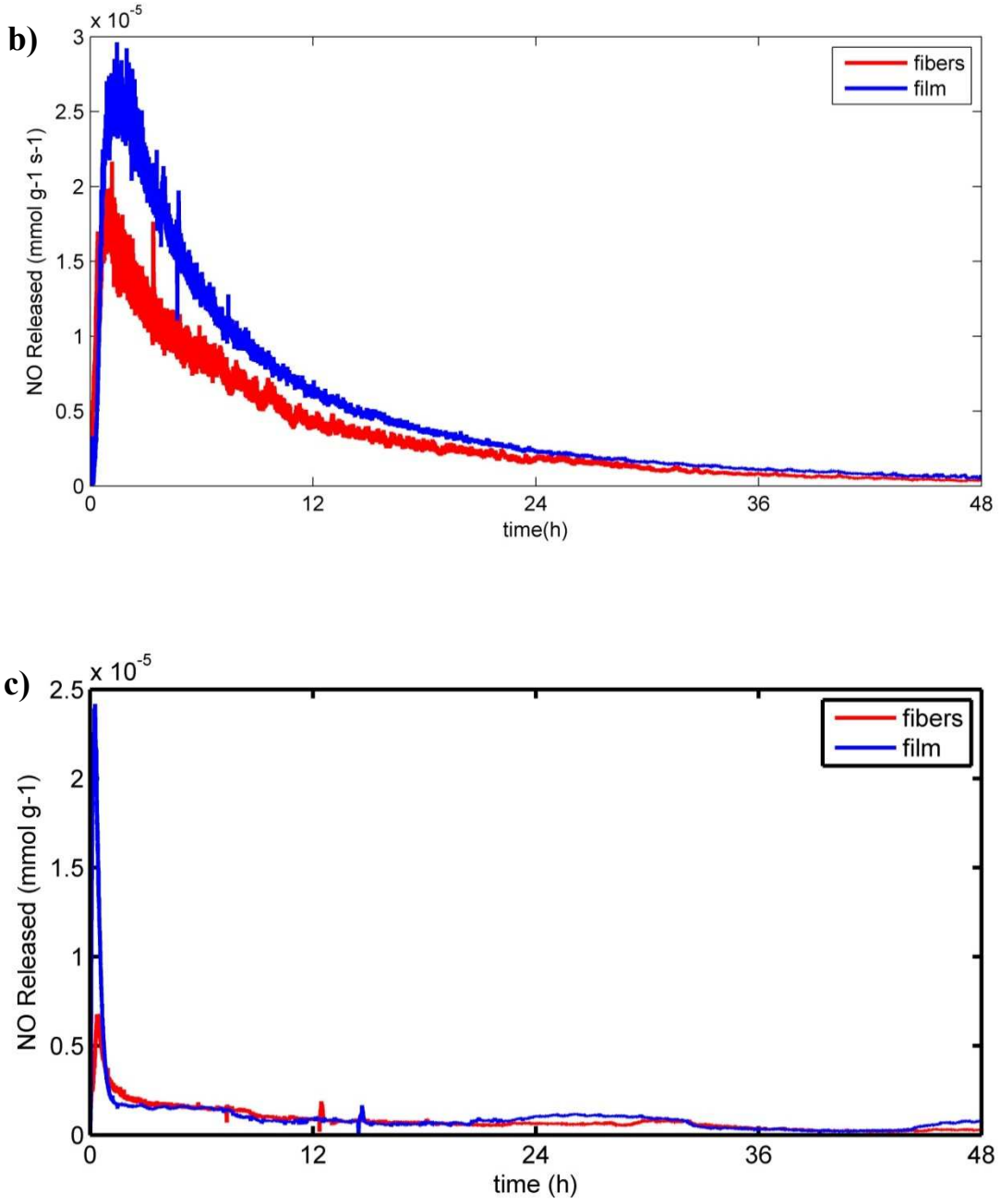


**Figure 5.8.** Representative NO release kinetic profiles from individual thin film and electrospun S-nitrosated polymers under experimental physiological conditions (10 mM PBS buffer/ pH 7.4/ 37 ºC) over 48 h for a) *S*-nitrosated PLGH-cysteamine, b) *S*-nitrosated PLGH-cysteine and c) *S*-nitrosated PLGH-homocysteine.

**Table 5.5.** Comparison between NO released over 48 h from polymers processed into thin-films and nanofibers

| ***S-nitrosated* Polymer** | **NO released after 48 h**[b] | |
|---|---|---|
| | Thin-film[a] $\mu$mol g$^{-1}$ | Nanofibers $\mu$mol g$^{-1}$ |
| PLGH-cysteamine SNO | 0.241 ± 0.004 | 0.281 ± 0.016 |
| PLGH-cysteine SNO | 0.155 ± 0.009 | 0.110 ± 0.007 |
| PLGH-homocysteine SNO | 0.033 ± 0.007 | 0.026 ± 0.004 |

[a]As reported previously[13]
[b]10 mM PBS/ pH 7.4/ 37°C

### 5.3.4 Comparison between S-nitrosated nanofibers

The NO release profiles of all *S*-nitrosated nanofibers can be characterized by an initial rapid release of NO followed by a slower release rate over the remaining 48 h (Figure 5.8). In general, the higher storage capacity materials exhibited the larger initial rate of NO release. Nanofibers made from *S*-nitrosated PLGH-cysteamine demonstrated the greatest release rate over 48 h, followed by the cysteine and homocysteine analogs. The instantaneous NO release peaked between 30 min to 1 h for all three polymer systems. The relatively lower NO release level of the homocysteine derivative can be attributed to the relative higher stability of the *S*-nitrosated homocysteine species compared to the cysteine and cysteamine derivatives under the release conditions. The trends in NO release from the different *S*-nitrosated nanofibers are consistent with those of thin films.

While we report the amount of NO released from the nanofibers over 48 h, none of these materials had exhausted their NO release capacity during this period. The 48 h release profiles for *S*-nitrosated PLGH-cysteamine and *S*-nitrosated PLGH-cysteine fit well to an exponential function. Based on this fit, the *S*-nitrosated cysteamine and cysteine nanofibers would be expected to release NO for 85 h before reaching baseline. On the other hand, the NO release

from the homocysteine analog quickly achieved a steady state release level that was maintained for 46 h after the initial 2 h spike. As such, if these fibers maintained this rate of NO release, the material would actively release NO for 198 h before reaching baseline.

One of the major advantages of this electrospun polymer system over small molecular donor blends is the sustained release of NO over multiple days. In previous work using NO donor blended electrospun systems,[6, 8] NO release from composite electrospun fiber material occurred rapidly over the period of minutes, extinguishing their NO release capability within an hour. The *S*-nitrosated PLGH electrospun materials provide continuous release of NO over the period of days, creating a more sustained release window. This is important for aiding these materials in their potential for therapeutic use. As the process of fighting infection causing bacteria and initiating cell proliferation at a wound site occurs on the time scale of days, these materials exhibit the appropriate release characteristics for potentially aiding in the wound healing processes.

### 5.3.5 Nanofiber morphological stability after immersion in PBS

For a nanofiber material to function to promote wound healing, the fiber morphology of the material must be maintained in physiological conditions long enough to promote cell attachment. Degradation properties of the bulk PLGH materials have been previously conducted and demonstrated a complete degradation of the material over nearly 40 weeks for PLGH-cysteamine, 30 weeks for PLGH-cysteine and 20 weeks for PLGH and PLGH-homocysteine polymer derivatives.[13] As such, we wanted to ensure the fibers were capable of maintaining morphology under physiological conditions as well. The exposure of these fibers to physiological conditions for 48 h demonstrated that the electrospun matrix maintains its characteristic fibrous form. Figure 5.9 shows the random orientation of the fibers after NO

release. The maintenance of fiber form over a period of days is beneficial for applications in wound healing when the material must initially remain intact in order to provide a strong scaffold for cell growth and proliferation. Based on the previous findings with the bulk material, it is expected the scaffold will completely degrade over the period of months. If applied as a wound healing aid, the complete degradation of the material is intended and advantageous after cell infiltration into the scaffold has occurred.

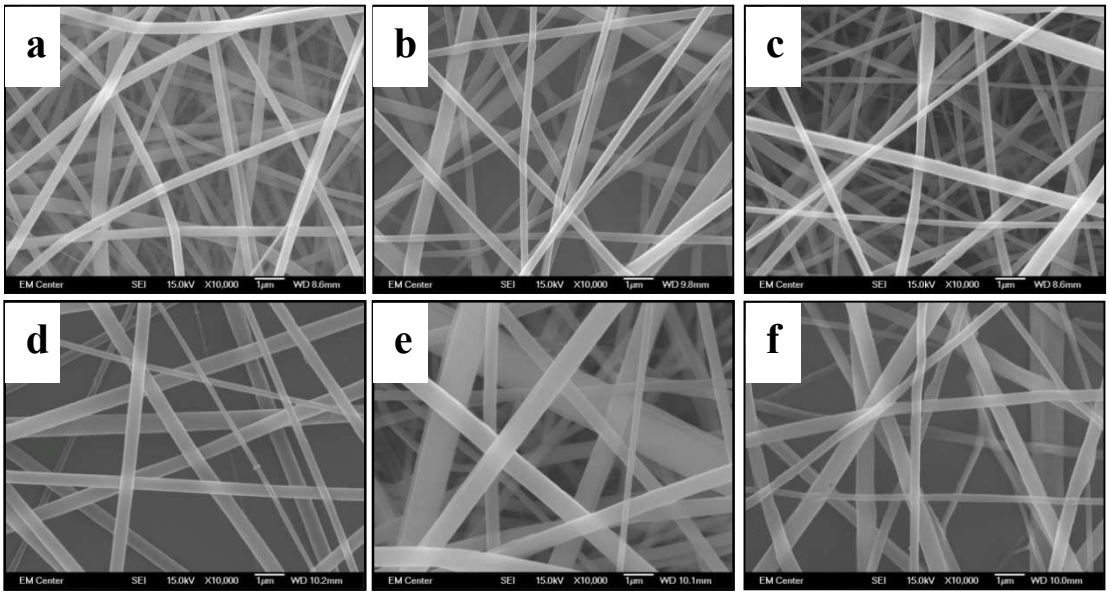


**Figure 5.9.** Representative SEM images at 10,000x of electrospun nanofibers of a) *S*-nitrosated PLGH-cysteamine, b) *S*-nitrosated PLGH-cysteine, c) *S*-nitrosated PLGH-homocysteine. Electrospun fibers after exposure to physiological pH and temperature in PBS for 48 h d) *S*-nitrosated PLGH-cysteamine, e) *S*-nitrosated PLGH-cysteine and f) *S*-nitrosated PLGH-homocysteine.

## 5.4 Conclusion

In this study, a series of thiolated and NO releasing biodegradable PLGH polymers were successfully electrospun to create nanofiber scaffolds capable of continuous NO release over a period of days when submerged in PBS under physiological temperature and pH. Each material exhibited its own unique NO release properties. Short term exposure to aqueous conditions did

not alter the morphology of the fibers as all materials were shown to maintain their nanofibrous forms after 48 h. The development of biodegradable nanofibers containing covalently attached NO donors may provide a novel paradigm for applications in wound healing. The nanofibers act to mimic the natural extracellular matrix while controlled and extended NO release provides bactericidal activity. With both properties combined into one material, further investigation into the impact of these materials in preventing bacterial responses and promoting cell attachment in wounded tissue are warranted.

REFERENCES


1. Hunley, M. T.; Long, T. E., Electrospinning functional nanoscale fibers: a perspective for the future. *Polymer International* **2008,** 57, (3), 385-389.

2. Kumbar, S. G.; et al., Electrospun nanofiber scaffolds: engineering soft tissues. *Biomedical Materials* **2008,** 3, (3), 034002.

3. Blackwood, K. A.; McKean, R.; Canton, I.; Freeman, C. O.; Franklin, K. L.; Cole, D.; Brook, I.; Farthing, P.; Rimmer, S.; Haycock, J. W.; Ryan, A. J.; MacNeil, S., Development of biodegradable electrospun scaffolds for dermal replacement. *Biomaterials* **2008,** 29, (21), 3091-3104.

4. Powell, H. M.; Supp, D. M.; Boyce, S. T., Influence of electrospun collagen on wound contraction of engineered skin substitutes. *Biomaterials* **2008,** 29, (7), 834-843.

5. Liu, S. J.; Kau, Y. C.; Chou, C. Y.; Chen, J. K.; Wu, R. C.; Yeh, W. L., Electrospun PLGA/collagen nanofibrous membrane as early-stage wound dressing. *Journal of Membrane Science* **2010,** 355, (1-2), 53-59.

6. Coneski, P. N.; Nash, J. A.; Schoenfisch, M. H., Nitric Oxide-Releasing Electrospun Polymer Microfibers. *ACS Applied Materials & Interfaces* **2011,** 3, (2), 426–432.

7. Lopez-Jaramillo, P.; Rincon, M. Y.; Garcia, R. G.; Silva, S. Y.; Smith, E.; Kampeerapappun, P.; Garcia, C.; Smith, D. J.; Lopez, M.; Velez, I. D., A Controlled, Randomized-Blinded Clinical Trial to Assess the Efficacy of a Nitric Oxide Releasing Patch in the Treatment of Cutaneous Leishmaniasis by Leishmania (V.) panamensis. *American Journal of Tropical Medicine and Hygiene* **2010,** 83, (1), 97-101.

8. Liu, H. A.; Balkus, K. J., Novel Delivery System for the Bioregulatory Agent Nitric Oxide. *Chemistry of Materials* **2009,** 21, (21), 5032-5041.

9. Bohlender, C.; Wolfram, M.; Goerls, H.; Imhof, W.; Menzel, R.; Baumgaertel, A.; Schubert, U. S.; Mueller, U.; Frigge, M.; Schnabelrauch, M.; Wyrwa, R.; Schiller, A., Light-triggered NO release from a nanofibrous non-woven. *Journal of Materials Chemistry* **2012,** 22, (18), 8785-8792.

10. Koh, A.; Carpenter, A. W.; Slomberg, D. L.; Schoenfisch, M. H., Nitric Oxide-Releasing Silica Nanoparticle-Doped Polyurethane Electrospun Fibers. *Acs Applied Materials & Interfaces* **2013,** 5, (16), 7956-7964.

11. Joslin, J. M.; Lantvit, S. M.; Reynolds, M. M., Nitric Oxide Releasing Tygon Materials: Studies in Donor Leaching and Localized Nitric Oxide Release at a Polymer-Buffer Interface. *Acs Applied Materials & Interfaces* **2013,** 5, (19), 9285-9294.

12. Annich, G. M.; Meinhardt, J. P.; Mowery, K. A.; Ashton, B. A.; Merz, S. I.; Hirschl, R. B.; Meyerhoff, M. E.; Bartlett, R. H., Reduced platelet activation and thrombosis in extracorporeal circuits coated with nitric oxide release polymers. *Critical Care Medicine* **2000,** 28, (4), 915-920.

13. Damodaran, V. B.; Joslin, J. M.; Wold, K. A.; Lantvit, S. M.; Reynolds, M. M., S-Nitrosated biodegradable polymers for biomedical applications: synthesis, characterization and impact of thiol structure on the physicochemical properties. *Journal of Materials Chemistry* **2012,** 22, (13), 5990-6001.

14. Katti, D. S.; Robinson, K. W.; Ko, F. K.; Laurencin, C. T., Bioresorbable nanofiber-based systems for wound healing and drug delivery: Optimization of fabrication parameters. *Journal of Biomedical Materials Research Part B-Applied Biomaterials* **2004,** 70B, (2), 286-296.

15. Duan, B.; Wu, L. L.; Yuan, X. Y.; Hu, Z.; Li, X. L.; Zhang, Y.; Yao, K. D.; Wang, M., Hybrid nanofibrous membranes of PLGA/chitosan fabricated via an electrospinning array. *Journal of Biomedical Materials Research Part A* **2007,** 83A, (3), 868-878.

16. Reynolds, M. M.; Hrabie, J. A.; Oh, B. K.; Politis, J. K.; Citro, M. L.; Keefer, L. K.; Meyerhoff, M. E., Nitric Oxide Releasing Polyurethanes with Covalently Linked Diazeniumdiolated Secondary Amines. *Biomacromolecules* **2006,** 7, (3), 987-994.

17. You, Y.; Min, B.-M.; Lee, S. J.; Lee, T. S.; Park, W. H., In vitro degradation behavior of electrospun polyglycolide, polylactide, and poly(lactide-co-glycolide). *Journal of Applied Polymer Science* **2005,** 95, (2), 193-200.

18. Bashur, C. A.; Dahlgren, L. A.; Goldstein, A. S., Effect of fiber diameter and orientation on fibroblast morphology and proliferation on electrospun poly(d,l-lactic-co-glycolic acid) meshes. *Biomaterials* **2006,** 27, (33), 5681-5688.

19. Sill, T. J.; von Recum, H. A., Electro spinning: Applications in drug delivery and tissue engineering. *Biomaterials* **2008,** 29, (13), 1989-2006.

20. Xin, X.; Hussain, M.; Mao, J. J., Continuing differentiation of human mesenchymal stem cells and induced chondrogenic and osteogenic lineages in electrospun PLGA nanofiber scaffold. *Biomaterials* **2007,** 28, (2), 316-325.

21. Ma, Z. W.; Kotaki, M.; Inai, R.; Ramakrishna, S., Potential of nanofiber matrix as tissue-engineering scaffolds. *Tissue Engineering* **2005,** 11, (1-2), 101-109.

22. Pham, Q. P.; Sharma, U.; Mikos, A. G., Electrospinning of polymeric nanofibers for tissue engineering applications: A review. *Tissue Engineering* **2006,** 12, (5), 1197-1211.

23. Pillay, V.; Dott, C.; Choonara, Y. E.; Tyagi, C.; Tomar, L.; Kumar, P.; du Toit, L. C.; Ndesendo, V. M. K., A Review of the Effect of Processing Variables on the Fabrication of Electrospun Nanofibers for Drug Delivery Applications. *Journal of Nanomaterials* **2013**.

24. Meng, Z. X.; Zheng, W.; Li, L.; Zheng, Y. F., Fabrication, characterization and in vitro drug release behavior of electrospun PLGA/chitosan nanofibrous scaffold. *Materials Chemistry and Physics* **2011,** 125, (3), 606-611.

# CHAPTER 6: CONCLUSION AND FUTURE DIRECTIONS

## 6.1 Conclusion

Chronic, infected wounds represent a major burden to the healthcare industry. Current treatment methods fail due to the inability to stimulate healthy growth from the wounded tissue and prevent bacterial infection. As bacteria strains continue to develop resistance to the antibiotics used to treat them, new methods of infection control must be developed. Recently, there has been an interest in investigating the development of wound treatments that incorporate nitric oxide (NO), a small molecule naturally up-regulated by cells during wound healing.

In this work, two polymeric NO-releasing material systems, *S*-nitrosated dextran and PLGH, were synthesized and studied for their potential application as wound healing materials. This research focused on the effect of dextran polymer derivatives on bactericidal activity and cell functionality in addition to the processing capabilities of PLGH. *S*-nitrosated dextran represented a biodegradable water-soluble dextran based system tailored to incorporate the thiol group cysteamine onto which NO is covalently attached. *S*-nitrosated PLGH represented a biodegradable water-insoluble polymer system, which also incorporates an NO group attached to a thiol modification on the PLGH backbone. Both polymer systems were characterized for thiol incorporation using a modification of the Ellman's assay, NO incorporation was characterized using UV-visible spectroscopy, and NO release was determined using real time NO analysis in PBS at 37°C and pH 7.4. The synthesis methods used resulted in repeatable thiol incorporation, NO storage and NO release properties. NO incorporation and release of these polymers was similar to that of other reported NO-incorporated materials exhibiting bactericidal activity, indicating their potential efficacy for reducing bacteria burden. Additionally, NO release from

both materials is characterized by a high initial release of NO followed by a lower steady release. These properties are advantageous as they mimic *in vivo* NO release in wounds where higher NO release is needed to induce bactericidal activity, after which lower NO release is necessary for promoting proliferative and protective effects on eukaryotic cells.

Bactericidal activity was evaluated for *S*-nitrosated dextran in solutions of planktonic gram-negative *E. coli* and *A. baumannii* as well as gram-positive *S. aureus.* The design of the experiment allowed for the observation of bacteria activity over 24 h while providing bacteria with an environment conducive to growth. In this work, 6- and 7-log reductions were observed in bacteria over 24 h. This is within the first NO-releasing systems, and the first polymeric NO-releasing system, to, over 24 h, achieve log reductions of 7 or greater. These results represent the achievement of clinically relevant reductions of planktonic bacteria, suggesting potential for the polymer system as a treatment for *in vivo* infection.

Cell functionalization of human dermal fibroblasts (HDF) was investigated by determining cell viability and morphology. Cell function was determined after 24 h using a cell viability assay and after 5 days using florescent imaging techniques. The results of this study led to the understanding of dosages of *S*-nitrosated dextran between which cytotoxic and non-cytotoxic effects on cell viability were observed. Reducing the polymer concentration in cell solution reduced observed cytotoxic effects to the HDF cells *in vitro,* which is consistent with observations of a concentration dependence of NO on cell function *in vivo.*

Processing capabilities were explored for PLGH and dextran polymer derivatives using the electrospinning with the goal of forming uniform fibers with nano-scale diameters. Parameters for developing electrospun fibers of *S*-nitrosated PLGH and its derivatives were

established and the morphology of the fibers was confirmed using SEM. Release of NO was found to be retained by the polymer after the electrospinning process, and, using SEM, the fibrous morphology was confirmed to be maintained after exposure to aqueous conditions. The development of these fibers marks the first published example of an electrospun macromolecular scaffold of a NO-releasing polymer. The morphological structure of the electrospun polymer mimics the fibrous structure of the ECM. This property could promote enhanced cell proliferation and infiltration at a wound site. The NO release from the fibers is characterized by an initially high release, which could be beneficial for inducing bactericidal activity. This high release is followed by a steady, low release similar to levels of NO released by the endothelium. This second stage could prove beneficial for promoting cellular proliferation. The structural maintenance of the fibers under aqueous conditions suggests the processed polymer could maintain morphology if applied to a wound site.

The results of this research suggest clinically relevant bacteria reductions and processing potential coupled with retained release characteristics for these *S*-nitrosated polymeric materials. Evidence of potential efficacy of the polymers is proven through the demonstration of high log-reductions of clinically relevant bacteria; determination of polymer concentrations limits for promoting and inhibiting skin cell functionality; and demonstration of processing techniques that mimic the ECM while maintaining NO release and structural morphology under aqueous conditions over 48 h. These results represent promising advancements in the development of NO releasing materials as efficacious treatments for enhancing the healing of chronic, infected wounds.

## 6.2 Future directions

The results presented in this dissertation only begin to show the potential of electrospun nitrosated materials for their *in vivo* application in wound healing and therefore further studies on these materials are suggested. The studies presented in Chapter 3 examined the bactericidal activity of the *S*-nitrosated dextran-cysteamine polymer against planktonic bacteria, yet bacteria in chronic wounds are more likely to be present in the form of a biofilm. As discussed in Chapter 1, bacteria biofilms are highly difficult to eradicate once they start to form and exhibit low susceptibility to traditional antibiotics. Therefore, the next step in determining the antibacterial potential of the material should focus on examining the ability of *S*-nitrosated PLGH and dextran materials to both disperse biofilms and prevent their formation. In biofilm dispersal experiments, biofilms could be grown to maturation in well plates before being treated with varying concentrations of *S*-nitrosated dextran-cysteamine, dispersed in nutrient media. Live/dead fluorescent assays could be utilized to visualize any dispersal or disruption of the biofilm resulting from the polymer treatment. The results of the planktonic bacteria assays suggest *S*-nitrosated dextran-cysteamine would be capable of preventing biofilm formation on surfaces as the material kills the vast majority of bacteria in solution, but this must be confirmed. First, methods for developing films or coatings from these materials should be developed so surface interactions can be assessed. Bacteria should be exposed to the polymer surfaces and attachment assessed using a live/dead fluorescence assays to visualize attached and viable bacteria. Along with bactericidal activity, potential cytotoxicity of the material must also be further assessed. These studies should also be carried out using the *S*-nitrosated PLGH polymer systems.

To determine the cytotoxicity of the materials, further *in vitro* studies should be conducted analyzing human dermal fibroblast and endothelial cells viability when exposed to a variety of concentrations of polymer, starting at the highest concentration reported for bactericidal activity in Chapter 3, as well as films of the polymers. Currently, the Reynolds group is working to develop processes of blending dextran derivatives with commercially available polyurethane materials to develop a thin film, which could be applied to mouse models for performing *in vivo* cutaneous wound healing analysis.

Despite the fact that the thin polymer films mentioned above are one processing alternative, the three-dimensional structure observed on electrospun fibers would be a more biologically relevant as it mimics the extracellular matrix. This three-dimensional interface is probably a more suitable set-up for enhancing cell growth and proliferation during wound healing. The electrospun nanofibers developed within this dissertation present significant challenges in terms of application as they are fragile and exhibit no mechanical strength. One potential way to improve the mechanical properties of the fibers would be through experimenting with coaxial electrospinning, where the NO-donor polymer is electrospun along with another polymer system- one with potential for flexible but handleable properties. This process would result in a core/sheath fiber structure where the NO-donor polymer forms the inner core with the more mechanically robust as the surrounding sheath. With optimized processing techniques and a better understanding of therapeutic dosages, the polymers presented in this dissertation would have potential for further investigation as viable wound healing materials.